

# **Forensic Hyperpolarisation Using SABRE**

Thomas Tennant

A thesis submitted in fulfilment of the requirements of the Manchester Metropolitan University for the degree of Master of Science (by Research)

Division of Chemistry & Environmental Science

School of Science and the Environment

Manchester Metropolitan University

2018

## **Dedication**

It is with genuine gratitude that I dedicate this thesis to Rev. Fr. Ron McGivern, my Grandad. Without his support, I would not have been able to take this opportunity and I would not be where I am today. For that, I thank him.

## **Acknowledgements**

Firstly, I would like to thank my supervisor's Dr Ryan Mewis and Dr Oliver Sutcliffe for not only providing me with this opportunity, but for having patience and helping me along the way with invaluable advice and research insight. I would also like to extend thanks to the analytical support team, in particular Lee Harman, for providing me with crucial training on various laboratory instruments.

I would like to thank the various post docs and PhD students in and around the laboratory who have without doubt offered help and advice in some way at some point. These include Michael Foley, James Ryan, Chris Foster, and Lysbeth Antinodes, but in particular Tom Robertson, Jack Marron and Matt Hulme.

On a more personal note, I would like to thank my family and friends for constantly supporting me throughout my undergraduate and postgraduate degrees.

## Abstract

The purpose of this study is to develop the application of Signal Amplification By Reversible Exchange (SABRE) hyperpolarisation to New Psychoactive Substance (NPS) analysis. Piperazine derivatives are the compounds under investigation due to their strong prevalence in the last ten years as a New Psychoactive Substances (NPS) which posed/poses a threat to the general public, particularly the younger generation. Firstly, this study aimed to fully characterise 1-[(2-pyridyl)methyl]piperazine, 1-[(3-pyridyl)methyl]piperazine and 1-[(4-pyridyl)methyl]piperazine (2, 3 and 4-PMP respectively). Secondly, it was important to develop a quantitative method for detection of these compounds using bench top  $^1\text{H}$  Nuclear Magnetic Resonance (NMR). Standard addition (SA) and Internal Standard (IS) calibrations were the methods investigated for their suitability. The largest part of the project was to explore the feasibility to hyperpolarise the compounds under investigation due to the presence of a pyridyl functionality. Hyperpolarisation can lower detection limits, cut costs and offer quicker and better results than conventional NMR. SABRE was the hyperpolarisation method employed due to its ease, low cost and impressive literature results. The final aim was to develop/optimize and apply a method to extract and detect the NPS from a common formulation. It was discovered that 3 equivalents of triethylamine was the optimum amount to freebase 4-PMP.3HCl. The method of standard addition using bench-top NMR was incredibly accurate in determining the concentration of PMP samples with unknown concentrations. Finally, a mixture of all three isomers was distinguishable through the use of GC-MS. In addition to this, it was also possible to extract the drug from a common formulation (tablet) in its un-hyperpolarisable state, freebase it and

then successfully hyperpolarise. This thesis provides an acceptable application of SABRE to the analysis of NPS.

## Acronyms

(1-methyl-4-phenyl-1,2,3,6-tetrahydropyridine) (MPTP)

1-(cyclohexylmethyl)-1*H*-indole-3-carboxylic acid 8-quinolinyl ester (BB-22)

1-[(2-pyridyl)methyl]piperazine (2-PMP)

1-[(3-pyridyl)methyl]piperazine (3-PMP)

1-[(4-pyridyl)methyl]piperazine (4-PMP)

3,4-methylenedioxy-methamphetamine (MDMA)

Active Pharmaceutical Ingredient (API)

Adiabatic longitudinal transport after dissociation engenders net alignment (ALTADENA)

Benzylpiperazine (BZP)

Dynamic Nuclear Polarisation (DNP)

Gamma-hydroxybutyrate (GHB)

Gas Chromatography Mass Spectrometry (GC-MS)

Hyperpolarisation (HP)

Internal Standard (IS)

Magnetic field (*B*)

Magnetic Resonance Imaging (MRI)

New Psychoactive Substances (NPS)

Nuclear Magnetic Resonance (NMR)

*para*-Hydrogen (*p*-H<sub>2</sub>)

*Para*-hydrogen and synthesis allow dramatic enhanced nuclear alignment (PASADENA)

*Para*-Hydrogen Induced Polarisation (PHIP)

Psychoactive Substances Act 2016 (PSA 2016)

Signal Enhancement By Reversible Exchange (SABRE)

Spin Exchange Optical Pumping (SEOP)

Standard Addition (SA)

Temperature (K)

Tesla (T)

Triethylamine (TEA)

United Nations Office on Drugs and Crime (UNODC)

# Contents

1. Introduction .....	15
1.1. New Psychoactive Substances (NPS) .....	15
1.1.1. Prevalence of NPS.....	15
1.1.2. Prevalence of Piperazines .....	17
1.1.3. Research Importance .....	18
1.2. <sup>1</sup> H Nuclear Magnetic Resonance (NMR) Spectroscopy .....	19
1.2.1. Magnetic Field Alignment .....	20
1.2.2. Chemical Shift .....	20
1.3. Hyperpolarisation .....	21
1.3.1. Brute-Force .....	22
1.3.2. Dynamic Nuclear Polarisation (DNP) .....	22
1.3.3. Spin-Exchange Optical Pumping (SEOP) .....	23
1.3.4. <i>Para</i> -Hydrogen Induced Polarisation (PHIP) .....	24
1.3.5. PASADENA (Para-hydrogen and synthesis allow dramatic enhanced nuclear alignment) .....	25
1.3.6. ALTADENA (Adiabatic longitudinal transport after dissociation engenders net alignment) .....	25
1.3.7. SABRE (Signal amplification by reversible exchange) .....	26
2. Experimental Methodologies.....	28
2.1. Reagents.....	28
2.2. Instrumentation.....	28



2.3.	Generic Hyperpolarisation Sample Preparation and Method .....	29
2.3.1.	Adaptations to the Generic Hyperpolarisation Method .....	30
2.4.	Analysis 4-PMP.3HCl Tablet by GCMS.....	32
2.4.1.	Calibration Standards .....	32
2.4.2.	Test Solution (Quantitative GC-MS Analysis).....	33
2.4.3.	Test Solution (Qualitative GC-MS Analysis) .....	33
2.4.4.	GC-MS Method Validation .....	33
2.5.	Standard Addition (SA) and Internal Standard (IS) Calibration .....	34
2.5.1.	Preparation from Stock Solutions.....	34
3.	Hyperpolarisation of PMP Compounds .....	36
3.1.	Characterisation and Resolution <i>via</i> Bench-top NMR (BT-NMR) .....	36
3.2.	Hyperpolarisation of 4-PMP (freebase) .....	37
3.3.	Freebasing 4-PMP.3HCl <i>in-situ</i> .....	40
3.4.	Hyperpolarisation of 4-PMP.3HCl .....	41
3.5.	Does Triethylamine 'Poison' the Catalyst? .....	43
3.6.	Effect of Excess Triethylamine on Hyperpolarisation .....	44
3.7.	The Sequential Addition of Triethylamine.....	46
3.8.	Changing the Order of Addition .....	49
3.9.	The Sequential Addition of Triethylamine (4-PMP.3HCl).....	50
3.10.	The Sequential Addition of Triethylamine to 4-PMP (freebase).....	54
3.11.	2-PMP and 3-PMP .....	56

3.11.1.	Hyperpolarisation .....	57
3.12.	Summary.....	58
4.	Hyperpolarisation of 4-PMP Tablet .....	60
4.1.	Adapting the Hyperpolarisation Method .....	60
4.2.	Results and discussion .....	61
4.3.	Summary .....	65
5.	Standard Addition (SA) and Internal Standard (IS) – Quantitative NMR (QNMR)	
	67	
5.1.	Standard Addition.....	67
5.1.1.	Proof of Concept.....	68
5.2.	Calibration (TMS Internal Standard) .....	68
5.3.	Results and Discussion.....	69
5.4.	Summary .....	72
6.	GC-MS Analysis .....	73
6.1.	Characterisation and Separation of PMP Isomers.....	73
6.2.	Validation and the Quantification of a PMP Tablet .....	74
6.3.	Results and discussion .....	75
6.4.	Summary .....	79
7.	Hyperpolarisation of 1-(cyclohexylmethyl)-1 <i>H</i> -indole-3-carboxylic acid 8-	
	quinolinyl ester (BB-22).....	79
7.1.	Results and Discussion.....	80

7.2. Summary .....	81
8. Conclusion.....	82
9. Future Work.....	84
10. Appendix.....	85
10.1. Characterisation Data for 2-PMP.....	85
10.2. Characterisation Data for 3-PMP.....	88
10.3. Characterisation Data for 4-PMP.....	91
10.4. Characterisation Data for 4-PMP.3HCl.....	93
10.5. Characterisation Data for 4-PMP.3HCl Tablet.....	94
10.6. Characterisation Data for BB-22.....	96
11. Bibliography.....	99

## List of Figures

Figure 1: Low-field $^1\text{H}$ NMR spectra for 2, 3 and 4-PMP (freebase). .....	36
Figure 2: Hyperpolarised $^1\text{H}$ NMR spectrum of 4-PMP (freebase). .....	40
Figure 3: Hyperpolarised $^1\text{H}$ NMR spectrum of 4-PMP.3HCl after the addition of 1.2eq triethylamine. ....	42
Figure 4: Hyperpolarised $^1\text{H}$ NMR Spectra of 4-PMP (freebase): A) No Triethylamine added, B) 1.2 eq Triethylamine added. ....	44
Figure 5: $^1\text{H}$ NMR SABRE spectra for addition of 5eq TEA to 4-PMP (freebase). (A) is the thermal spectrum, (B) was taken after the first para-hydrogen purge, (C) and (D) are the result of the 2nd and 3rd tube shake from the 1st purge. (E), (F) and (G) correspond to the 1 <sup>st</sup> , 2 <sup>nd</sup> and 3 <sup>rd</sup> tube shake after the introduction of the 2 <sup>nd</sup> para-hydrogen purge. ....	46
Figure 6: Stacked $^1\text{H}$ NMR spectra for the sequential addition of triethylamine to 4-PMP freebase. ....	47
Figure 7: Graph showing how increasing amounts of TEA effect the hyperpolarisation levels of 4-PMP.3HCl. ....	48
Figure 8: $^1\text{H}$ NMR spectra for experiments 8 and 9; determining how much the order of addition effects hyperpolarisation. Experiment 8 (Green), Experiment 9 (Maroon). ....	50
Figure 9: Graph showing how increasing the concentration of TEA effects the hyperpolarisation of 4-PMP.3HCl. ....	53
Figure 10: Graph showing how increasing the concentration of TEA effects the hyperpolarisation of 4-PMP (freebase). ....	55
Figure 11: Structures for 3-pyridylmethylpiperazine (3-PMP) and 2-pyridylmethylpiperazine (2-PMP). ....	56
Figure 12: Hyperpolarised $^1\text{H}$ NMR spectra for 2-PMP. ....	58

Figure 13: 4-PMP.3HCl Tablet. ....	60
Figure 14: Hyperpolarised <sup>1</sup> H NMR spectrum (turquoise) and <sup>1</sup> H NMR thermal background spectrum (maroon) of 4-PMP.3HCl pill. The thermal spectrum is shown at x32 vertical magnification. ....	62
Figure 15: Hydride region taken from the hyperpolarised spectra of the 4-PMP.3HCl based pill. Bottom to top: Thermal background, 1 <sup>st</sup> para-hydrogen purge A, 1 <sup>st</sup> para-hydrogen purge B, 2 <sup>nd</sup> para-hydrogen purge A, 2 <sup>nd</sup> para-hydrogen purge B, 3 <sup>rd</sup> para-hydrogen purge. (A = first shake, B = second shake). ....	63
Figure 16: Standard addition calibration graph for 4-PMP (freebase). ....	69
Figure 17: Standard addition calibration graph for 3-PMP (freebase). ....	69
Figure 18: Standard addition calibration graph for 2-PMP (freebase). ....	70
Figure 19: Internal standard (TMS) calibration graph for 4-PMP (freebase). ....	70
Figure 20: GC-MS chromatograph for the separation of 2-, 3- and 4-PMP. ....	74
Figure 21: GC-MS calibration graph of average Integrated Area Ratio (IAR) for each concentration. ....	75
Figure 22: GC-MS calibration for all IAR points at each concentration. ....	76
Figure 23: 150 ugml-1 GCMS calibration chromatograph (4-PMP.3HCl). ....	77
Figure 24: Graph showing how increasing sample mixing time effects its Integrated Area Ratio (IAR). ....	77
Figure 25: GC-MS chromatograph for the tablet analysis. ....	79
Figure 26: Low-field NMR spectrum for attempted hyperpolarisation of BB-22. ....	80
Figure 27: IR Spectrum for 2-PMP. ....	85
Figure 28: High-field <sup>1</sup> H NMR spectrum for 2-PMP. ....	85
Figure 29: High-field NMR <sup>1</sup> H- <sup>1</sup> H COSY for 2-PMP. ....	86
Figure 30: High-field DEPT NM for 2-PMP. ....	86

Figure 31: High-field $^{13}\text{C}$ NMR for 2-PMP.....	87
Figure 32 LC-MS spectrum for 2-PMP.....	87
Figure 33: IR spectrum for 3-PMP.....	88
Figure 34: High-field $^1\text{H}$ NMR spectrum for 3-PMP. ....	88
Figure 35: High-field $^1\text{H}$ - $^1\text{H}$ COSY NMR for 3-PMP. ....	89
Figure 36: High-field DEPT NMR for 3-PMP. ....	89
Figure 37: High-field $^{13}\text{C}$ NMR. ....	90
Figure 38: LC-MS spectrum for 3-PMP.....	90
Figure 39: High-field $^1\text{H}$ NMR spectrum for 4-PMP. ....	91
Figure 40: High-field $^1\text{H}$ - $^1\text{H}$ COSY spectrum for 4-PMP.....	91
Figure 41: High-field DEPT NMR for 4-PMP. ....	92
Figure 42: High-field $^{13}\text{C}$ NMR for 4-PMP.....	92
Figure 43: LC-MS spectrum for 4-PMP.....	93
Figure 44: IR spectrum for 4-PMP.3HCl. ....	93
Figure 45: LC-MS spectrum for 4-PMP.3HCl. ....	94
Figure 46: LC-MS spectrum for 4-PMP.3HCl tablet.....	94
Figure 47: GC-MS for 4-PMP.3HCl tablet. ....	95
Figure 48: IR spectrum for BB-22. ....	96
Figure 49: High-field $^1\text{H}$ NMR spectrum for BB-22.....	96
Figure 50: High-field $^1\text{H}$ - $^1\text{H}$ COSY NMR spectrum for BB-22. ....	97
Figure 51: High-field HMQC NMR spectrum for BB-22.....	97
Figure 52: High-field $^{13}\text{C}$ NMR spectrum for BB-22.....	98

Table 1 - Quantities used in the SABRE studies throughout this project. ....	30
Table 2 - Information regarding the make-up of the calibration standards for GCMS. .	32
Table 3 - Information detailing the make-up of the SA calibration solutions. ....	34
Table 4 - Information detailing the work up of IS calibrations standards. ....	35
Table 5 - Table showing NMR tube concentrations for sequential addition of TEA to 4-PMP.3HCl. Catalyst stock (2 mg / 100 $\mu$ L).....	51
Table 6 - How 4-PMP.3HCl and 4-PMP (freebase) were compared in terms of eq of TEA added. E.g. 3 eq TEA with 4-PMP.3HCl was compared to 0 eq TEA with 4-PMP (freebase). .....	54
Table 7 - Standard addition results. ....	71

## 1. Introduction

### 1.1. New Psychoactive Substances (NPS)

Over the years the terms research drugs, legal highs, designer drugs and NPS have become increasingly familiar, which is no doubt a result of their growing popularity. NPS are described as “narcotic or psychotropic drugs that are not scheduled under the United Nations 1961 or 1971 Conventions, but which may pose a threat to public health comparable to scheduled substances”.<sup>1</sup> They are synthetically made substances, often produced by underground chemists in China and India, that are designed to mimic the behaviour of popular illicit drugs such as cocaine, 3,4-methylenedioxymethamphetamine (MDMA) and cannabis.<sup>2</sup>

#### 1.1.1. Prevalence of NPS

What are now known as NPS established a solid presence on society in the United States in 1984, when a number of fentanyl derivatives made their way on to the illicit drug market. Despite its imprecision, the name ‘designer drugs’ was coined in respect to the lab made opioids.<sup>1, 3</sup> Interest in the substances faded, however, when a synthetic impurity (1-methyl-4-phenyl-1,2,3,6-tetrahydropyridine) (MPTP) found in a proline derivative led to users chemically inducing themselves with Parkinson’s disease.<sup>1</sup> A number of phenethylamine based drugs made attempts at finding a long-lasting place on the market with little success. Gamma-hydroxybutyrate (GHB), a ‘failed pharmaceutical’, was at first believed to aid muscle development and so found a niche market within the bodybuilding community. Although it was not incredibly popular, it



did not take long for recreational drug users to discover its potential to offer experiences of euphoria or sedation.<sup>1, 4</sup> NPS prominence was re-established, despite being short-lived, lasting in to the early 2000's after the production of hallucinogenic analogues made their way on to the scene. Benzylpiperazine (BZP), a piperazine derivative, is arguably the first NPS to maintain a solid hold on the drug market. Legally marketed in New Zealand from the start of the 21<sup>st</sup> century as a safer alternative to 3,4-methylenedioxy-methamphetamine (MDMA), millions of BZP pills were sold before the drug was detected in Europe.<sup>1, 5</sup> A curious bit of research emerged when it became apparent that BZP had transitioned from being sold as a pill to being sold as a powder. The compelling fact here is that production had shifted from underground laboratories to established chemical companies, notoriously situated in Asia.<sup>1</sup> The next phase in the emergence of NPS is based around synthetic cathinones and synthetic cannabinoids, such as mephedrone and Spice respectively. The start of this phase is subjective in the literature, with evidence to suggest cathinones properly surfaced substantially later than in the Soviet Union in the 70's and 80's or Germany in 1997. The use of Google Insights showed that there were almost no searches for synthetic cathinones before 2008.<sup>6</sup> However, this could be dismissed by looking at internet access data. The early 2000's saw the rise of the internet no doubt, but knowledge of using it to research drugs at that time remains an unanswered question. More recently, synthetic cannabinoids have caught the attention of researchers and the public. Prior to the passing of the Psychoactive Substances Act 2016 (PSA 2016), synthetic cannabinoids such as Spice were marketed legally as incense or room odorizers. Despite being labelled 'not for human consumption', synthetic cannabinoids were regularly purchased as a legal alternative to cannabis.<sup>7</sup> Commonly the synthetic cannabinoid is sprayed onto plant material, which does not offer any psychoactive effects itself. In addition to this, they

can be purchased as a liquid or in the form of pills. With over 240 different synthetic cannabinoids reported to UNODC between 2008 and 2016, they form the largest NPS group. This is due to the fact there are an overwhelming amount of different structures reported. Additionally, twenty-nine fatalities throughout 2014 and 2015 directly linked to synthetic cannabinoids shows how much of a risk they pose to public health.<sup>8,9</sup>

### 1.1.2. Prevalence of Piperazines

The start of the 21<sup>st</sup> century saw the growing popularity of MDMA and amphetamines alike, which influenced an influx of similarly structured compounds known as piperazines.<sup>10, 11</sup> BZP became the most popular MDMA/amphetamine substitute, with most of its distribution found in New Zealand (under the name BZP party pills), however BZP was also detected in the U.K, Brazil and Japan.<sup>5, 12</sup> Astonishingly, after many failed attempts by clandestine laboratories to make designer drugs fashionable, BZP broke the mould and stamped its mark on the world. Their attractive euphoric effects saw them become prominent on the club scene as a safer alternative to MDMA, with an estimated 8 million servings sold between 2000 and 2005 in New Zealand.<sup>1, 5, 13</sup> To put this into perspective, this is the same as 40% of New Zealand's population purchasing one BZP pill per year in the 5-year period (2000–2005). To further confirm BZP's use in the club scene, data collected in a report on BZP party pills conducted in New Zealand in 2006, reported that the most common age group to confirm use of the substance was 20-24 year olds (48.8% of respondents). In addition to this, the report not only clarified that 15-18 years of age were the most common reported ages of first use, it also stated that 75.7% of respondents describe getting hold of BZP as 'very easy'. This highlights the importance of the PSA 2016 in the UK.<sup>14, 15</sup> Interestingly, a UK study in 2010 claimed

piperazines were the most common drugs in tablets bought over the internet, however, there is no data post-PSA 2016 unfortunately.<sup>12</sup> Considering this comes years after the reign of BZP throughout New Zealand, it is intriguing to see that piperazines were still rife. The population of the UK is magnitudes larger than New Zealand and thus an influx of BZP of some kind, despite being safe guarded by the PSA, would prove tough to manage, particularly due to the demographic showing peak popularity amongst young people.<sup>15</sup> Abuse and dependence potential is evident and has been confirmed by research, even though there are no clinical studies to support this, with 2.2% of respondents classifying themselves as dependant on BZP in New Zealand.<sup>15, 16</sup> Furthermore, like other illicit drugs, the risk of overdose is still present. In 2004 alone, 21 people were reported to have overdosed due to BZP consumption (five solely due to BZP).<sup>5</sup> In light of this, a study by Butler and Sheridan concluded by reporting that despite reports of young people suffering dangerous side effects as a result of BZP consumption, there was no evidence to back them up.<sup>17</sup> The literature does, however, make a point of highlighting the potential need for harm reduction interventions in cases of risky use.<sup>17</sup>

### 1.1.3. Research Importance

The introduction of the 2016 Psychoactive Substances Act in the UK forced the distribution of the substance out of the hands of 'head shops' and retailers, and into the hands of drug dealers who work under no regulations. The amount of NPS substances reported is increasing year on year, thus, it is imperative to progress research in order to stay on top of the situation.<sup>8</sup> Developing a wider range of detection and characterisation techniques is of benefit to reduce the risk posed to public health and safety by these substances. Literature states that there is a possibility of alternatives to

BZP surfacing to replace the drug in the future, adding another dynamic to the importance of research into potential future variants of these drugs.<sup>18</sup> This study aims to characterise the NPS 4-PMP and its regioisomers before exploring the feasibility of their hyperpolarisation. Further to this, the development of a viable quantitation method using bench-top NMR will take place. Finally, a method will be developed to extract, detect and hyperpolarise the NPS from a common formulation.

## 1.2. <sup>1</sup>H Nuclear Magnetic Resonance (NMR) Spectroscopy

The phenomenon that is NMR was first successfully detected in December 1945 by two separate groups of physicists in the United States. When Edward M. Purcell *et al.* at Harvard University and Felix Bloch *et al.* at Stanford University in California succeeded in detecting the first lucrative observation of NMR in solids and liquids, they set in motion the development of a new branch of science.<sup>19, 20</sup> Their discovery was recognized worldwide and they were awarded the Nobel Prize in Physics in 1952.<sup>21</sup> Today NMR spectroscopy is one of the most powerful and versatile analytical techniques available to scientists and is most commonly used in structure elucidation. NMR utilises the quantum mechanics of subatomic particles (protons, neutrons and electrons) due to their spin properties. In atoms such as <sup>12</sup>C, <sup>16</sup>O, <sup>32</sup>S these spins are paired and therefore cancel each other out producing zero overall spin. However, there are a scope of atoms (<sup>1</sup>H, <sup>13</sup>C, <sup>31</sup>P, <sup>15</sup>N, <sup>19</sup>F etc.) whose nuclei do possess an overall spin allowing for analysis through NMR. Determining the spin of a given nucleus is relatively simple and can be done so by following the subsequent rules. If both the number of protons and neutrons are even, the nucleus will possess zero spin. When added together, if the number of protons plus the number of neutrons is odd, the nucleus will possess a half-integer spin

(1/2, 3/2, 5/2). If both the number of protons and neutrons are odd, the nucleus has a full integer spin (1, 2, 3).<sup>22</sup>

### 1.2.1. Magnetic Field Alignment

For  $^1\text{H}$ , upon the application of a magnetic field there are two possible alignments, orientation either with the magnetic field (alpha =  $\alpha$ ) or against it (beta =  $\beta$ ).  $\alpha$  is preferred due to its lower energy; however, the energy difference between both alignments is so small that natural population of both can be expected at room temperature. During the acquisition of an NMR spectrum, energy from a radio-frequency (RF) coil is applied to the system, promoting a transition of  $\alpha$  orientated nuclei to  $\beta$  nuclei. When the RF coil is turned off, relaxation of the nuclei begins (transitions from  $\beta$  back to  $\alpha$  until thermal equilibrium reached), generating resonances which are recorded and displayed in a spectrum following Fourier transformation.<sup>23</sup>

### 1.2.2. Chemical Shift

Since the magnetic moment of specific nuclei, such as  $^1\text{H}$ , remains constant indefinitely, it could be presumed that  $^1\text{H}$  would give resonance signals at the same field/frequency values every time. To a scientist's advantage this does not hold true and so chemical shift enables us to identify and characterise structures. Chemical shifts are the signature appearance of signals on an NMR spectrum derived from functional groups. These are a result of electrons in the surrounding environment of the proton responding to the external magnetic field they are subjected to, and so different  $^1\text{H}$  environments produce different chemical shifts. Electrons generate a conflicting field to the much stronger,

external magnetic field. The conflicting field acts as a shield to the nucleus (Zeeman interactions ( $H_z$ )) from the external magnetic field. These interactions are amended by the chemical shielding effect described by the shielding constant, and the indirect spin-spin coupling contribution ( $H_j$ ), which outlines the connection between two neighbouring nuclei.<sup>24, 25</sup> It is for this reason, to overcome shielding effects, that NMR spectrometers typically employ magnets between 1 and 20 Tesla (T).<sup>26</sup> It is understood that nuclei with more shielding will have a lower ppm (parts per million) and will be situated in the aliphatic region of the spectrum (right side), whilst nuclei with less shielding will have a higher ppm and will be situated in the aromatic region (left side).

### 1.3. Hyperpolarisation

One of NMR's greatest disadvantages is its inherent low sensitivity, which arises from the very small population differences that exist between nuclear spin states. Hyperpolarisation, which is comprised of a variety of techniques, has proven successful in improving the sensitivity of NMR spectroscopy whilst also providing the fundamental building blocks for advancement in drug detection, characterisation and quantification, as well as Magnetic Resonance Imaging (MRI).<sup>27</sup> Each of the six techniques; Brute force, Dynamic Nuclear Polarisation (DNP), Spin Exchange Optical Pumping (SEOP), *Para*-hydrogen and synthesis allow dramatic enhanced nuclear alignment (PASADENA), Adiabatic longitudinal transport after dissociation engenders net alignment (ALTADENA) and Signal Enhancement By Reversible Exchange (SABRE), achieve enhanced polarisation in a different way. Where some are invasive and chemically change the substrate, others are not and propagate magnetisation in other ways. Essentially, non-

Boltzmann distributions are the desired outcome, of which some methods to achieve this are discussed below.

### 1.3.1. Brute-Force

Often referred to as the simplest HP method, Brute-Force enhances NMR signals by simply altering the conditions of the environment a sample is polarised in. Two factors crucial to NMR are altered: Temperature ( $K$ ) and magnetic field ( $B$ ). By polarising a sample in a high-field – low temperature environment (lowering  $T$  to  $<4$  K and increasing  $B$  to 14 T), Brute-Force polarisation can take place. Lowering  $T$  prevents population of the thermal equilibrium energy level whilst increasing  $B$  helps to provide energy to promote  $\alpha$  orientated spins to  $\beta$  orientated spins. The main advantage of Brute-Force is the simplicity of the method; there is no requirement to chemically alter the target compound, thus HP acquisition is quicker as it relies solely on Boltzmann-law polarisation rather than secondary chemistry or physics. A further advantage is the unnecessary for free radicals, microwave excitation or co-solvents that are essential in DNP.<sup>28, 29</sup> It is worth noting that detection is carried out at a much lower magnetic field, commonly below 40 mT.<sup>30</sup>

### 1.3.2. Dynamic Nuclear Polarisation (DNP)

Expanding hyperpolarisation in its most simple form is the promising technique, DNP.<sup>29</sup> Moving away from harnessing the power of low temperatures and high magnetic fields, DNP provides hyperpolarisation through the application of microwave excitation to electron spins.<sup>31</sup> Polarisation is transferred to neighbouring nuclei contained in a glass-

forming matrix at cryogenic temperatures ( $100\text{ K} \geq$ ).<sup>32, 33</sup> In comparison to Brute-force, the increase in temperature offered by DNP is an advantage in terms of experimental difficulty, while impressive signal enhancements (80-fold  $<$ ) have provided momentum to the method, probing the development of an ever increasing range of systems.<sup>33</sup> Interestingly, lower enhancements can reduce experiment times massively as the amount of time required for signal averaging is inversely proportional to the square of the enhancement.<sup>34</sup> With this being said DNP does come with its fair share of limitations. Firstly, when  $T_1$  (relaxation time) times are short, the detection of nuclei becomes difficult or impossible. This causes identification of unknown compounds to be challenging requiring the need for extra analysis by conventional NMR spectroscopy. Secondly, the pre-condition of radical insertion to the sample (electron source) is often an un-desirable action to scientists, especially after time consuming isolation and purification methods have been used to isolate and/or purify a product.<sup>35</sup> The application of DNP to  $^{13}\text{C}$  can increase sensitivity by many orders of magnitude, thus, providing a solution to the low gyromagnetic ratio of  $^{13}\text{C}$  in regard to NMR, making it applicable to MRI.<sup>36</sup>

### **1.3.3. Spin-Exchange Optical Pumping (SEOP)**

The development of SEOP has advanced the resolution of MRI by providing a niche pathway for the HP of  $^3\text{He}$  and  $^{129}\text{Xe}$ .<sup>37</sup> It works by utilising circularly polarised light to excite alkali-metal atoms, which in turn collide with a larger quantity of noble-gas atoms ( $^3\text{He}$  and  $^{129}\text{Xe}$ ). The excitation transfers close to 50% of the spin angular momentum to the alkali-metal atoms, causing subsequent collisions with noble-gas atoms to transfer some of the electron-spin polarization to noble-gas nuclei.<sup>38</sup> Primarily, hyperpolarised



noble gasses such as helium and xenon offer an improvement to current methods of determining the health and condition of lung space. Inhaled hyperpolarised noble gasses, used as 'imaging agents', offer clearer, more resolute images as a result. The technique isn't massively time consuming (producing 0.3 L of 64% polarised  $^{129}\text{Xe}$  per hour) but isn't remarkably fast at the same time.<sup>39</sup> Compared to DNP, SEOP is generally favoured as a producer of MRI agents because of its focus on gasses, despite its limitation to noble gasses. However, in terms of speed, *Para*-Hydrogen Induced Polarisation (PHIP) techniques perform better and can achieve enhancements far greater than what has been seen with Brute-force, DNP and SEOP.

#### 1.3.4. *Para*-Hydrogen Induced Polarisation (PHIP)

A very effective approach to altering the Boltzmann distribution is PHIP. This technique provides polarisation through the use of a spin isomer of hydrogen, *para*-Hydrogen (*p*-H<sub>2</sub>). *p*-H<sub>2</sub> contains a pair of protons that form a singlet spin state which has no magnetic moment and thus does not give rise to a signal when probed *via* NMR.<sup>30</sup> Following a prediction in 1986 that PHIP could be used to increase NMR signal intensities, Bowers and Weitekamp successfully proved the concept by achieving enhancement factors between 100 and 200 on several samples.<sup>40</sup> PHIP itself has three different approaches; PASADENA, ALTADENA and SABRE.<sup>30, 41, 42</sup> Whereas DNP and SEOP are generally considered for use in MRI, PHIP methods are more suited towards chemical analysis, characterisation, and to provide insight into the species involved in reaction mechanisms.<sup>43</sup>

### 1.3.5. PASADENA (Para-hydrogen and synthesis allow dramatic enhanced nuclear alignment)

*p*-H<sub>2</sub> hydrogenates an unsaturated substrate in a high magnetic field with the *p*-H<sub>2</sub> nuclei consequently taking up magnetically inequivalent sites in said substrate, before polarisation is detected using radio-frequency pulses. Polarisation is relayed dominantly through the resulting (dynamic) dipolar coupling network.<sup>44</sup> This method is mostly used to study homogeneously catalysed hydrogenation reactions, not just for the detection of low concentration intermediates, but also to evaluate reaction mechanism and the kinetics involved. Characterised by its use of both high and low-field magnets, PASADENA is often employed over alternative PHIP methods due to its ease and reproducibility of handling, spectra quality and potential applications for *in situ* studies.<sup>45</sup> Despite its reputation among scientists as one of the most effective hyperpolarisation methods, it is however intrusive. The substrate is chemically different following the addition of *p*-H<sub>2</sub>, therefore reducing its applicability in work such as drug detection, characterisation and discovery.

### 1.3.6. ALTADENA (Adiabatic longitudinal transport after dissociation engenders net alignment)

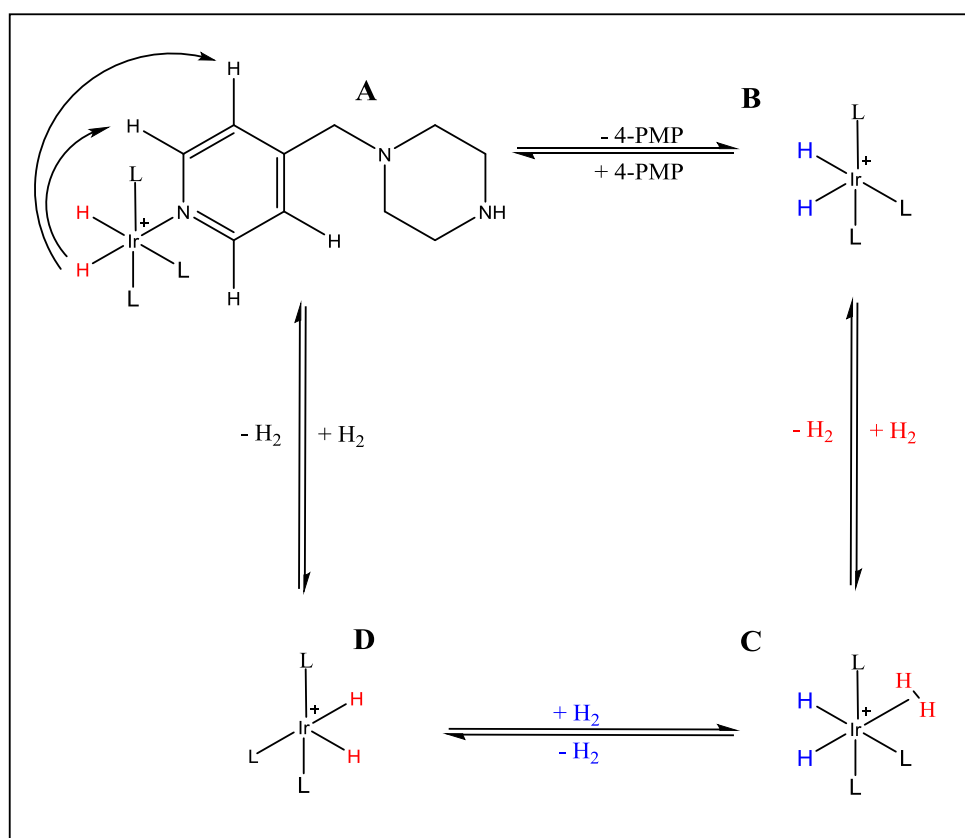
The sibling of PASADENA, ALTADENA offers a slightly different approach towards PHIP. The requirement of an unsaturated substrate remains, as hydrogenation with *p*-H<sub>2</sub> of a double/triple bond is fundamental. As it states in the name, ALTADENA conditions involve adiabatic transfer.<sup>44, 46</sup> Instead of polarisation taking place at high-field prior to detection at low-field, ALTADENA does the exact opposite and adopts a concept known as 'isotropic mixing'. Samples are polarised in the stray field of the NMR magnet before

detection in the high-field magnet. Precession frequencies of individual protons are much more similar in the stray field as opposed to the high-field. Since isotropic mixing defines the transfer of PHIP-derived polarisation between protons as an exchange of energy between nuclear spins having different temperatures, conducting these experiments in the stray field is accordingly more efficient. The difference in efficiency is evident when spectra attained from both PASADENA and ALTADENA methods are compared. Enhancements could be somewhat increased if polarisation could be solely directed to protons, excluding heteronuclei. It can be said that high *para*-hydrogenation rates significantly increase transfer of PHIP to heteronuclei in both cases of PASADENA and ALTADENA.<sup>44</sup>

#### 1.3.7. SABRE (Signal amplification by reversible exchange)

The more recent development of a non-intrusive PHIP technique has gained massive popularity in the polarisation community. Signal Amplification by Reversible Exchange transfers polarisation from *p*-H<sub>2</sub> derived hydride ligands bound to a SABRE catalyst, to the protons of the hyperpolarisable substrate *via* the establishment of a J-coupling (scalar) network.<sup>42</sup> A simple catalytic cycle for the process can be seen in Scheme 1 and in a review by Mewis.<sup>42</sup> SABRE first appeared in the literature in 2009, when Duckett *et al.* indicated that PHIP was possible without hydrogenating an analyte.<sup>47</sup> This offered a new alternative to conventional PHIP. There was now a method which hyperpolarised an analyte without chemically altering it. This in turn opened up a whole host of potential hyperpolarisable analytes, as the pre-requisite for a double/triple bond to necessitate hyperpolarisation transfer was no more. Though the process does require a carefully constructed metal-centred catalyst (normally Ir), experimental times can be

made strikingly short (~seconds) as catalyst activation can occur at ambient temperatures (catalyst decomposes upon heating) without the need of sophisticated equipment (as demonstrated in this work).<sup>48</sup> There has been extensive development of SABRE catalysts in order to achieve the optimum ligand exchange rates. The exchange rates of substrate and hydrogen to and from the catalyst need to complement each other (in order for catalytic cycle to be maintained) to achieve optimal hyperpolarisation.<sup>42</sup> Early work suggested phosphine ligands facilitated maximum hyperpolarisation, however upon analysis of different nitrogen *N*-heterocyclic carbenes (NHC), IMes (1,3-bis(2,4,6-trimethylphenyl)imidazole-2-ylidene) proved to be the most effective.<sup>49</sup>



Scheme 1: Catalytic cycle for SABRE.<sup>42</sup>

## 2. Experimental Methodologies

### 2.1. Reagents

1-(4-pyridylmethyl)piperazine hydrochloride (4-PMP.3HCl) was prepared by treating a solution of 1-(4-pyridylmethyl)piperazine (0.5 g, 2.82 mmol) in diethyl ether (10 mL) with 4M hydrogen chloride in dioxane (5.6 mL, 11.2 mmol, 4 eq.). The crude product was purified by recrystallisation from acetone to give the target compound as a beige powder (0.81 g, 100%). The compound was fully characterised by NMR, IR and MS before use. 2, 3 and 4-PMP freebase were purchased from Fluorochem Ltd. (Hadfield, UK) and were used without further purification.<sup>50</sup> BZP.2HCl was purchased from Sigma-Aldrich. Solvents (Sigma-Aldrich, Gillingham, UK and Fisher Scientific, Loughborough, UK) were used as received. A tablet of 4-PMP.3HCl (circa. 100 mg) was prepared using an adaptation of the procedure reported by Hamad *et al.*<sup>51</sup> 1-(cyclohexylmethyl)-1*H*-indole-3-carboxylic acid 8-quinolinyl ester (BB-22) was obtained from BRC Fine Chemicals (London, UK; <https://www.brc-finechemicals.com>) and used without further purification. The compound was fully characterised by NMR, IR and MS before use (see Appendix).

### 2.2. Instrumentation

High field <sup>1</sup>H NMR and <sup>13</sup>C NMR (10 mg of compound to be analysed/600 µL in CDOD<sub>3</sub>) spectra were acquired on a JEOL AS-400 (JEOL, Tokyo, Japan) NMR spectrometer operating at a <sup>1</sup>H resonance frequency of 400 MHz and referenced to the residual solvent peak ( $\delta = 3.33$ ). Low field <sup>1</sup>H NMR spectra were acquired on an Oxford Instruments bench-top Pulsar<sup>®</sup> NMR spectrometer operating at a <sup>1</sup>H resonance frequency of 60 MHz and referenced to the residual solvent peak ( $\delta = 3.33$ ). GC-MS

analysis was performed using an Agilent 6850 GC and a MS5973 mass selective detector (Agilent Technologies, Wokingham, UK). The mass spectrometer was operated in the electron ionisation mode at 70 eV. Separation was achieved with a capillary column (HP5 MS, 30 m  $\times$  0.25 mm i.d. 0.25  $\mu$ m) with helium as the carrier gas at a constant flow rate of 1.0 mL min<sup>-1</sup>. The oven temperature programme started at 60 °C, increased at 15 °C/min and was held at 300 °C for 3 minutes, unless stated otherwise. A 1- $\mu$ L aliquot of the samples (qualitative analysis, calibration standards and test solutions) were injected (manually) with a split ratio of 20:1. The injector and the GC interface temperatures were both maintained at 280°C and 300°C respectively. The MS source and quadrupole temperatures were set at 230°C and 150°C, respectively. Mass spectra were obtained in full scan mode (50 – 550 amu). Calibration standards were made up as shown in table 1. Each calibration standard was injected six times.

### 2.3. Generic Hyperpolarisation Sample Preparation and Method

Five equivalents (eq) of substrate (relative to the catalyst), 2 mg [Ir(IMes)(COD)Cl] (catalyst) dissolved in 0.6 mL d<sub>4</sub>-methanol was added to a Young's capped NMR tube. \*  
<sup>1</sup>The sample was de-gassed three times using a freeze-thaw method that involved submerging the tube in an acetone/dry-ice slush bath and then removing the headspace using a Schlenk-line. The thermal (Boltzmann) one-scan spectrum was acquired using a low-field 60 MHz Oxford Instruments Pulsar® bench-top NMR spectrometer. *Parahydrogen* was introduced to the NMR tube at a pressure of 3.0 bar. The NMR tube

---

\* Some samples also had Triethylamine (TEA) added to them either at the start, or sequentially throughout an experiment.

was shaken vigorously in the vertical plane (in Earth's magnetic field (0.5 G)) for ten seconds, prior to being immediately transferred to the spectrometer to acquire the  $^1\text{H}$  NMR spectrum. The NMR tube was shaken and analysed three times for each addition of *parahydrogen* to the Young's capped NMR tube. Details of the quantities used in each study are listed in Table 1.

Table 1 - Quantities used in the SABRE studies throughout this project.

Study Number	Compound	Quantity of Compound	Catalyst (mg)	D <sub>4</sub> -Methanol (mL)	TEA (eq)	<i>p</i> -H <sub>2</sub> Pressure (bar)
1	4-PMP (f)	2.76 $\mu\text{L}$	2	0.6	0	3.0
2	4-PMP.3HCl	4.44 mg	2	0.6	1.2	3.0
3	BZP.2HCl	3.87 mg	2	0.6	1.2	3.0
4	4-PMP (f)	2.76 $\mu\text{L}$	2	0.6	1.2	3.0
5	4-PMP (f)	2.76 $\mu\text{L}$	2	0.6	5.0	3.0
6	4-PMP (f)	2.76 $\mu\text{L}$	2	0.6	10.0	3.0
7	4-PMP (f)	2.76 $\mu\text{L}$	2	0.6	0.4 – 2.0	3.0
8	4-PMP.3HCl	4.44 mg	2	0.6	1.2	3.0
9	4-PMP.3HCl	4.44 mg	2	0.6	1.2	3.0
10	4-PMP.3HCl	4.44 mg	2	0.6	0 – 10.0	3.0
11	4-PMP (f)	2.76 $\mu\text{L}$	2	0.6	0 – 7.0	3.0
12	4-PMP.3HCl Tablet	2.00 mg	1	0.6	3.0	3.0
13	BB-22	5.00 mg	2mg	0.6	0	3.0

### 2.3.1. Adaptations to the Generic Hyperpolarisation Method

For the experiments in which TEA was added, the generic hyperpolarisation method was adapted. For the sequential addition of TEA to one sample, the sample was considered a new sample after each addition, and so the experimental method is then re-followed

from the point of de-gassing. It should also be noted that from study 10 onwards a new order of addition was followed that saw the reactants added in the following order: substrate, TEA, catalyst and solvent.

Experiments 2 – 6, 8: TEA added to the other reagents at the start. Generic hyperpolarisation method followed.

Experiment 7: 0.4 eq TEA added after each purge with parahydrogen. Generic hyperpolarisation method then followed from de-gassing.

Experiment 9: TEA added directly to substrate before addition of catalyst and solvent. Generic hyperpolarisation method then followed.

Experiment 10: TEA added directly to substrate (0, 1, 2, 3, 4, 5, 10 eq of TEA) before addition of catalyst. A different sample was used each time due to the requirement that TEA is added prior to solvent and catalyst.

Experiment 11: TEA added directly to substrate (0, 1, 2, 7 eq of TEA) before addition of catalyst. A different sample was used each time due to the requirement that TEA is added prior to solvent and catalyst.

Experiment 12: 30 mg of the tablet (6 mg active pharmaceutical ingredient) (API) was added to 900  $\mu\text{L}$   $d_4$ -methanol before being filtered through a syringe filter. 300  $\mu\text{L}$  of the resulting filtered solution (which contains only the API) was added to a vial prior to the addition of 3 eq TEA, 150  $\mu\text{L}$  catalyst stock ( $6.66 \text{ mg mL}^{-1}$ ) and 147  $\mu\text{L}$   $d_4$ -methanol. The generic hyperpolarisation method then followed the de-gassing step.



Experiment 13: 1-(cyclohexylmethyl)-1*H*-indole-3-carboxylic acid 8-quinolinyl ester (BB-22). 100 eq Acetonitrile added in at the start. Generic hyperpolarisation method followed.

## 2.4. Analysis 4-PMP.3HCl Tablet by GCMS

### 2.4.1. Calibration Standards

An eicosane stock solution ( $50 \mu\text{g mL}^{-1}$ ) was made by dissolving 5 mg eicosane in 50 mL methanol before performing a 1 in 2 dilution. The 4-PMP.3HCl stock solution ( $50 \mu\text{g mL}^{-1}$  eicosane,  $200 \mu\text{g mL}^{-1}$  4-PMP.3HCl) was made by dissolving 10 mg of the analyte in 50 mL of the ( $50 \mu\text{g mL}^{-1}$ ) eicosane stock solution, to ensure the eicosane was at constant concentration. Aliquots of these two stock solutions were then mixed to give calibration standards containing 25, 50, 75, 100, 125  $\mu\text{g mL}^{-1}$  of the analyte and  $50 \mu\text{g mL}^{-1}$  eicosane.

Table 2 - Information regarding the make-up of the calibration standards for GCMS.

Calibration Standard ( $\mu\text{g mL}^{-1}$ )	[Eicosane] ( $\mu\text{g mL}^{-1}$ )	4-PMP.3HCl Stock ( $\mu\text{L}$ )	Eicosane Stock ( $\mu\text{L}$ )
50	50	200	600
75	50	250	417
100	50	500	500
125	50	500	300
150	50	600	200

#### 2.4.2. Test Solution (Quantitative GC-MS Analysis)

The tablet (502.2 mg) containing 100 mg active pharmaceutical ingredient (API), 4-PMP.3HCl, was made in house *via* the use of KBr disk equipment. A test solution (100  $\mu\text{g mL}^{-1}$ ) was made up by dissolving 5 mg of the tablet in 10 mL of an eicosane internal standard stock methanol solution (50  $\mu\text{g mL}^{-1}$ ). The test samples were injected six times.

#### 2.4.3. Test Solution (Qualitative GC-MS Analysis)

The tablet was weighed accurately prior to being homogenised *via* pestle and mortar. Testing solutions of each compound were made to the concentration 1  $\text{mg mL}^{-1}$  (all samples spiked with eicosane, tablet testing solution 1  $\text{mg mL}^{-1}$  API). The test samples were injected in duplicate.

#### 2.4.4. GC-MS Method Validation

The GC-MS method was validated in accordance with The International Council for Harmonisation of Technical Requirements for Pharmaceuticals for Human Use (ICH) guidelines using the following parameters: linearity, accuracy, precision, limit of detection (LOD) and limit of quantification (LOQ).<sup>12</sup> Linearity, precision: six replicate injections of the calibration standards were performed and the data analysed under the same conditions. The %RSD was calculated for each replicate test sample. Accuracy (percentage recovery study): determined from spiked samples prepared in triplicate at three levels over a range of 80-120 % of the target concentration (100  $\mu\text{g mL}^{-1}$ ). The percentage recovery and %RSD were calculated for each of the replicate samples. Limits of detection and quantification: six replicate injections of the calibration standards were

performed and the data analysed under the same conditions. The limits of detection and quantification were calculated based on the standard deviation of the response and the slope.<sup>52</sup>

## 2.5. Standard Addition (SA) and Internal Standard (IS) Calibration

### 2.5.1. Preparation from Stock Solutions

For the SA two stock solutions were made up of known concentrations, one acting as the known and the other as the unknown. The two stocks were mixed so that the overall volume of each NMR tube was maintained at 600  $\mu\text{L}$ , whilst the analyte concentration of the tubes increased. Table 3 details how this was completed.

Table 3 - Information detailing the make-up of the SA calibration solutions.

Tube Number	Stock A (Unknown) ( $\mu\text{L}$ )	Stock B (Known) ( $\mu\text{L}$ )	D <sub>4</sub> -Methanol ( $\mu\text{L}$ )	Final 4-PMP concentration ( $\mu\text{L mL}^{-1}$ )
0	100	0	500	0.460
1	100	100	400	1.293
2	100	200	300	2.126
3	100	300	200	2.960
4	100	400	100	3.793

For IS, 5.52  $\mu\text{L}$  4-PMP was dissolved in 2 mL d<sub>4</sub>-methanol to give a stock solution (C) of concentration 2.76  $\mu\text{L mL}^{-1}$ . 1  $\mu\text{L}$  Tetramethylsilane (TMS) was added to 0.5 mL d<sub>4</sub>-methanol to give a TMS stock solution (D) of concentration 2  $\mu\text{L mL}^{-1}$ . The TMS

concentration was maintained at  $0.33 \mu\text{L mL}^{-1}$  per calibration standard. Each tube was made up to  $600 \mu\text{L}$  with  $\text{d}_4$ -methanol. Table 4 details this.

Table 4 - Information detailing the work up of IS calibrations standards.

Tube Number	Stock C ( $\mu\text{L}$ )	Stock D ( $\mu\text{L}$ )	$\text{D}_4$ -Methanol ( $\mu\text{L}$ )	Final 4-PMP concentration ( $\mu\text{L mL}^{-1}$ )
0	100	100	400	0.460
1	200	100	300	0.920
2	300	100	200	1.380
3	400	100	100	1.840
4	500	100	0	2.300

### 3. Hyperpolarisation of PMP Compounds

#### 3.1. Characterisation and Resolution *via* Bench-top NMR (BT-NMR)

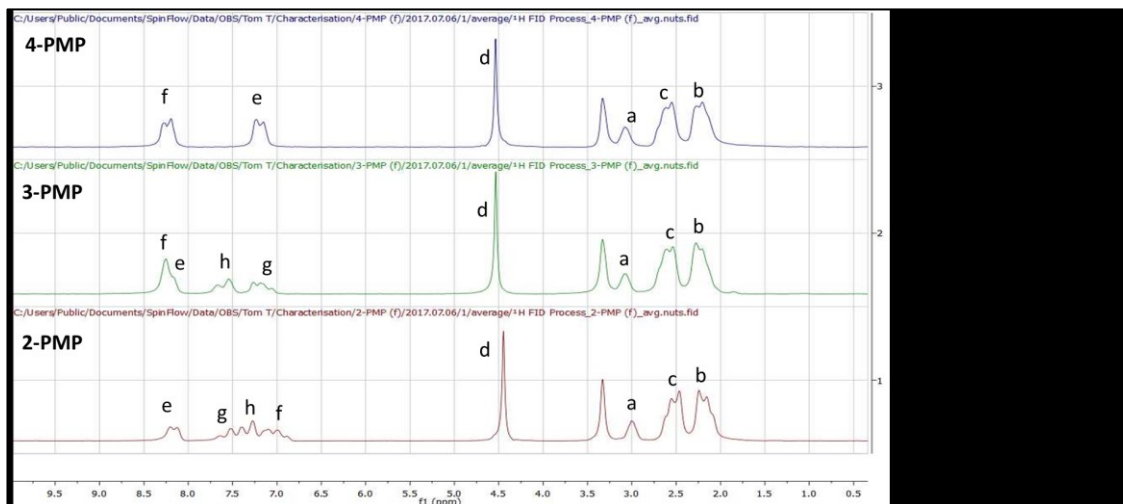


Figure 1: Low-field  $^1\text{H}$  NMR spectra for 2, 3 and 4-PMP (freebase).

Individually the PMP isomers are easily characterised using  $^1\text{H}$  BT-NMR, high-field NMR and GC-MS (see Appendix). Each signal is resolved to the baseline and can be assigned to its corresponding hydrogen environment (NMR). On the contrary, compared to high-field  $^1\text{H}$  NMR, the resolution suffers slightly with signals appearing broader and less sharp. However, bench-top NMR's ease of use, time efficient procedures and portability mean that these drawbacks are easily mitigated.  $^1\text{H}$  NMR spectra were collected for all three isomers. All three have an identical aliphatic region and this is because the backbone of the compound (methyl piperazine) remains the same (Figure 1). However, the change in the position of the pyridyl group does cause some changes to the resonances observed in the aromatic region. Figure 1, which depicts the  $^1\text{H}$  NMR spectra for 2, 3 and 4-PMP (freebase) with all peaks assigned, shows these changes in resonance very clearly. Looking at 4-PMP, two doublets are observed at  $\delta$  8.25 and  $\delta$  7.25 which

correspond to the *ortho*- and *meta*-H nuclei respectively. Comparing this spectrum to 3-PMP it is noticeable that there are now three signals present. This is a result of an increase in the number of  $^1\text{H}$  NMR environments present. The position of the pyridyl's nitrogen causes the symmetry of the  $^1\text{H}$  NMR environments to be broken, causing two  $^1\text{H}$  environments to become four. Similarly, in the  $^1\text{H}$  NMR spectrum of 2-PMP, there are now four individual environments leading to four individual resonances. This leads to the creation of what appears to be a multiplet at  $\delta$  7.25. The cause of this is simply down to the fact that a low-field 60 MHz BT-NMR was used. A weaker magnet naturally produces spectra that aren't as resolved compared with high-field NMR instruments. However, the resonances were able to be assigned when the low-field spectrum was compared to a high-field spectrum. The problem arises when analysing a mixture of all three isomers *via* BT-NMR. Due to the characteristic resonances of all three isomers occurring between  $\delta$  6.8 and  $\delta$  8.5, it is impossible to differentiate between the three. The point here is that in the case of a street sample containing all three isomers, although this is highly unlikely, separating the three and characterising them would not be possible by using a standard  $^1\text{H}$  BT-NMR method.<sup>11</sup> It would require the need for a more in-depth method to be employed, such as a  $^1\text{H}$ - $^1\text{H}$  COSY or GC-MS. The results of a GC-MS study to separate the three isomers is detailed in chapter 6.

### 3.2. Hyperpolarisation of 4-PMP (freebase)

The literature shows that SABRE hyperpolarisation is for the most part performed on nitrogen containing compounds.<sup>53-56</sup> A very small part of the literature reports hyperpolarisation of nitrogen containing drug compounds.<sup>57, 58</sup> Thus, PMP is of interest because of its potential ability to hyperpolarise well, but also because of its potential

future prevalence. To set a benchmark for the hyperpolarisation of the PMP family, 4-PMP (freebase) was the first compound to undergo hyperpolarisation. With its moiety to bind to the catalyst being through the nitrogen situated in the four position of its pyridyl functionality, enhancement ( $\epsilon$ ) levels (enhancements were measured by normalising the integration of a characteristic hyperpolarised NMR signal, to its un-hyperpolarised counter-part) were expected to be relatively high ( $\epsilon \approx 200$ ). This was a prediction based on literature involving the hyperpolarisation of pyridine, taking into account non-optimal experimental conditions, which has been reported to show enhancements well over the 5000 – fold mark.<sup>49</sup> Sterically speaking, the pyridyl nitrogen of 4-PMP (freebase) is not directly hindered, just like pyridine, and therefore should allow for most if not all the magnetization to be propagated from the *parahydrogen* derived hydride ligands through to the pyridyl protons. The piperazine nitrogen is ruled out as a potential ligation centre due to its protonation. It should be noted that polarisation *via* SABRE is not limited to protons; it has been reported that it can also be transferred to <sup>13</sup>C and <sup>15</sup>N.<sup>59</sup> It is understood that the polarisation transfer through the nitrogen is allowed due to the existence of a free orbital on the atom, which reaches out into space close to the protons without posing a steric barrier for the temporary addition to the catalyst. This, and the fact that  $J_{HH}$ -couplings are realistically limited to 5 bonds, explains why only the pyridyl protons become hyperpolarised.<sup>60</sup> Excess substrate (5 equivalents relative to the catalyst) was required in these studies in order to prevent side reactions (such as competition between solvent and substrate for the catalyst) during the activation of the catalyst. Failure to activate the catalyst effectively in the presence of sufficient substrate can lead to irreversible deactivation consistent with oligomerization of the catalyst molecules.<sup>61</sup> A catalytic cycle for the SABRE process can be seen in Scheme 1. A 313-fold <sup>1</sup>H NMR enhancement (Figure 2) was observed which

set a good benchmark for what could be expected from the PMP family. To contextualise this, 4-PMP freebase was hyperpolarised at low-field 0.5 G with 50% *para*-hydrogen, whereas Chekmenev. *et al.* achieved  $\epsilon \approx 2,900$  for pyridine at 9.4 T, using at least 65% *para*-hydrogen.<sup>62</sup> Considering 15% less *para*-hydrogen was used in tandem with a lower magnetic field (65 G has been shown to be optimal), where Boltzmann polarisation alone is one magnitude lower compared to at 9.4T,  $\epsilon \approx 300$  is an impressive result.<sup>63</sup> At first glance, it is clear to see the extent of the hyperpolarisation. Four hyperpolarised signals (2 emission; pointing down, and 2 absorption; pointing up) at  $\delta$  8.2,  $\delta$  8.0,  $\delta$  7.25 and  $\delta$  6.75 are the direct result of a J-coupling (scalar) network established between the *para*-hydrogen derived hydride ligands of  $[\text{Ir}(\text{IMes})(4\text{-PMP})_3(\text{H})_2]^+$  and 4-PMP's pyridyl group.<sup>42</sup> The signals observed at  $\delta$  8.2 and  $\delta$  8.0 correspond to the *ortho*-hydrogen environment of both the dissociated (free) substrate and the bound substrate respectively. Because 4-PMP is hyperpolarised whilst bound to the catalyst, and since exchange of the substrate on and off the catalyst continues when the sample is analysed, the resulting NMR spectrum shows hyperpolarised signals of both dissociated and bound substrate. This information can give insight into the dissociative nature of the substrate in relation to the catalyst.<sup>48, 64</sup>



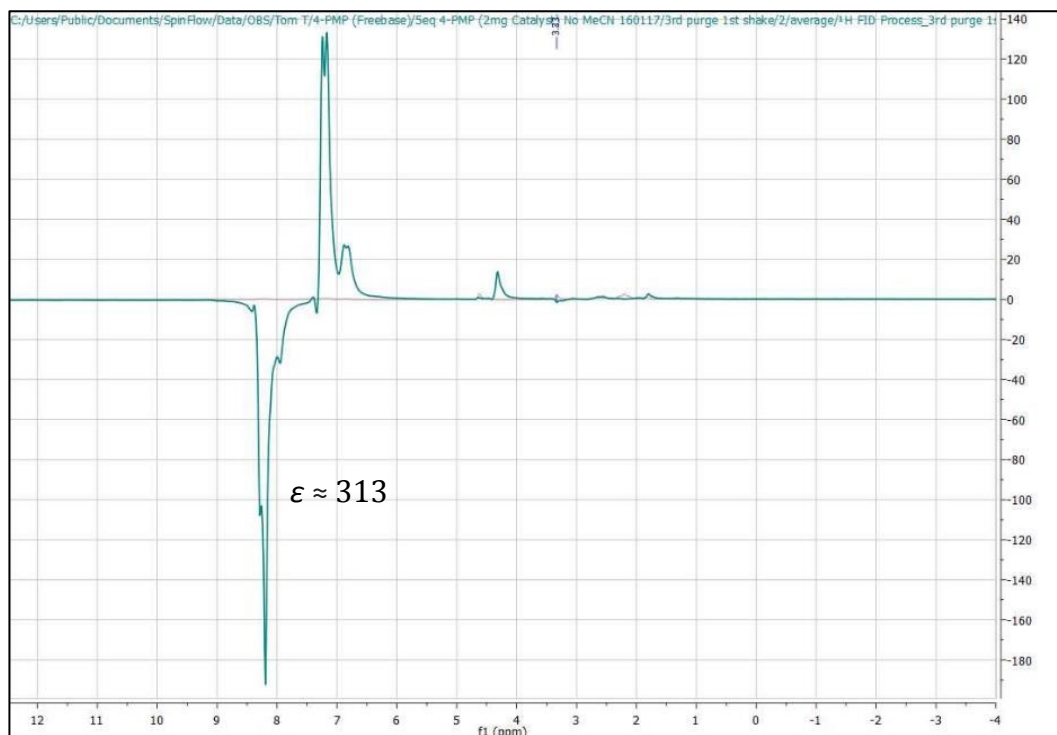


Figure 2: Hyperpolarised  $^1\text{H}$  NMR spectrum of 4-PMP (freebase).

### 3.3. Freebasing 4-PMP.3HCl *in-situ*

Being able to freebase a hydrochloride salt *in-situ* is vital in applying SABRE to drug analysis. It is very common for street drugs such as cocaine and ecstasy pills to have an API present in its hydrochloride salt. This is because it is very common for a nitrogen to become protonated and have a negatively charged counter ion. In order to hyperpolarise 4-PMP.3HCl, it was imperative that the salt was removed, as this would free up the pyridyl nitrogen to ligate to the SABRE catalyst. Attempting to hyperpolarise 4-PMP.3HCl on its own resulted in no enhancement, as expected, as it has no ligation centre. In removing the HCl, the pyridyl's nitrogen atom is freed up allowing for potential coordination to the catalyst during SABRE. The method adopted to freebase 4-PMP.3HCl (Scheme 2) utilises simple acid and base chemistry instead of freebasing *via* separation, which not only takes longer, but also cannot be done *in-situ*. The decision was made to



freebased to some extent, proving *in-situ* freebasing works. If the freebasing had been unsuccessful entirely there would be no observable hyperpolarisation. Assessing the hyperpolarisation gives an indication as to what degree the freebasing method worked. The *ortho*-hydrogen signal ( $\delta$  8.2) was chosen to calculate the enhancement, just like with 4-PMP (freebase). The result was  $\epsilon \approx 7.66$  which is magnitudes lower when compared to the 300-fold enhancement that resulted from 4-PMP (freebase). It has been recognised, and acknowledged, that the reproducibility of SABRE when manually shaking the sample in the 'stray field' of the magnet is no better than 20% at best.<sup>56</sup> However, this enhancement falls outside the expected range of variance. This is evidence of some kind of unwanted reaction between the base and the catalyst, or the HCl salt has not been completely stripped from the compound.

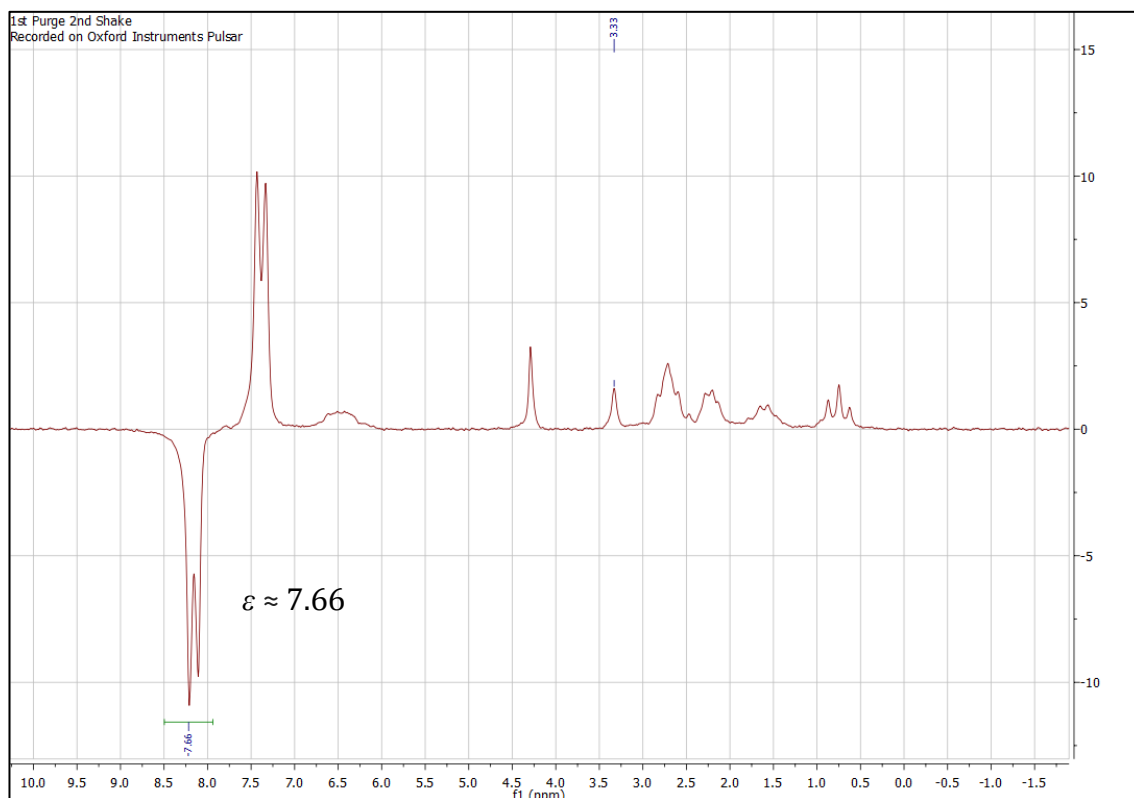


Figure 3: Hyperpolarised  $^1\text{H}$  NMR spectrum of 4-PMP.3HCl after the addition of 1.2eq triethylamine.

### 3.5. Does Triethylamine 'Poison' the Catalyst?

The first investigation focused on the interaction of TEA with the catalyst. After seeing lower enhancements than were expected, it seemed plausible that TEA could in some way prevent the catalyst from activating. Since 4-PMP (freebase) hyperpolarised well, adding TEA to a solution containing 4-PMP (freebase) and measuring the resulting hyperpolarisation made logical sense in determining the chemical role of TEA. Figure 4 shows that the signal enhancement for 4-PMP decreased by more than half from 313-fold to 142-fold, suggesting the base has a negative impact on the reaction. Evidently, there is still a good level of hyperpolarisation despite triethylamine playing some role in reducing it. This investigation showed that TEA does not block the catalyst from activating, it simply decreases the amount of hyperpolarised substrate allowed to build up.

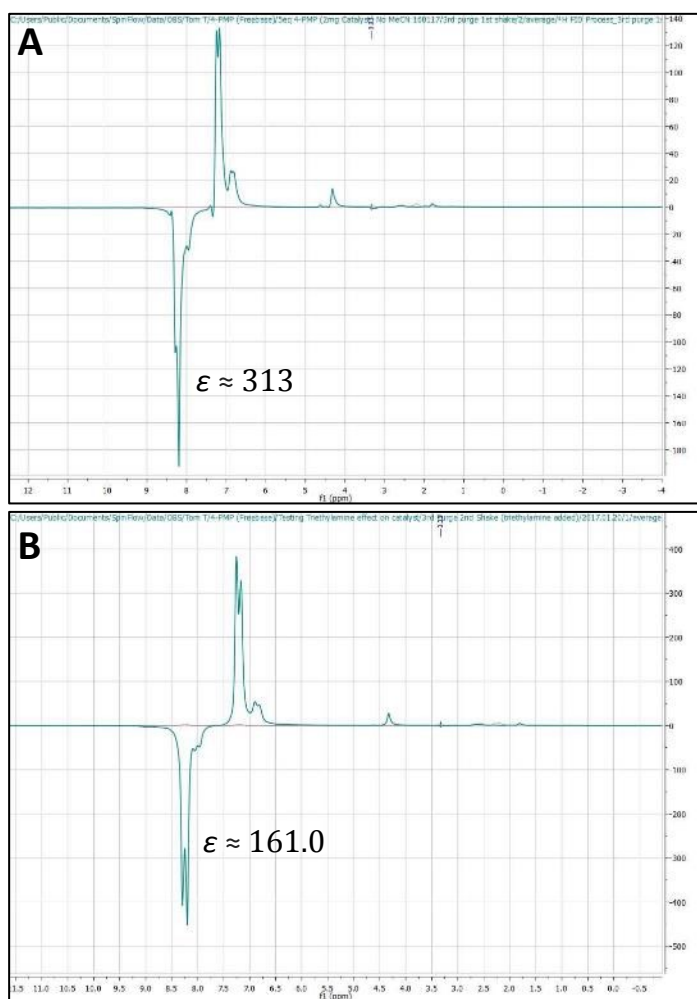


Figure 4: Hyperpolarised  $^1\text{H}$  NMR Spectra of 4-PMP (freebase): A) No Triethylamine added, B) 1.2 eq Triethylamine added.

### 3.6. Effect of Excess Triethylamine on Hyperpolarisation

An experiment was conducted to investigate how excess TEA effects hyperpolarisation. 5 eq of TEA was added, compared to 1.2 eq used in earlier experiments, to see if hyperpolarisation is prevented entirely at higher concentrations. In this instance, a sample of 4-PMP (freebase) was made up and hyperpolarised with one purge of *para*-hydrogen to achieve a 'baseline' for signal enhancement. Only after this was TEA introduced to the sample. This was done so that it was clear to see the effect TEA had on enhancement levels. The  $^1\text{H}$  NMR spectra for the sample containing 5 eq of TEA are shown in Figure 5. (A) is the thermal proton background taken prior to SABRE. It is

notable that there is no TEA present due to the lack of a signal (triplet) at  $\delta$  0.9. Catalyst activation can be confirmed in (B) due to the signal enhancements and the presence of hydride signals at  $\delta$  -12.5 and  $\delta$  -17.5. Furthermore, spectra C – G show small signals at  $\delta$  -23 which are further indication of a healthy catalyst.<sup>61</sup> The pinnacle of hyperpolarisation is observed in (C) ( $\epsilon \approx 23.18$ ) before it decreases in (D) ( $\epsilon \approx 8.6$ ), due to the majority of *para*-hydrogen becoming 'spent' and converting back into *ortho*-hydrogen. It is at this point the headspace of the NMR tube is removed making way for a fresh purge of *para*-hydrogen. 5 eq of TEA was added before the addition of more *para*-hydrogen and the collection of spectrum (E). Signal enhancement continues to decrease in (E) ( $\epsilon \approx 4.73$ ) before ceasing completely in (F). This comes immediately after the addition of TEA. Thus, increasing the concentration of TEA in the sample so that it is in excess causes hyperpolarisation to stop completely.

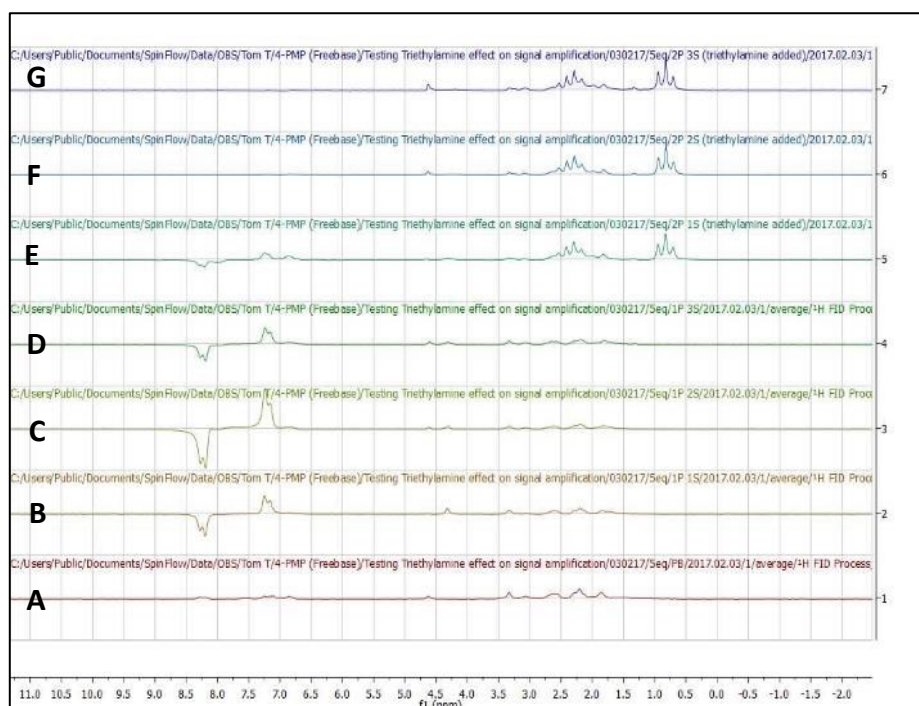


Figure 5:  $^1\text{H}$  NMR SABRE spectra for addition of 5eq TEA to 4-PMP (freebase). (A) is the thermal spectrum, (B) was taken after the first *para*-hydrogen purge, (C) and (D) are the result of the 2nd and 3rd tube shake from the 1st purge. (E), (F) and (G) correspond to the 1<sup>st</sup>, 2<sup>nd</sup> and 3<sup>rd</sup> tube shake after the introduction of the 2<sup>nd</sup> *para*-hydrogen purge.

### 3.7. The Sequential Addition of Triethylamine

Understanding that hyperpolarisation is suppressed at 5 eq (vast excess), a study working upwards from 0.4 eq was conducted on 4-PMP (freebase) to examine how hyperpolarisation changes at different concentrations. Incrementally increasing the concentration of TEA and recording the resulting hyperpolarisation essentially allows the bigger picture to be observed. Since 0.4 eq (0.434  $\mu\text{L}$ ) is such a small amount, and bearing in mind TEA is volatile, it was vital to check the NMR spectra to confirm its addition had taken place. Figure 6 shows this distinctly. The resonance (triplet) at  $\delta$  0.9, which is caused by TEA, increases in size after each addition. Thus, it is possible to confirm to a high degree of certainty that TEA was successfully added. In terms of hyperpolarisation, the signal enhancements calculated at each concentration of TEA are shown graphically in Figure 7. Overall, there is a slight positive correlation which shows

that TEA does aid hyperpolarisation. When focus is turned to equivalence (0 and 2 specifically), signal enhancement doubles from a 20-fold enhancement to a 43-fold enhancement. On the contrary, there is a lot of variance in-between these results, especially in regard to the signal enhancement calculated at 0.8 eq TEA. This result stands out as an anomaly more than any other data point for the simple reason that upon its removal, there would be a constant steady increase in signal enhancement as TEA concentration increases. Furthermore, the large amount of variance cannot be ignored or overlooked. Even when removing this anomaly there is still too much variance. Although the  $R^2$  value would rise to 0.8388 from 0.6205, which is an improvement in linearity, there is too much variance to make meaningful conclusions. This experiment was deemed inconclusive, thus necessitating further investigations.

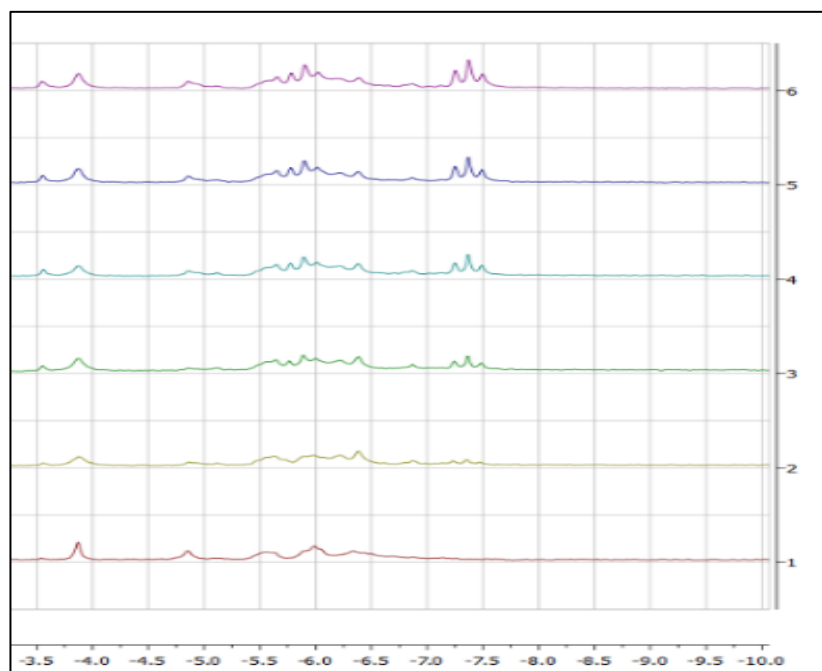


Figure 6: Stacked  $^1\text{H}$  NMR spectra for the sequential addition of triethylamine to 4-PMP freebase.



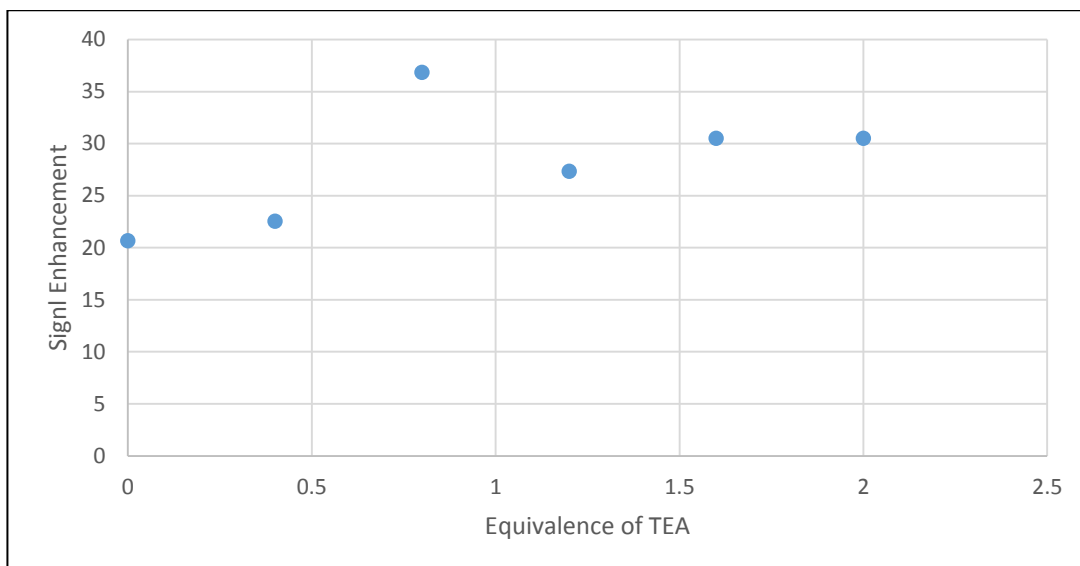


Figure 7: Graph showing how increasing amounts of TEA effect the hyperpolarisation levels of 4-PMP.3HCl

It was now known that adding an excess of TEA to 4-PMP.3HCl has a detrimental effect whilst not adding enough makes hyperpolarisation unlikely to occur. Therefore, the medium in which optimal hyperpolarisation can be seen with 4-PMP.3HCl needed to be discovered. After observing the large amount of variance in Figure 7 it became apparent that the order of addition of TEA to the reaction could be crucial. Perhaps TEA interacted with the catalyst preferentially over 4-PMP. Up unto this point the substrate was added first followed by the catalyst, solvent and then TEA. It was decided that the base should be moved up the order of addition, adding it directly to the substrate to maximise their interaction. This way, TEA would interact solely with the substrate and strip it of its HCl salt prior to the addition of the catalyst. This step is key as it means upon the catalyst being activated, 4-PMP.3HCl will essentially be 4-PMP (freebase) which is already known to enhance well (

Figure 2). The visible increase in enhancement at 0.8 eq of TEA is understood to be a result of the relatively large variance (20%) associated with the 'shake and analyse' technique.<sup>65</sup>

### 3.8.Changing the Order of Addition

To prove the importance of the order of addition, two experiments were conducted on 4-PMP.3HCl (Experiment 8 and 9, Table 1). Experiment 8 utilised the order of addition that had been used up until now whereas experiment 9 followed a proposed 'new order of addition' (added in the order of substrate, base, catalyst, solvent). Both were hyperpolarised using SABRE and their signal enhancements recorded in order to deduce which order of addition produces better enhancements. Figure 8 shows the hyperpolarised <sup>1</sup>H NMR spectra for experiments 8 and 9. The first thing that stands out from this data is how they look to be identical, but this is deceiving. The signal enhancement for experiment 8 was calculated to be 8-fold ( $\epsilon \approx 7.66$ ) whereas a 13-fold ( $\epsilon \approx 12.87$ ) enhancement was recorded for experiment 9. Despite the new order of addition giving an enhancement nearly two times that of the previous order of addition, the results are incredibly close to the 20% variance that is rife when using the 'shake and analyse' technique.<sup>65</sup> These results weren't as clear cut as they were expected to be, however, moving forward it made logical sense to follow the new order of addition. Adding TEA directly to the substrate allows for the formation of more 4-PMP (freebase) prior to the addition of the catalyst and solvent. This in turn reduces the chance of TEA interacting with the catalyst instead of the substrate, which prevents altering and/or blocking of the catalytic cycle.

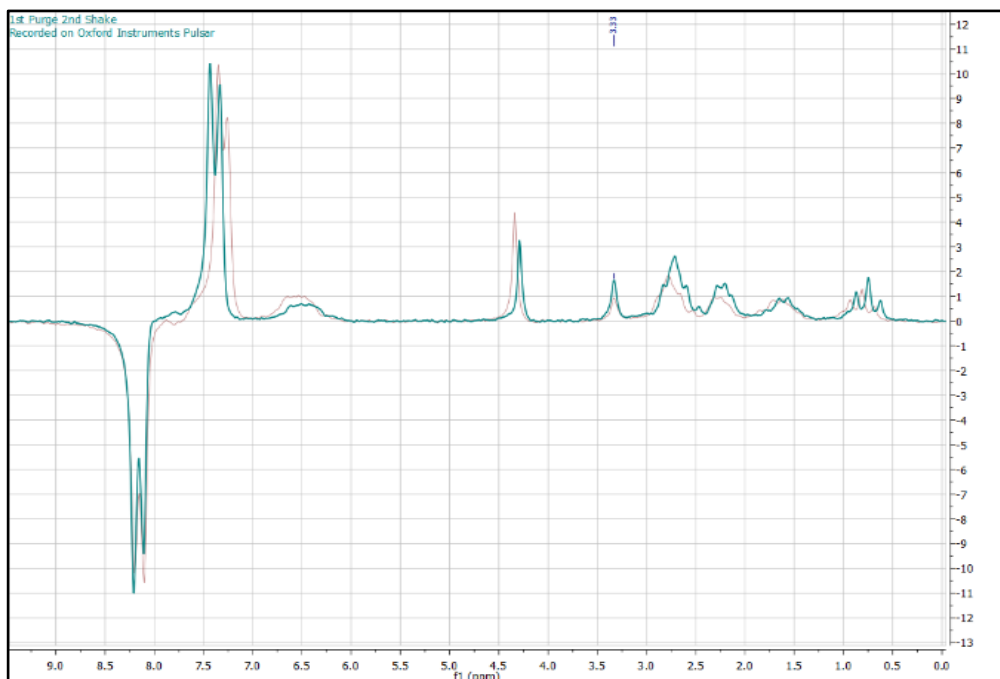


Figure 8:  $^1\text{H}$  NMR spectra for experiments 8 and 9; determining how much the order of addition effects hyperpolarisation. Experiment 8 (Green), Experiment 9 (Maroon).

### 3.9. The Sequential Addition of Triethylamine (4-PMP.3HCl)

Moving forward, the next step was to determine the concentration of TEA at which maximum hyperpolarisation could be observed in 4-PMP.3HCl. This experiment involved adding TEA in to the sample sequentially whilst using the new order of addition. When TEA was added to the sample last, it was a simple procedure that allowed for the same sample to be analysed throughout the whole study. In order to add more TEA to the sample, the screw top of the Young's NMR tube would be removed, the TEA added and the sample de-gassed. As TEA is now being introduced directly to the substrate before the addition of the catalyst, this is no longer achievable. There is now the requirement for a new sample to be made up for each TEA concentration tested. To do this appropriately, concentrations of substrate and catalyst had to be kept the same throughout the study, therefore stock solutions of substrate and catalyst were created. However, the solubility of 4-PMP.3HCl posed a problem when trying to achieve this. 4-

PMP.3HCl has a solubility of 0.74 mg  $\mu\text{L}^{-1}$  in methanol- $d_4$ . To attain a substrate concentration of 4.44 mg in the NMR tube would require 600  $\mu\text{L}$  of solvent, leaving no room for the catalyst stock (100  $\mu\text{L}$ ) and 0 - 22  $\mu\text{L}$  (0 – 10 eq) of TEA. It was vital to maintain a total NMR tube volume of 600  $\mu\text{L}$  as this is the volume used in every study in this project. The only way to solve this complication was to weigh out seven batches of 4.44mg (4-PMP.3HCl), adding to each batch the TEA, 100  $\mu\text{L}$  of catalyst stock (2 mg / 100  $\mu\text{L}$ ) and solvent to reach a total tube volume of 600  $\mu\text{L}$ . Details of the sample concentrations are shown in Table 5.

Table 5 - Table showing NMR tube concentrations for sequential addition of TEA to 4-PMP.3HCl. Catalyst stock (2 mg / 100  $\mu\text{L}$ ).

<b>Tube No.</b>	<b>Vol Cat. Stock (<math>\mu\text{L}</math>)</b>	<b>4-PMP.3HCl (mg)</b>	<b>Vol. TEA (<math>\mu\text{L}</math>)</b>	<b>Vol. MeOD (<math>\mu\text{L}</math>)</b>	<b>TEA Eq.</b>	<b>Total Vol. (<math>\mu\text{L}</math>)</b>
1	100	4.44	0	500	0	600
2	100	4.44	2.18	497.82	1	600
3	100	4.44	4.35	495.65	2	600
4	100	4.44	6.53	493.47	3	600
5	100	4.44	8.70	491.30	4	600
6	100	4.44	10.90	489.10	5	600
7	100	4.44	21.75	478.25	10	600

The enhancement data can be seen in Figure 9, which shows graphically how each addition of TEA affects the hyperpolarisation of 4-PMP.3HCl. When there are 0 eq of TEA in the sample, no hyperpolarisation is reported. This was carried out to reinforce that addition of TEA is necessary. Upon the addition of 1 eq TEA, hyperpolarisation begins to be evident. A 5-fold enhancement was recorded which signifies that the catalyst has

become activated, which in turn allows for the catalytic cycle to take place. In addition, this is a very similar result to the first attempt at hyperpolarising 4-PMP.HCl, meaning the 13-fold enhancement previously seen when testing the new order of addition has been verified as a trusted result. Moreover, at 2 eq TEA, a significant amount of hyperpolarised substrate can build up. At this concentration of TEA, a 193-fold increase in signal is observed. This is both interesting and significant as it is larger than the enhancement seen when TEA was added to 4-PMP freebase (161-fold). At 3 eq of TEA, the substrate is now theoretically 4-PMP (freebase) as all the HCl should have been removed, leaving  $\text{NEt}_3\cdot\text{HCl}$  in solution. At this TEA concentration the largest signal enhancement of 363-fold was observed. As predicted, this is directly comparable to the signal enhancement seen with 4-PMP (freebase) without TEA (313-fold). This confirms that at 3 eq TEA, 4-PMP.3HCl is completely converted to 4-PMP (freebase). In comparison to a study carried out on nicotinamide, where the hyperpolarisation was conducted at  $6\pm 4$  mT and detected at 9.4 T (0.5 G and 1.4 T respectively in this work), the reported signal enhancement of the *ortho*-protons is 77.2-fold and 88.1-fold. At a lower magnetic field, with increased competition for the catalyst after freebasing and without bubbling of *para*-hydrogen through the sample, the 363-fold signal enhancement reported in this work is exceptional.<sup>61</sup> In the same study, higher concentrations of catalyst and substrate also struggled to better the results done in this study. A SABRE experiment on pyridine using concentrations of 8 mM and 32 mM for catalyst and substrate respectively (5 mM and 25 mM in this study), achieved enhancements barely larger than that seen in the corresponding  $^1\text{H}$  NMR thermal spectrum (enhancement values were not reported, shown through NMR spectrum). This study was again carried out at high-field 9.4 T compared to 1.4 T in this work.<sup>61</sup> Furthermore, work done by P. Spannring *et. al.* only managed to achieve an

enhancement of  $\epsilon \approx 24$  for free pyridine in D<sub>2</sub>O using a 300 MHz spectrometer, despite using 10 eq substrate relative to the catalyst. Their work utilised an IDEG SABRE catalyst as opposed to IMes in this study, however, this shows why IMes is generally the preferred SABRE catalyst.<sup>66</sup> Interestingly, when 4 eq of TEA is added to the sample, hyperpolarisation levels begin to drop off, dipping to a 197-fold signal enhancement. This suggests that after 4-PMP.3HCl becomes 4-PMP (freebase) and an excess of TEA starts to build up, which inhibits the catalytic cycle in some way leading to a drop in the amount of hyperpolarised substrate present. Again, the addition of 5 eq of TEA sees hyperpolarisation decrease further. At this concentration, the enhancement observed was 85-fold. This is further confirmation that excess TEA is unfavourable when achieving optimal hyperpolarisation. Finally, the addition of 10 eq TEA to the sample sees the hyperpolarisation stay at a similar level, rising ever slightly to a 95-fold enhancement. It is fair to say that hyperpolarisation plateaus after the addition of 5 eq TEA due to the build-up of a huge excess of TEA.

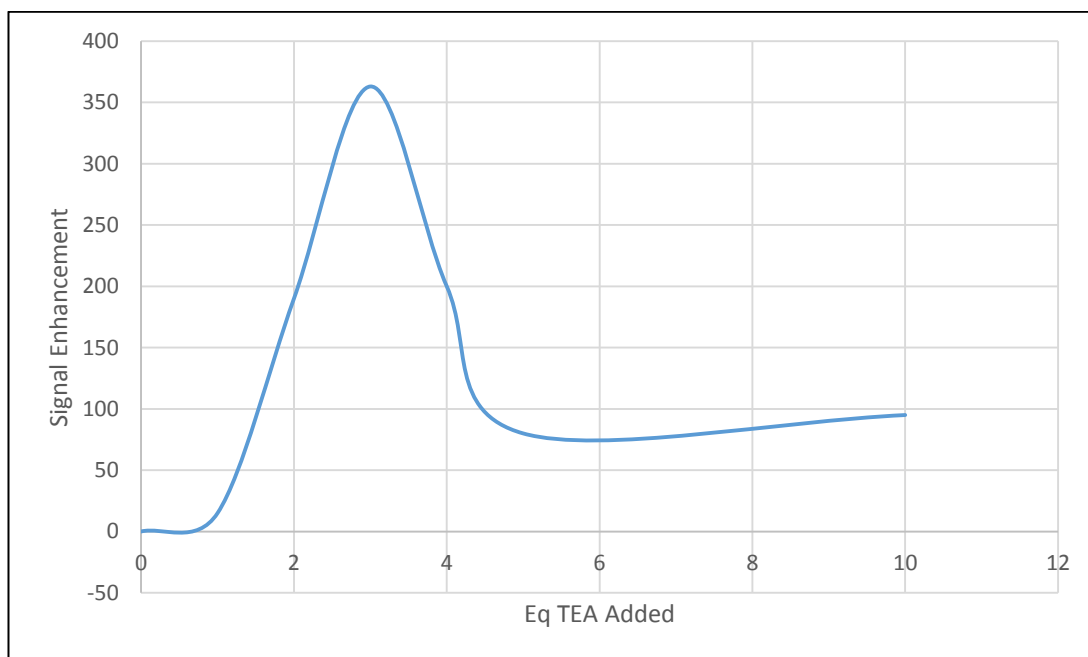


Figure 9: Graph showing how increasing the concentration of TEA effects the hyperpolarisation of 4-PMP.3HCl.

Table 6 - How 4-PMP.3HCl and 4-PMP (freebase) were compared in terms of eq of TEA added. E.g. 3 eq TEA with 4-PMP.3HCl was compared to 0 eq TEA with 4-PMP (freebase).

Compound	Equivalence of TEA			
	3	4	5	10
4-PMP.3HCl	3	4	5	10
4-PMP (freebase)	0	1	2	7

### 3.10. The Sequential Addition of Triethylamine to 4-PMP (freebase)

A lot was gained from the sequential addition of TEA to 4-PMP.3HCl. Firstly, using 3 eq of TEA provides the optimum level of hyperpolarisation. This is because 4-PMP.3HCl transforms to its freebase at 3 eq of TEA. Secondly, after 3 eq of TEA is added hyperpolarisation can be expected to decrease and eventually plateau at a significantly lower level. This is due to a vast excess of TEA building up and blocking access to the catalyst. A similar trend was expected in this study. When trying to uncover a hyperpolarisation correlation between TEA and PMP, it helps to consider 4-PMP.3HCl being in its freebased form in the presence of 3 eq of TEA. In addition, 4-PMP freebase is already in its freebased form at 0 eq of TEA. It is for this reason that during experiment 11, the sequential addition of triethylamine to 4-PMP freebase, 3 eq TEA with 4-PMP.3HCl was compared to 0eq TEA with 4-PMP freebase and so forth. This is better visualised in Table 6. Hyperpolarisation levels should be highest at 0 eq TEA before dropping off and plateauing. At a TEA concentration of 0, a 105-fold signal enhancement was recorded. This is 66% lower than what was observed with the previous order of addition, and 3 eq of TEA (4-PMP.3HCl) experiment. When 1 eq TEA was added, hyperpolarisation began to decrease following the trend set by 4-PMP.3HCl. A signal enhancement of 25 was observed which is one quarter the size of the signal seen with

4-PMP.3HCl. Despite being much lower than expected these results follow the expected trend. Moving forward, hyperpolarisation decreased even further when 2 and 5 eq of TEA were added to the sample. The signal enhancements reported here were 15-fold and 4-fold respectively. Despite the measurements of hyperpolarisation not matching up with 4-PMP-3HCl, the trend is obeyed completely. This can be seen in Figure 10. If Figure 9 is compared to Figure 10, the similarities are clear to see. Optimal hyperpolarisation occurs at 3 eq of TEA in both substrates before decreasing substantially and plateauing. Therefore, the same can be said for 4-PMP freebase that was said for its HCl salt. As there is no HCl to remove, the concentration of TEA builds up until it is in vast excess. In the process, it blocks and reduces the chance of any substrate-catalyst interaction, resulting in decreasing amounts of hyperpolarisation being observed. Excess TEA is detrimental to hyperpolarisation.

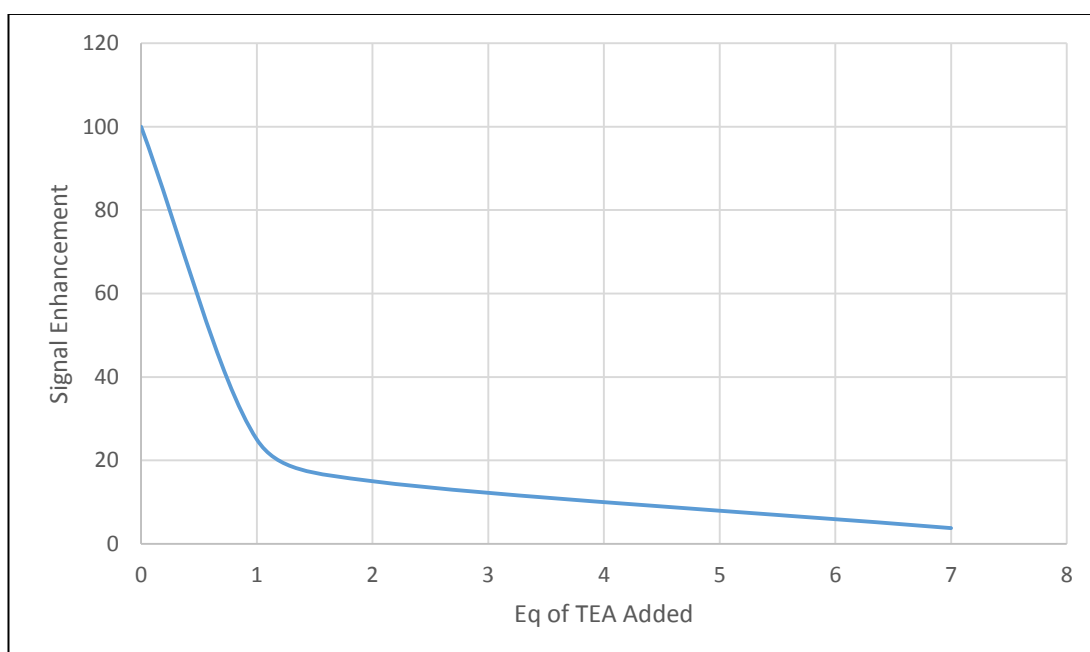


Figure 10: Graph showing how increasing the concentration of TEA effects the hyperpolarisation of 4-PMP (freebase).



### 3.11. 2-PMP and 3-PMP

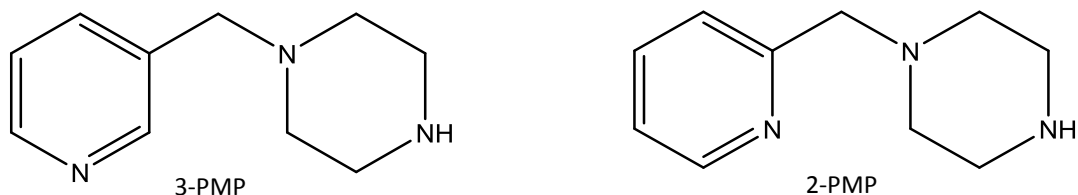


Figure 11: Structures for 3-pyridylmethylpiperazine (3-PMP) and 2-pyridylmethylpiperazine (2-PMP).

3-PMP and 2-PMP, two isomers of 4-PMP, were also studied regarding their hyperpolarisability, characterisation and separation. The only difference between the isomers is the position of the pyridyl ring, this is shown in Figure 11. Each isomer was characterised successfully *via* both high and low-field BT-NMR. The one problem that was encountered arose when attempting to separate and characterise a mixture of all three isomers. This would have huge implications when trying to determine the concentration of a sample.<sup>67</sup> In terms of quantification of a mixture, integrating the signals of the separate isomers cannot be achieved with 100% accuracy. Some resonances overlap meaning the true integral of a signal is problematic to determine. Moreover, as the position of the pyridyl changes from 3 to 2, steric hindrance acting on the nitrogen is increased. The cause of the steric hindrance is from the methylene connecting the pyridyl to the piperazine, and the piperazine functionality itself. Steric hindrance plays no role in the characterisation of these isomers but does come into play during hyperpolarisation. Literature reports the more sterically hindered a compounds moiety to bind to the catalyst is, the lower the resulting hyperpolarisation.<sup>62</sup> With this in mind it was expected that hyperpolarisation would decrease the closer the nitrogen moves to the rest of the structure.

### 3.11.1. Hyperpolarisation

Taking into account what was reported by Chekmenev *et. al.* that steric hindrance alters the time scale of the SABRE exchange process, or reduces the association constant, it was expected that lower levels of hyperpolarisation would be observed in these isomers.<sup>62</sup> As the pyridyl nitrogen moves closer to the methyl piperazine part of the compound, steric hindrance increases and alters its ability to bind to the SABRE catalyst, ultimately reducing the accessibility of N to the catalyst.<sup>62, 68, 69</sup> The free orbital of the nitrogen is increasingly inhibited by the piperazine group in the 2- and 3-isomers, significantly reducing the amount of hyperpolarisable substrate allowed to build up due to being unable to efficiently ligate to the iridium centre. The enhancements confirmed overall the pattern Chekmenev reported.<sup>62</sup> The hyperpolarisation of 3-PMP shows symptoms of steric hindrance effects with an 8-fold signal enhancement (*ortho*-hydrogen signal) being observed. Compared to the 300-fold enhancement seen with 4-PMP (least hindered) (Figure 2), this is a massive indication of how sensitive the SABRE process is in regard to a sterically hindered substrate. Furthermore, with 2-PMP, negligible increase in signal intensity is observed. The presence of an emission resonance exists, however it is negligible in size (see Figure 12). This study gives insight into the limits of SABRE substrates when using an IMes SABRE catalyst. It also paints a clear picture of how subtle changes to the structure of a substrate can have huge impacts on its hyperpolarisability.

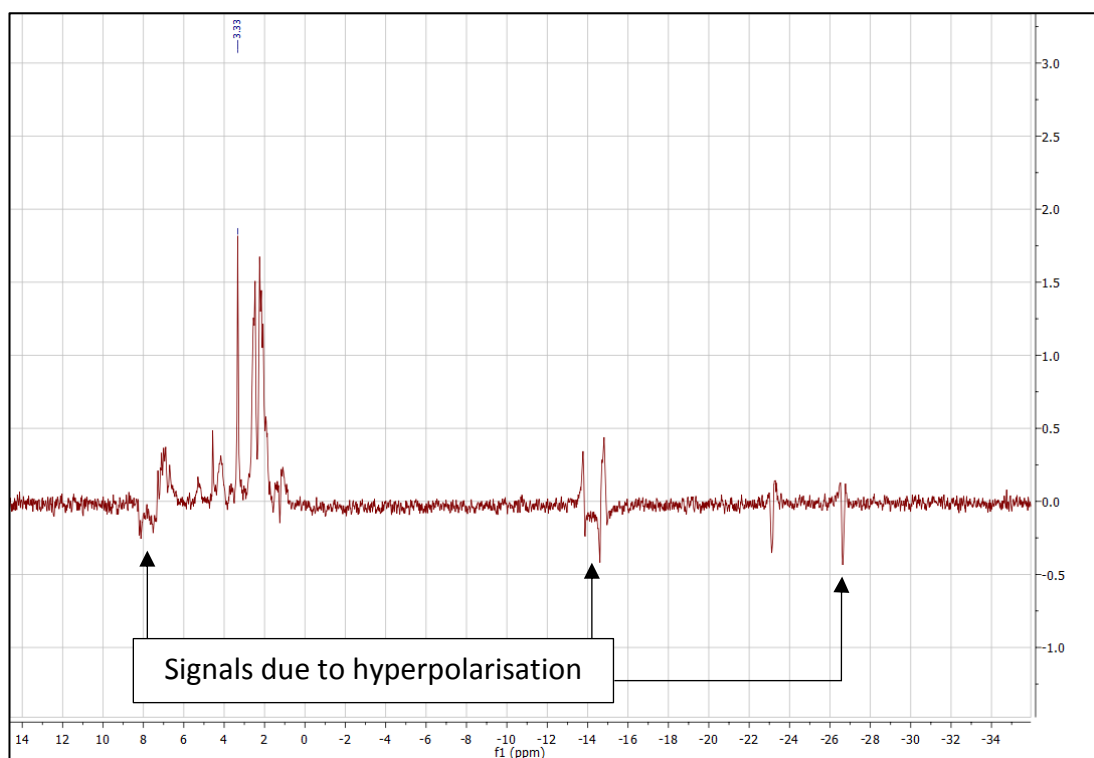


Figure 12: Hyperpolarised  $^1\text{H}$  NMR spectra for 2-PMP.

### 3.12. Summary

TEA proved to be a good choice of base for the removal of the HCl from 4-PMP.3HCl. The discovery of the optimal [TEA] paved the way for some outstanding signal enhancements, the largest being a 363-fold enhancement which was observed after freebasing 4-PMP.3HCl with 3 eq of TEA (see Figure 10). It is now also apparent that adding less than 3 eq of TEA could cause disproportionate deprotonation, leading to a mixture of compounds present, potentially with different protonated/deprotonated sites. This could be the cause for the variance in results in Figure 7. Changing the order of addition was a logical move to make. Although experiments 8 and 9 showed that the new order of addition offers a slight advantage in terms of signal enhancement, the two results looked comparable. Moving forward, it made sense to follow the new order of addition. Despite the 20% variance associated with shaking and analysing, some great

enhancements have been achieved in this work,<sup>65</sup> as well as the unearthing of a pattern for how TEA affects PMP hyperpolarisation. Of course, access to a polarisation system like the one reported by Duckett *et. al*, would be beneficial and would no doubt improve reproducibility.<sup>65</sup> Working at higher magnetic fields and lower temperatures would also improve hyperpolarisation levels, however, the importance here is that it is shown to be possible to achieve strong hyperpolarisation at lower magnetic fields/temperatures. This makes way for the application of bench-top NMR hyperpolarisation to mobile drug analysis, detection and/or characterisation. The most explanatory reason for the decrease in hyperpolarisation at high [TEA] is down to base-catalyst interaction. As excess [TEA] builds up, the chance of interactions between itself and the catalyst increases. As TEA begins to interact more with the catalyst, it proceeds to prevent 4-PMP doing so. Furthermore, it is thought that as TEA is less dissociative than 4-PMP (4-PMP is a weakly interacting ligand), the catalytic cycle which relies on the non-hydride ligand dissociating, is no longer obeyed resulting in the impossibility of hyperpolarisation.<sup>70</sup> This in turn explains why there is no evidence of hyperpolarised TEA. It is not impossible for 4-PMP to coordinate to the catalyst in these conditions resulting in some hyperpolarisation being seen, it just becomes less likely as [TEA] increases. The one thing that stands out more than anything else in this study is the signal enhancement for 4-PMP freebase observed during the sequential addition study. The same methodology was followed, this includes techniques and concentrations of reactants right down to using the same Gilson pipettes throughout. It is possible that different batches of catalyst (synthesised in house) perform slightly better or worse. However, the results are still remarkable. The hyperpolarisation of 2- and 3-PMP shows that steric hindrance plays a huge part in whether a substrate will hyperpolarise well or not. As shielding of the pyridyl increases, enhancement levels drop.

#### 4. Hyperpolarisation of 4-PMP Tablet

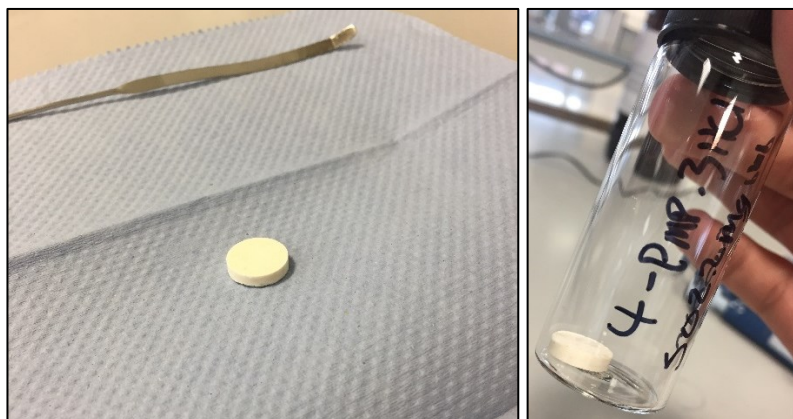


Figure 13: 4-PMP.3HCl Tablet.

The culmination of this work brings together everything that was learned throughout the analysis of the PMP isomers and applies it to a potential ‘street sample’. By hyperpolarising a pill, it shows that hyperpolarisation can be applied to drug research, opening a whole new route of research for both hyperpolarisation and NPS. The extraction method developed allowed 4-PMP.3HCl to be freebased and isolated from the surrounding impurities before being successfully hyperpolarised.

##### 4.1. Adapting the Hyperpolarisation Method

Hyperpolarising a street sample is not as straight forward as dissolving a small amount of it in the presence of the catalyst and some solvent, especially in the case of a pill. Since pills are solid, the API is going to be present in its hydrochloride salt form, meaning that potential ligand sites are protonated. Since this experiment was a ‘proof of concept’ it was already known that the API was in its HCl salt form and that the ligating pyridyl group was protonated. With this known, what was gathered from experiment 10 and 11

(the sequential addition of TEA to 4-PMP.3HCl and 4-PMP (freebase)) was put into action in this experiment (see details of experiment 12). Once the API was separated from the binding agents and fillers of the pill by syringe filtration, the general hyperpolarisation method could be followed.

#### 4.2. Results and discussion

Figure 14 shows the thermal and hyperpolarised  $^1\text{H}$  NMR spectra of the 4-PMP.3HCl Tablet. The maroon spectrum (bottom) belongs to the thermal background taken prior to any hyperpolarisation of the sample. This spectrum had to be magnified by a magnitude of 32 to make it visible in the presence of the hyperpolarised spectrum (top). It is hard to make out the characteristic resonances of 4-PMP in the un-hyperpolarised spectrum, however, the hyperpolarised spectrum contains the correct peaks at 8.2 ppm to confirm firstly, that it is 4-PMP and secondly, that it has hyperpolarised. This proves the extraction method worked correctly. As expected, the *ortho*- and *meta*- hydrogen environments hyperpolarised well. In line with how all previous enhancements have been calculated, the *ortho*-H signal was analysed for its hyperpolarisation, recording a 138-fold enhancement. This value follows the trend seen with the sequential additions, as  $\epsilon \approx 138$  falls between the enhancements of 100 and 363 seen with 4-PMP (freebase) and 4-PMP.3HCl respectively, at  $[\text{TEA}] = 3$  eq. The three eq of TEA used was based on the fact the pill contains 100 mg of 4-PMP.3HCl. The size of this enhancement was expected, based on the trends discovered earlier in this work. One fear was that a proportion of the API would not freebase and so would be collected in the filter, resulting in a lower enhancement being observed. This was not the case due to the extraction method performing correctly.

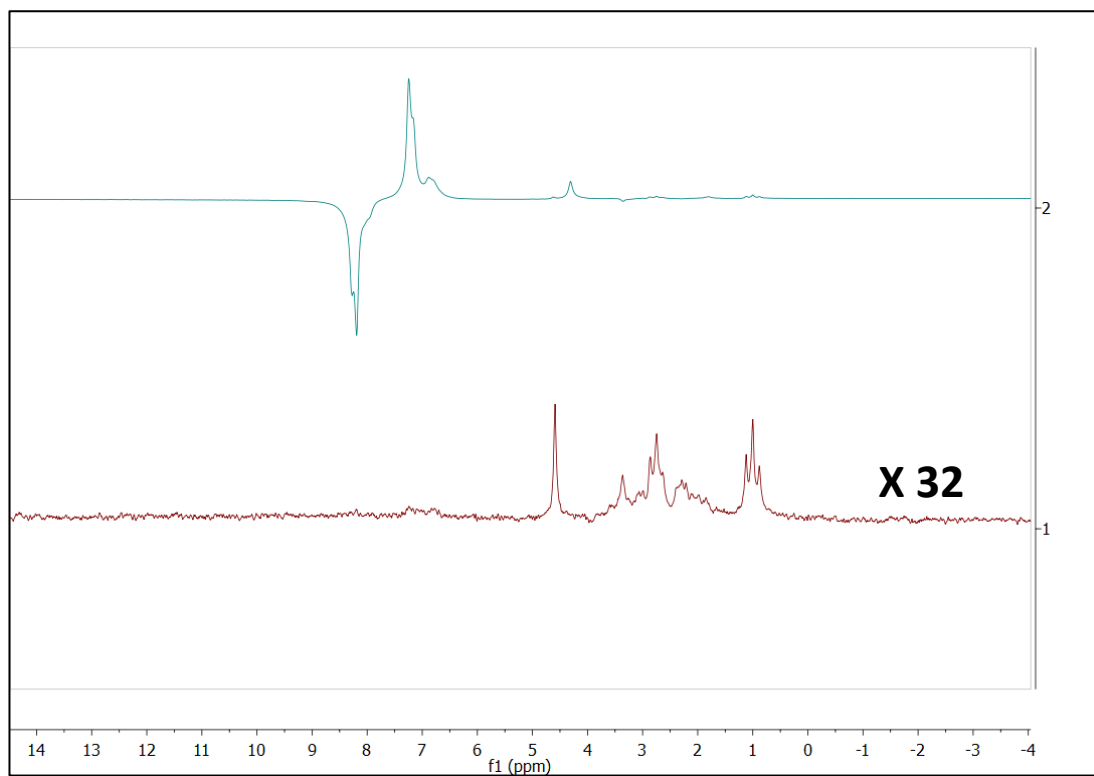


Figure 14: Hyperpolarised <sup>1</sup>H NMR spectrum (turquoise) and <sup>1</sup>H NMR thermal background spectrum (maroon) of 4-PMP.3HCl pill. The thermal spectrum is shown at x32 vertical magnification.

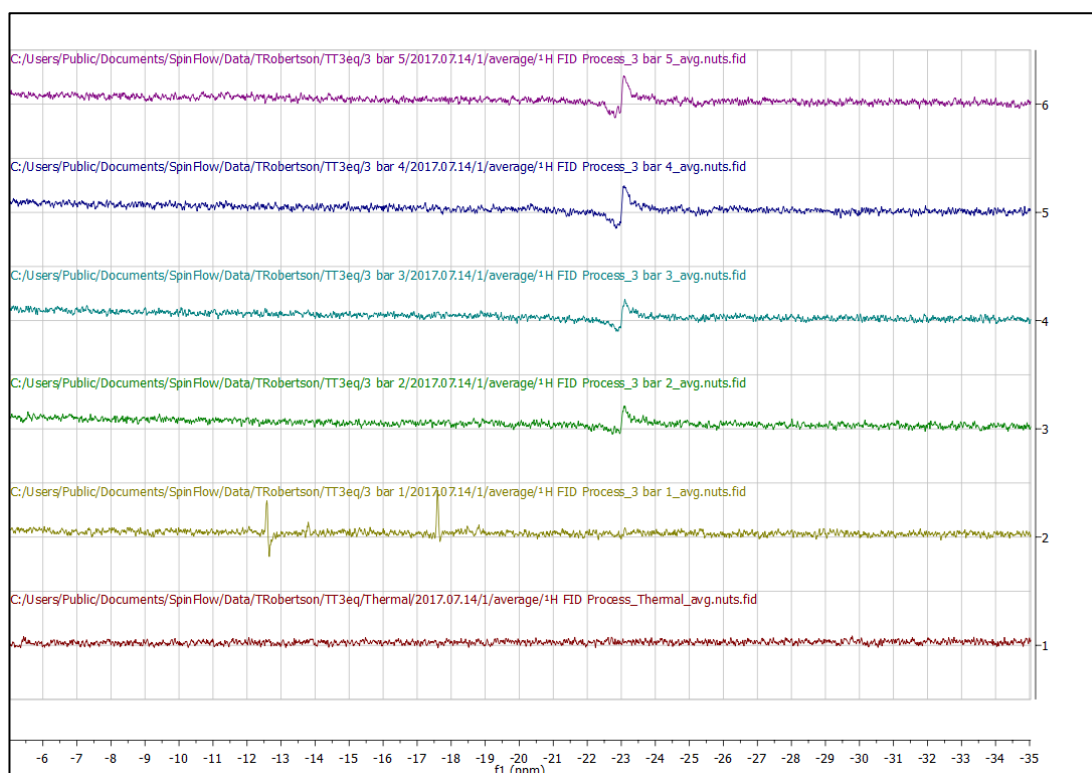


Figure 15: Hydride region taken from the hyperpolarised spectra of the 4-PMP.3HCl based pill. Bottom to top: Thermal background, 1<sup>st</sup> *para*-hydrogen purge A, 1<sup>st</sup> *para*-hydrogen purge B, 2<sup>nd</sup> *para*-hydrogen purge A, 2<sup>nd</sup> *para*-hydrogen purge B, 3<sup>rd</sup> *para*-hydrogen purge. (A = first shake, B = second shake).

A good indicator of successful catalyst activity is the appearance of the hydride region.

After the first purge of *para*-hydrogen there should be two hydride resonances present.

After further purges with *para*-hydrogen, there should be one characteristic resonance

at -23 ppm which is in line with other experiments conducted. Figure 15 shows the

hydride region for the hyperpolarised spectra of the 4-PMP.3HCl based pill. Firstly, the

two resonances at -12.5 and -17.5 ppm result from the COD component undergoing

hydrogenation. Once hydrogenated, the catalyst is fully activated and ready to

propagate hyperpolarisation efficiently to the substrate. The addition of *para*-hydrogen

to the complex means that Ir(I) is now Ir(III) which coincides with a change in geometry

from square planar to octahedral. Furthermore, the consistent resonance at -23 ppm

thereafter is confirmation of a single catalytic species in solution and that a methanol



adduct, as described elsewhere, is not observed.<sup>49, 61</sup> This experiment worked with great success as the API hyperpolarised as expected. A 138-fold enhancement after extraction from a pill whilst using the 'shake and analyse' technique is remarkable, especially when compared to the hyperpolarisation of nicotinamide, which shows 77- to 300-fold enhancements, the latter of which was observed using a unique flow-system.<sup>56, 65, 66</sup> The extraction method was key to achieving such a high enhancement in this experiment, without it the API simply would not hyperpolarise. Working with knowledge of the optimum TEA concentration required to freebase 4-PMP.3HCl meant that the salt could be freebased and isolated from the insoluble binding/filling agents of the pill, prior to filtration. This meant that upon filtration, most if not all the freebased API passed through the filter, leaving the impurities behind. It is fair to say the extraction method works well, presented no problems and is simple enough that it could be taken and applied in real world situations. One other important aspect in this study is the fact that only 2 mg of the API was used. This highlights the employment of SABRE to detect molecules at low concentration, as exemplified elsewhere and again backs up how efficient the extraction method was.<sup>54, 62, 71</sup> 2 mg is such a small amount that any loss of analyte in the filter would have resulted in a poor enhancement value. Furthermore, to obtain a creditable <sup>1</sup>H NMR spectrum, around 10 mg of analyte and multiple scans are needed. This experiment produced far larger signals with a far smaller amount of analyte and in a single scan. What sets this work apart from some literature is its novel application to the real world. The aim is not to prove something is hyperpolarisable, it is to prove that a hyperpolarisation technique, SABRE, can be used for the benefit of the many. Some drugs do hyperpolarise. The literature is rife with the hyperpolarisation biologically relevant compounds used to treat diseases, such as tuberculosis and cancer.<sup>57, 65, 72</sup> A report by P. Rayner *et al.* goes a step further by hyperpolarising the

crucial building blocks of some medicinal compounds; pyridazine, pyrimidine, pyrazine and isonicotinamide.<sup>58</sup> In addition, investigations have also taken place into the behaviour of drug compounds in the SABRE catalytic cycle, in particular, how they exchange with iridium complexes.<sup>73</sup> There have been some great advances in SABRE applications, particularly in the field of Magnetic Resonance Imaging (MRI), which suffers from the same sensitivity issues as NMR.<sup>43, 53, 74</sup> Finding a need for hyperpolarisation is niche, and that is what this work does, by going a step further than addressing the inherent lack of sensitivity in NMR, which has been addressed greatly by L. S. Lloyd *et al.*<sup>71</sup> It has been demonstrated here that it is possible to extract a NPS from a common formulation and then hyperpolarise it. The SABRE aspect of this process reduces the time taken to acquire spectra, the extraction process removes unwanted impurities that might otherwise cause resonance overlapping in the spectra, all the while the compound of interest is more importantly isolated for SABRE analysis. This opens up a whole host of possibilities for drug analysis, for example, developing further detection and extraction methods from more complex mixtures at low concentrations that would otherwise be un-detectable.

### 4.3. Summary

The experiment was successful in that the 4-PMP contained within the pill was successfully extracted and polarised by SABRE. Ultimately, this procedure could be applied to real world situations. The fact that the 138-fold enhancement is in line with all previous work done in this project backs up the legitimacy of the trends found. This is important due to the 20% variance threshold, that comes with the shake and analyse technique, which casts a small shadow of uncertainty.<sup>56, 65</sup> Not only does this bring drug

analysis closer together with hyperpolarisation, it proves the two can work well with each other. It also offers major benefits to the analytical side of drug analysis due to the small amount of analyte required and the reduced time it takes to gather the data. This work goes beyond providing a solution to the notorious sensitivity issues associated with NMR, providing SABRE with another real world purpose.

## 5. Standard Addition (SA) and Internal Standard (IS) – Quantitative NMR (QNMR)

Quantification in NMR is usually achieved using a referencing standard to calibrate the intensity scale of the measurement to a high degree of accuracy.<sup>75, 76</sup> Method development in this area could also form part of the solution to the innate challenge within NMR spectroscopy, achieving absolute quantification of a chemical compound.<sup>75</sup> Optimising this quantification method for use on the bench-top NMR works toward achieving this and will provide a simple, cheaper and more portable solution to drug detection and quantification. In this project, it was useful to utilise both techniques and show that they can both be performed successfully *via* bench-top NMR, as they both have their advantages and disadvantages. SA is only possible when the concentration of an analyte is known, whereas the IS method does not have this requirement. Although, in the case that SA can be performed, it is slightly more time efficient compared to IS.

### 5.1. Standard Addition

The method of SA is a relatively simple, quantitative approach for calculating the concentration of an unknown sample, which has been shown to improve results when experiments were redesigned from simple calibration plots.<sup>77</sup> It is carried out by analysing samples prepared from two stock solutions; one of a known concentration and another (the analyte under investigation) of an unknown concentration.<sup>78</sup> The concentration of the unknown sample is calculated by either extrapolating the trend line of the plotted data back to the X-axis, or algebraically by re-arranging the equation of

the trend line ( $y = mx + c$ ) to calculate  $x$ .<sup>79</sup> When the x-axis is labelled 'concentration of known stock added', the calculated x-intercept reflects the concentration of the unknown that is present in the sample.<sup>80</sup> Due to the time consuming manner of sample preparation, sample analysis and data interpretation, this method is best suited for studies involving a small number of samples, hence its employment in this study. However, SA has the potential to be extremely accurate due to the target analyte behaving as its own reference.<sup>79</sup>

#### 5.1.1. Proof of Concept

In an attempt to prove that this method was applicable to this study, the concentration of the analyte that would otherwise be unknown in this instance, was known. Thus, when extrapolating the line of best-fit back to the x-axis to determine the unknown concentration, the value observed should correlate with the known unknown. This allows the accuracy of this method to be determined.

#### 5.2. Calibration (TMS Internal Standard)

An IS of TMS was used as the reference in a separate calibration experiment. In this case, the response of the analyte is normalised to the response of the IS and plotted as a function of the analyte standard concentration. This is arguably more accurate than SA as the concentration of the IS is the same throughout the study.<sup>78, 81</sup> Furthermore, this method is often argued to be a better choice for calibration due to strict SA requirements relating to the precision of a method.<sup>82</sup> Quantification of street samples was not carried out.

### 5.3. Results and Discussion

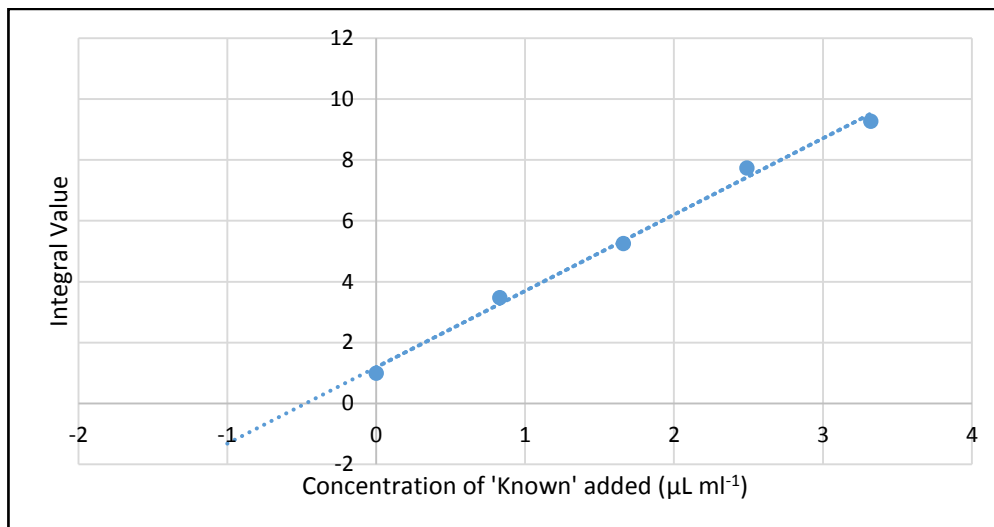


Figure 16: Standard addition calibration graph for 4-PMP (freebase).

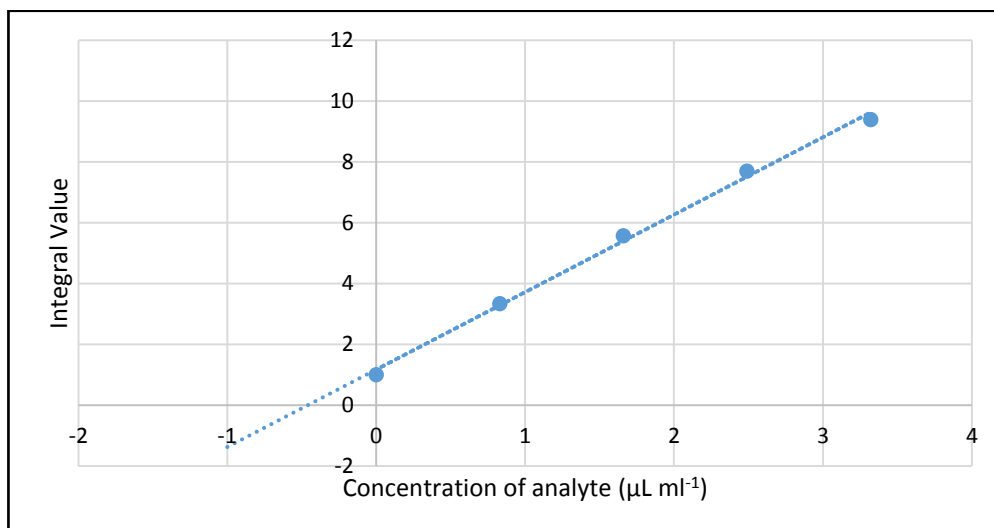


Figure 17: Standard addition calibration graph for 3-PMP (freebase).

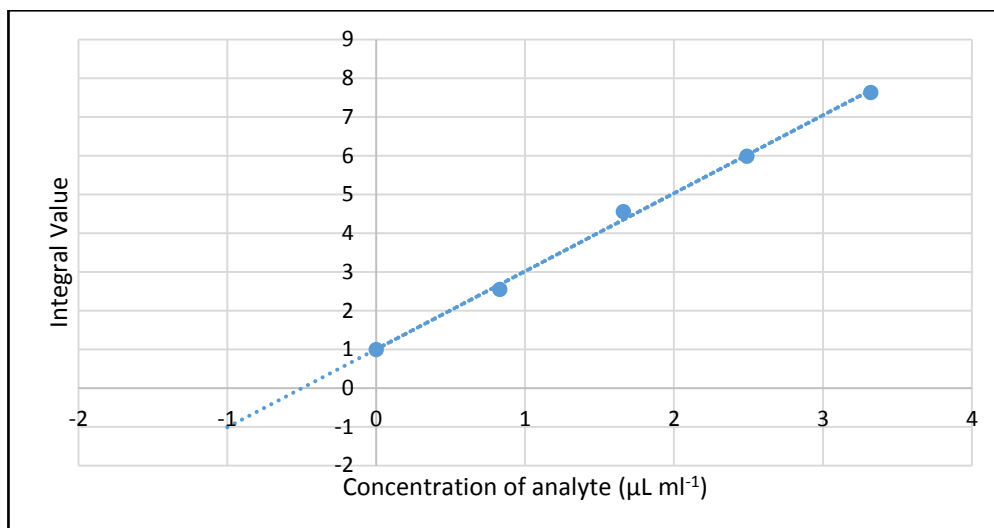


Figure 18: Standard addition calibration graph for 2-PMP (freebase).

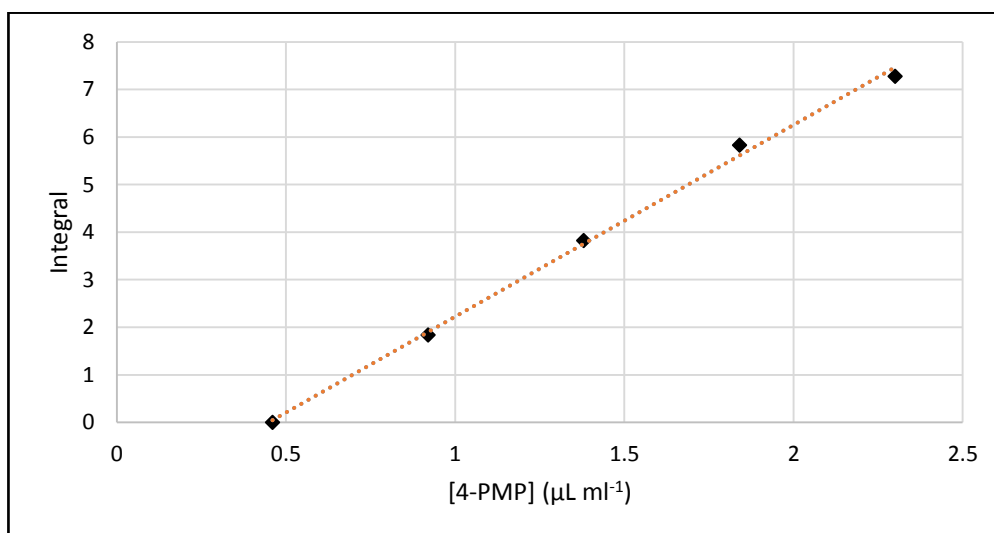


Figure 19: Internal standard (TMS) calibration graph for 4-PMP (freebase).

The method of SA was subjected to method development. Spiking samples manually with the analyte proved very unsuccessful and resulted in poor accuracy. Since the analyte (PMP) is an oil and such a small amount was up taken each time, it was difficult to ensure all the analyte was expelled from the pipette tip. This led to an inaccuracy in the spiking of each sample and it is therefore believed to be the cause behind the large

amount of variance seen in the results of this experiment. This led to further samples being prepared from stock solutions. The results, shown in Table 7, show an acceptable accuracy. The concentration of tube 0 was already known to be  $0.46 \mu\text{L mL}^{-1}$  (as this is a proof of concept), therefore this was the expected value for  $x$ . In regard to 4-PMP (Figure 16), this technique was 100% accurate the second time round (three repetitions in total) with an average concentration of  $0.47 \mu\text{L mL}^{-1}$ . A standard deviation (SD) of  $s = 0.057$  and an average  $R^2$  value of 0.993 show how close the data points are when related to the mean. The range in the determined concentration was  $0.11 \mu\text{L mL}^{-1}$ . For 3-PMP (Figure 17), 100% accuracy was achieved on the first repetition whilst the average concentration ( $0.37 \mu\text{L mL}^{-1}$ ) was out by  $0.11 \mu\text{L mL}^{-1}$ . However, this experiment reports the largest range of results ( $0.14 \mu\text{L mL}^{-1}$ ). A SD of  $s = 0.08$  was calculated which reflects this. 2-PMP (Figure 18) was accurate to within  $0.8 \mu\text{L mL}^{-1}$  whilst showing a more concise range of results ( $0.04 \mu\text{L mL}^{-1}$ ). This precision is shown through the SD (0.02). The average 2-PMP concentration determined was  $0.51 \mu\text{L mL}^{-1}$ . In regards to the IS method, a clear linear positive correlation can be seen (Figure 19). This shows that 60 MHz BT-NMR can offer top class precision and accuracy with more than one technique.

Table 7 - Standard addition results.

Analyte	Average Concentration ( $\mu\text{L mL}^{-1}$ )	Range ( $\mu\text{L mL}^{-1}$ )	Standard Deviation
4-PMP	0.47	0.11	0.057
3-PMP	0.37	0.14	0.080
2-PMP	0.51	0.04	0.020



#### 5.4. Summary

SA used in tandem with 60 MHz NMR was very accurate, determining concentrations within 0.01  $\mu\text{L}$  (2%) of the true concentration with 4-PMP. This shows the strong potential for SA methods when quantifying with a bench-top NMR spectrometer. SA would be a great choice in method if/when using bench top NMR to quantify out in the field when the quantity of samples is small. The linearity of the IS method also proves that bench-top NMR can perform to a very high standard using more than one technique. Comparing the two methods, SA would have to be run for each unknown sample in order to determine their concentration, whereas with an IS, once the calibration is completed, each unknown sample concentration can be found with one run.

## 6. GC-MS Analysis

### 6.1. Characterisation and Separation of PMP Isomers

Gas chromatography mass spectroscopy (GCMS) was utilised to characterise and separate a mixture of the PMP isomers. Despite its unlikelihood in a street sample, the ability to separate a mixture of all three PMP isomers was vital for proof of concept. GCMS is the instrument of choice among scientists when a separation of similar compounds is required and thus was chosen for this work due to its high precision, accuracy and above all else, power. With the PMP isomers all having very similar structures and the same molecular weights (not including 4-PMP.3HCl), this technique was the only valid option. It was possible after extensive method development to successfully characterise a mixture of all three isomers. 2-PMP eluted first (17.6 minutes), with 3 and 4-PMP co-eluting shortly after (21.9 and 22.0 minutes respectively). Despite the co-elution, it is easy to visually determine which peak is which (Figure 20). In terms of method development, altering the ramping of the oven temperature played a crucial role in separating 3- and 4-PMP as much as possible. Changing this ramp so that the oven temperature increased at a slower rate meant that the two isomers would separate enough to be distinguishable. The starting temperature was maintained at 100 °C for 50 minutes before ramping up at 30 °C/min until 310 °C was reached. This temperature was then held for 3 minutes.

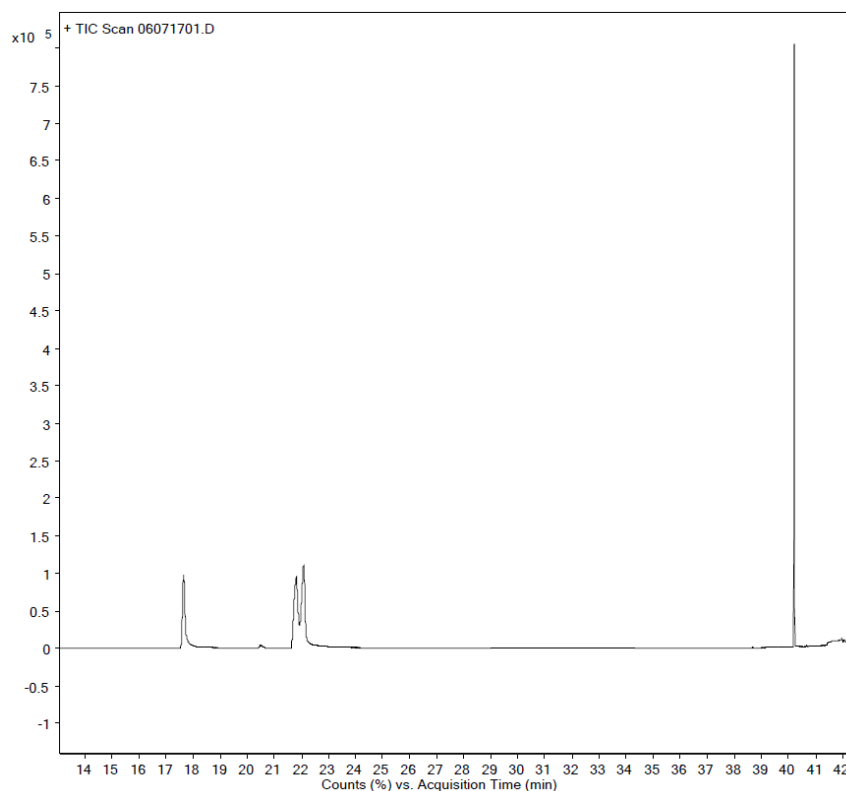


Figure 20: GC-MS chromatograph for the separation of 2-, 3- and 4-PMP.

## 6.2. Validation and the Quantification of a PMP Tablet

As an extension to the hyperpolarisation of the 4-PMP.3HCl tablet, GC-MS was employed to provide a validated qualitative and quantitative method for the API of the tablet.<sup>83</sup> The binding and filling agents present in the tablet formulation were removed prior to analysis *via* an extensively developed extraction method. The method development focused on testing the mixing times of the tablet when dissolved in a methanol-eicosane solution. The samples were made up the same, only the length of time they were placed in to the ultrasonic bath was varied. Sonication times of 1 min, 5 mins, 10 mins, 15 mins, 20 mins, 25 mins, 30 mins and 50 mins were examined.

### 6.3. Results and discussion

The method used to prepare the sample for GC-MS analysis was extremely simple. It required only that the analyte be dissolved in a methanol-eicosane solution before sonication and syringe filtration to dissolve the API and remove the adulterants respectively. In terms of the validation, the calibration standards demonstrated an acceptable correlation coefficient ( $r^2 = 0.995$ ) over an appropriate concentration range of  $50.0 - 150.0 \mu\text{g mL}^{-1}$  with sufficient repeatability ( $\text{RSD} = 4.81-10.37\%$ ,  $n = 5$ ). The Limit of Detection (LoD) and Limit of Quantification (LoQ) for the analyte were  $15.64$  and  $47.38 \mu\text{g mL}^{-1}$  respectively. The RSD for the tablet analysis was calculated to be  $4.13\%$  and the averaged integrated area ratio fitted onto the calibration graph. The two calibration graphs in Figure 21 and Figure 22 take into account all the Integrated Area Ratio(s) (IAR) at each concentration, and the average IAR at each concentration respectively.

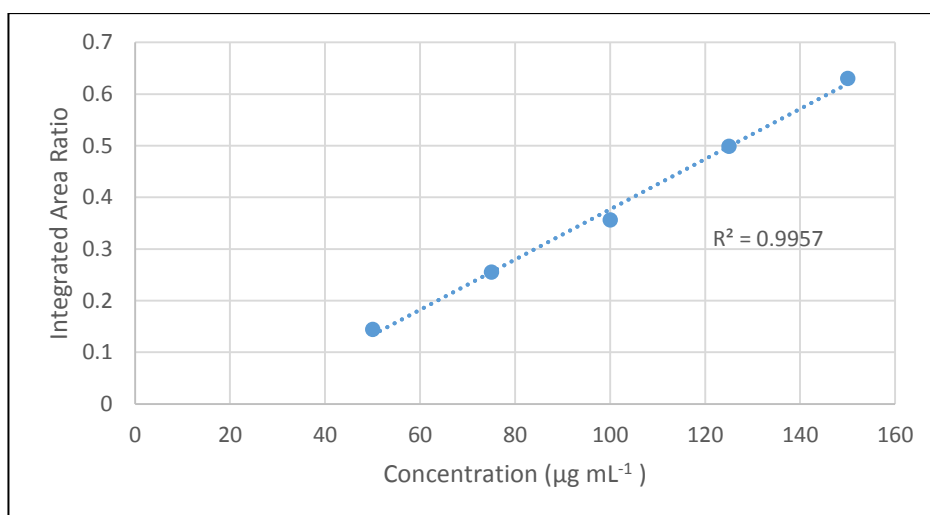


Figure 21: GC-MS calibration graph of average Integrated Area Ratio (IAR) for each concentration.

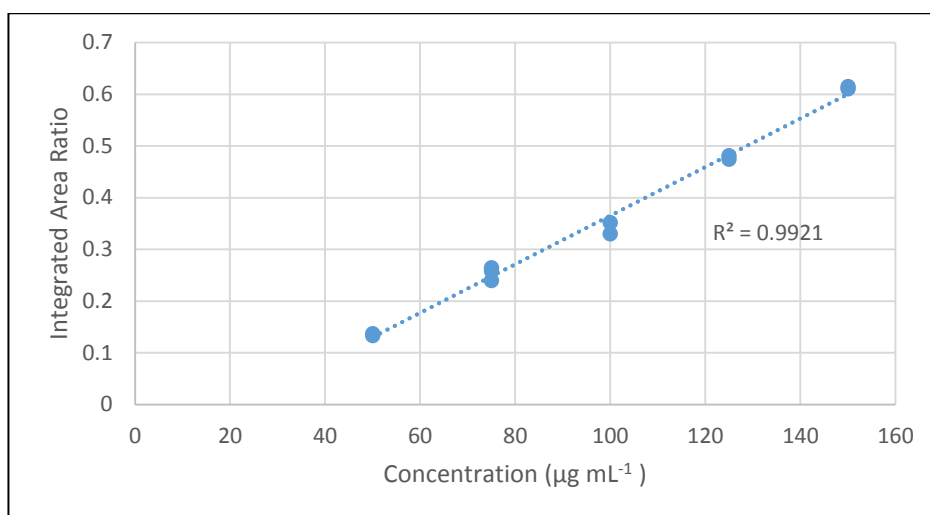


Figure 22: GC-MS calibration for all IAR points at each concentration.

The correlation coefficients of both graphs in Figure 21 and Figure 22 are acceptable and therefore either could be used to quantify. Since the tablet was made to prove a concept, the concentration of the API was known to be  $\sim 100$  mg. When quantifying the tablet by GC-MS, a concentration of this amount was expected. However, the concentration of the API in the tablet was calculated to be 72 mg, somewhat lower than the expected 100 mg. The validation was carried out using 4-PMP.3HCl, the API, with no issues whatsoever resulting in chromatographs that were clear, resolved to the baseline and provided great validation data (Figure 23). This provided reason to investigate the extraction process with the results of this shown in Figure 24.

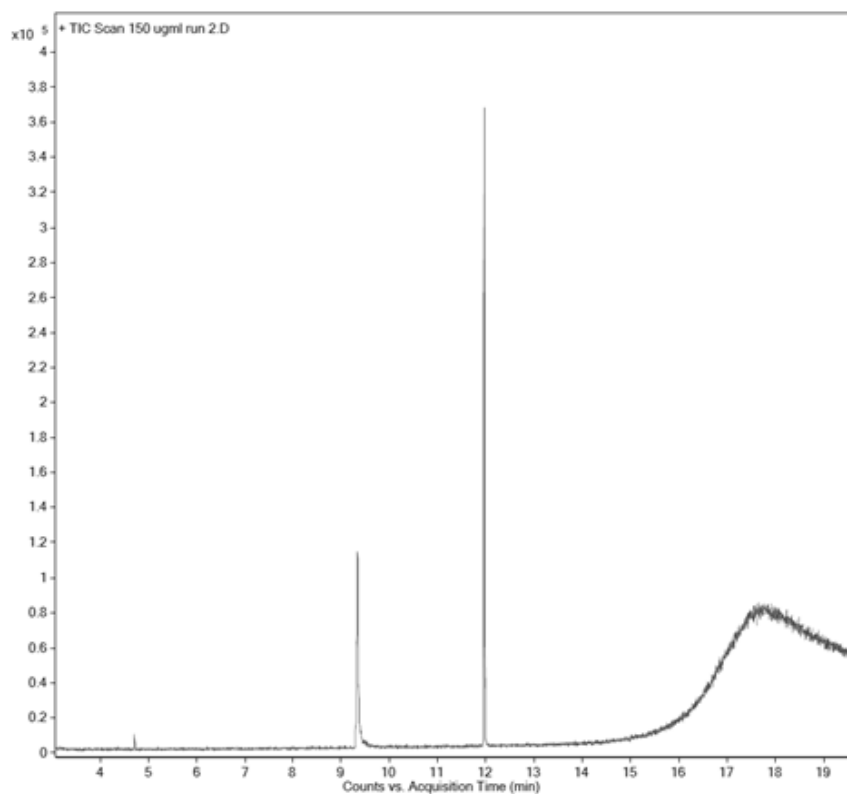


Figure 23: 150 ug/ml-1 GCMS calibration chromatograph (4-PMP.3HCl).

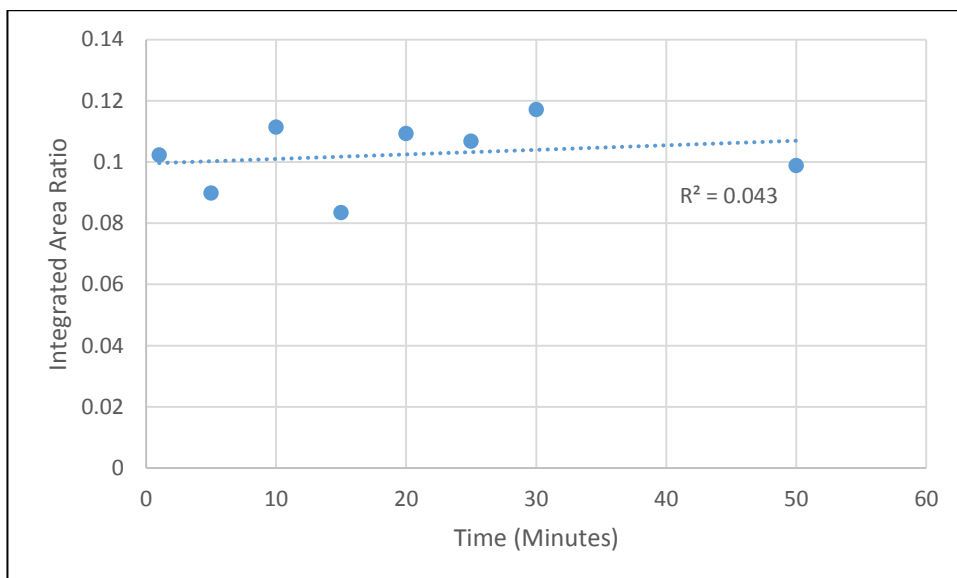


Figure 24: Graph showing how increasing sample mixing time effects its Integrated Area Ratio (IAR).

There is no correlation or linearity in Figure 24, thus showing that longer mixing times are not key in extracting the full amount of API. The potential for losing some analyte in the filter is present. In addition to this, as the tablet was made in-house there is the possibility that some of the API did not make it into the pill press. This would amount to a small proportion of the API not making it into the analysis sample. However, it is unlikely that so much would be lost due to this. This probed thoughts into another potential factor that could be restricting the amount of API extracted, polarity. Since methanol is moderately polar and the polarity of 4-PMP is unknown, it could be a possibility that 4-PMP (HCl) is a lot less polar than methanol or not polar at all and thus has reduced solubility in methanol. This question was raised earlier in this thesis resulting in a solubility test taking place. This test proved that 4-PMP.3HCl's solubility limit is  $7.2 \text{ mg mL}^{-1}$ , suggesting that there should be no solubility issues in this experiment. To completely rule out polarity being an issue, this experiment would need to be re-run in a range of solvents.

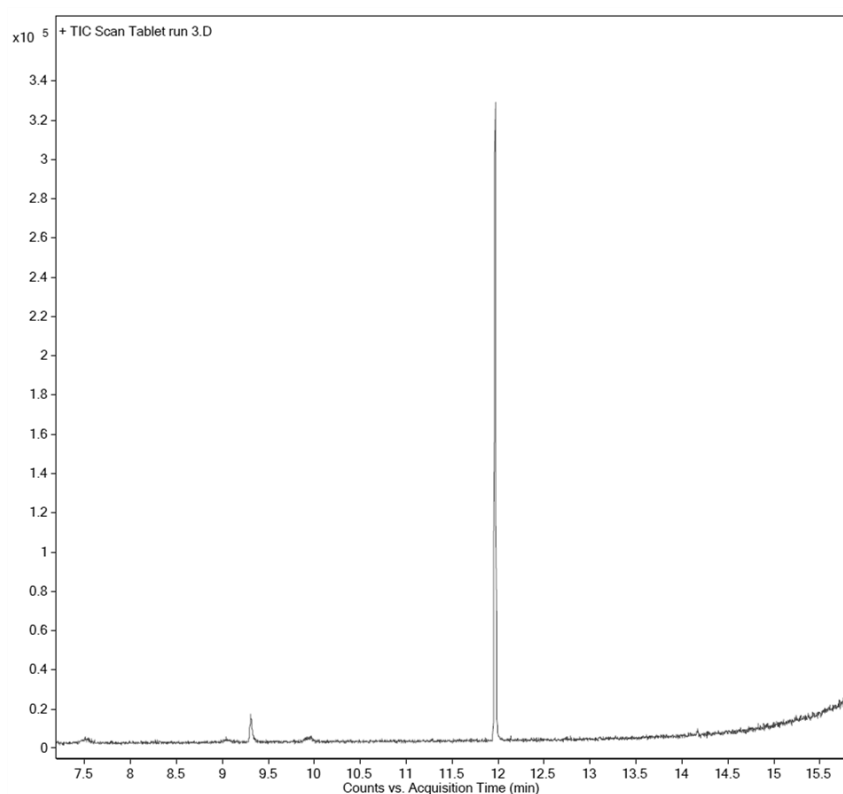


Figure 25: GC-MS chromatograph for the tablet analysis.

#### 6.4. Summary

The calibration standards performed correctly and led to a successful validation, which shows that this method has a lot of potential going forward. However, to successfully quantify the tablet, the extraction issues need to be addressed. Increasing the time in which the sample was sonicated for made no real difference to the result. In saying this, determining how polar the analyte is would also be extremely helpful. Furthermore, looking into other types of extraction methods could also be favourable. A common extraction method used for GC-MS is solid-phase micro extraction (SPME) which can completely remove the need for a solvent.<sup>84</sup>

#### 7. Hyperpolarisation of 1-(cyclohexylmethyl)-1*H*-indole-3-carboxylic acid 8-quinolinyl ester (BB-22)

Hyperpolarisation studies into BB-22 were undertaken to expand this work to another prevalent group of NPS, synthetic cannabinoids.<sup>7</sup> BB-22 was chosen because it offered a route into another group of NPS whilst creating another challenge in hyperpolarising such a bulky compound. The application of SABRE to bulkier and more sterically hindered compounds would be a breakthrough, as at the minute steric hindrance massively debilitates SABRE enhancements.



## 7.1. Results and Discussion

Resonances at  $\delta$  -13, -17 and -22 are indicative of the oxidative addition of *parahydrogen* to the catalyst, [Ir(IMes)(COD)Cl] (Figure 26). In addition to this the sample turned from dark yellow to light yellow in colour as a result of a change in oxidation state of the Ir centre, which is further evidence of this addition. In terms of hyperpolarisation, the observation of multiple hydride resonances suggests the formation of a number of complexes. Furthermore, the presence of an emission resonance at 8 ppm is exemplary of some minor hyperpolarisation, although the enhancement is less than unity. 2-PMP behaved very similarly (Section 3.11.1).

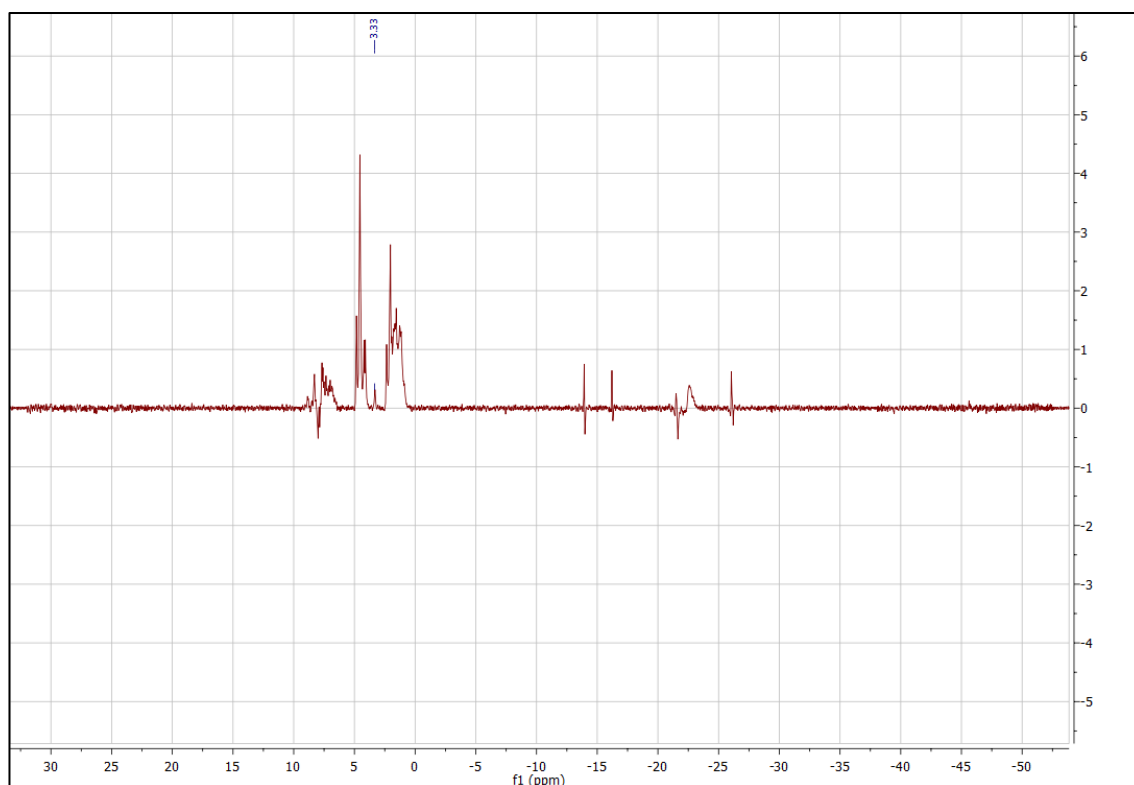


Figure 26: Low-field NMR spectrum for attempted hyperpolarisation of BB-22.

## 7.2.Summary

The potential to hyperpolarise big compounds such as BB-22 is there, just right now it is difficult to find the optimum parameters. A breakthrough in this area would open up a whole host of compounds to hyperpolarisation that were previously unhyperpolarisable.

## 8. Conclusion

To conclude, this work shows that it is possible to extract a compound of interest (NPS) from a common formulation (tablet) and subsequently hyperpolarise it. When the three freebased isomers were mixed together and analysed by NMR, it proved impossible to resolve the three. In light of this, all three were visually characterised by GC-MS as a mixture. This was made possible by firstly investigating the extent to which a group of piperazine isomers (2-, 3-, 4-PMP and 4-PMP.3HCl) hyperpolarise. As expected 4-PMP produced the largest enhancement ( $\epsilon \approx 300$ ). This is because of the decreased steric crowding compared to 2- and 3-PMP. In terms of hyperpolarisation, determining the optimum concentration of TEA was crucial in the development of an extraction method. TEA proved to be a good choice of base with enhancements as large as  $\epsilon \approx 363$  being observed (4-PMP.3HCl, 3 eq TEA). No other bases were investigated. It was found that a lower than optimum TEA concentration results in lower enhancement levels, thought to be the result of disproportionate deprotonation of the protonated nitrogen's. Excess TEA also resulted in lower enhancements. This is understood to be because TEA can compete with 4-PMP for binding sites on the catalyst. The 'shake and analyse' technique used through this work casted a shadow of doubt over results early on, due to the potential 20% variance that comes with it.<sup>65</sup> However, three eq of TEA relative to 4-PMP.3HCl was proven to be the ideal concentration to convert 4-PMP.3HCl to 4-PMP freebase. Upon evaluation of the literature, this work would have no doubt benefitted from a system similar to that used by S. B. Duckett *et al.*, demonstrated in their work.<sup>65</sup> The hyperpolarisation of the 4-PMP tablet really epitomises the work done as a whole in this study. The 138-fold enhancement observed when 4-PMP was isolated from the tablet and swiftly hyperpolarised, is a direct result of a simple but effective extraction

process. This also makes the method easily applicable to real world situations. Furthermore, since low substrate concentrations are permitted (as SABRE boosts detection limits of low-level analytes), sample preparation is relatively simple and data acquisition is very quick, making the novelty of this approach comprehensible. Moreover, in the grand scheme of SABRE hyperpolarisation, this research goes a step further than simply hyperpolarising compounds. It provides a niche application to an ever-evolving research area, NPS, opening the door for further development. The tablet was also analysed by GC-MS in an attempt to quantify. The linearity shown in Figure 21 and Figure 22 are acceptable, however, API extraction issues meant the concentration calculated was 28 mg lower than expected. Some loss of API is expected due to human/systematic error during weighing, tablet pressing and filtration, however this is too large a loss for any or all of those factors to be the cause. Increasing the time that the sample was subjected to ultrasonication made no difference, leading to the belief that polarity may be the concern since methanol is moderately polar and the polarity of 4-PMP is unknown. This would cause a reduction in the amount of dissolved analyte. The SA quantification method provided a strong level of accuracy (accurate to within 2% with 4-PMP), giving the technique strong potential as a method of choice, particularly due to its suitability to small sample sizes. The method of IS also provided acceptable linearity and is more favourable to large sample sizes whilst eliminating SA's requirement for an analyte stock.

## 9. Future Work

It would be great to continue this work to understand in more detail how the protonated nitrogen atoms of the NPS are deprotonated with TEA. This could be done by investigating NPS in their HCl salt form, which contain both more and less nitrogen's. One experiment that is of particular interest would be to slightly alter what was done in this work, to see if the observed results were similar. It would involve adding HCl to a freebased PMP isomer, essentially changing it to its HCl form, before analysing it like seen in this work. In this instance, the product may contain a mixture of freebased and HCl salt isomers and it would be interesting to see how such a mixture would react to the addition of TEA prior to hyperpolarisation. Another route for future work would be to analyse a wider range of NPS. This would help to build a bigger picture around freebasing and hyperpolarising NPS. The question 'would the same trends seen in this work carry through to other drug compounds?' is one that if answered, would further the research conducted herein. Furthermore, seeing this work applied to an established drug analysis group is also possible. Due to the relative simplicity of the extraction and analysis method, it isn't so farfetched that it couldn't be situated in police stations or at borders. Finally, in terms of hyperpolarisation, it would be truly fantastic to broaden the horizons of the topic and try to 'rock the apple cart' in terms of hyperpolarisation limits. Working with bigger and bulkier compounds to see if they are hyperpolarisable is a very feasible route of research and would open a whole host of avenues for hyperpolarisation to combine with.

## 10. Appendix

### 10.1. Characterisation Data for 2-PMP

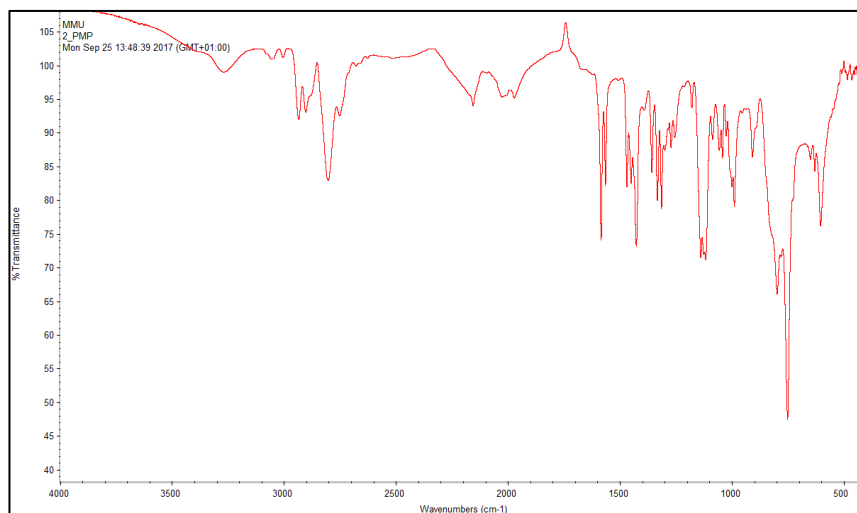


Figure 27: IR Spectrum for 2-PMP.

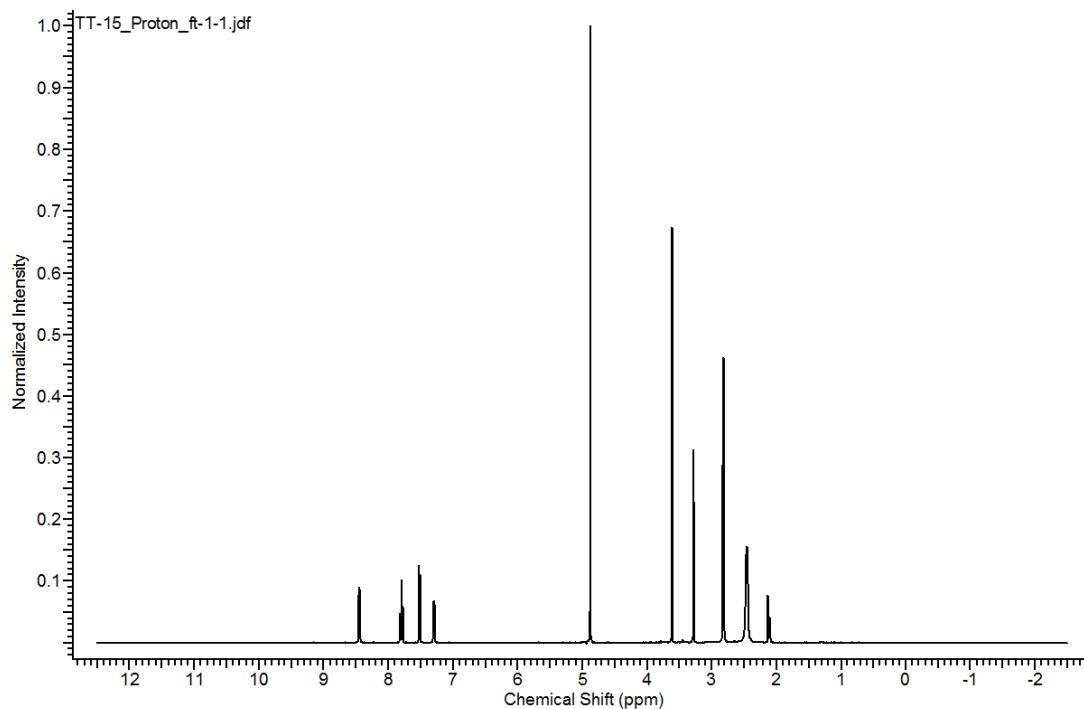


Figure 28: High-field  $^1\text{H}$  NMR spectrum for 2-PMP.

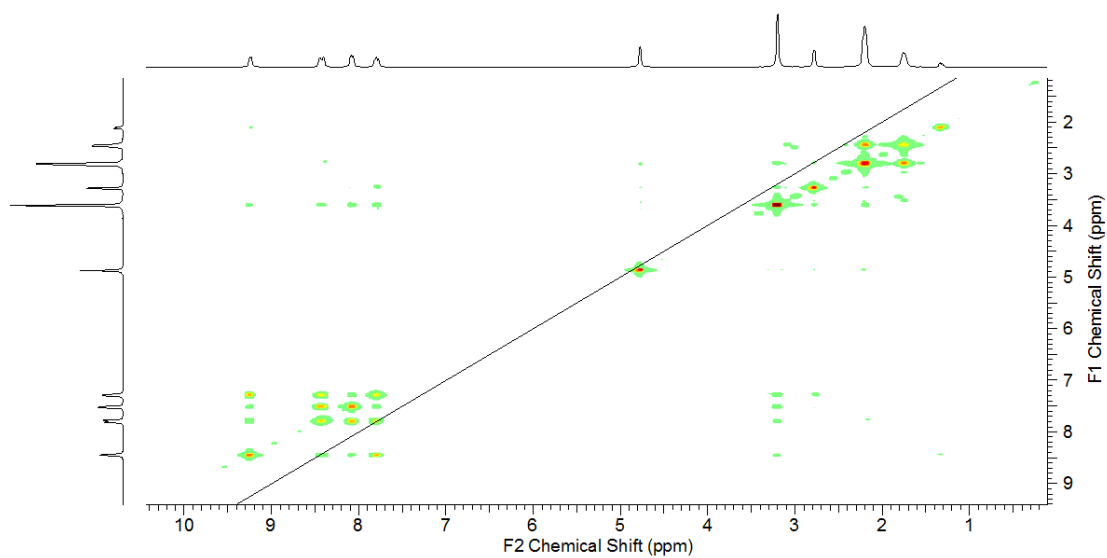


Figure 29: High-field NMR  $^1\text{H}$ - $^1\text{H}$  COSY for 2-PMP.

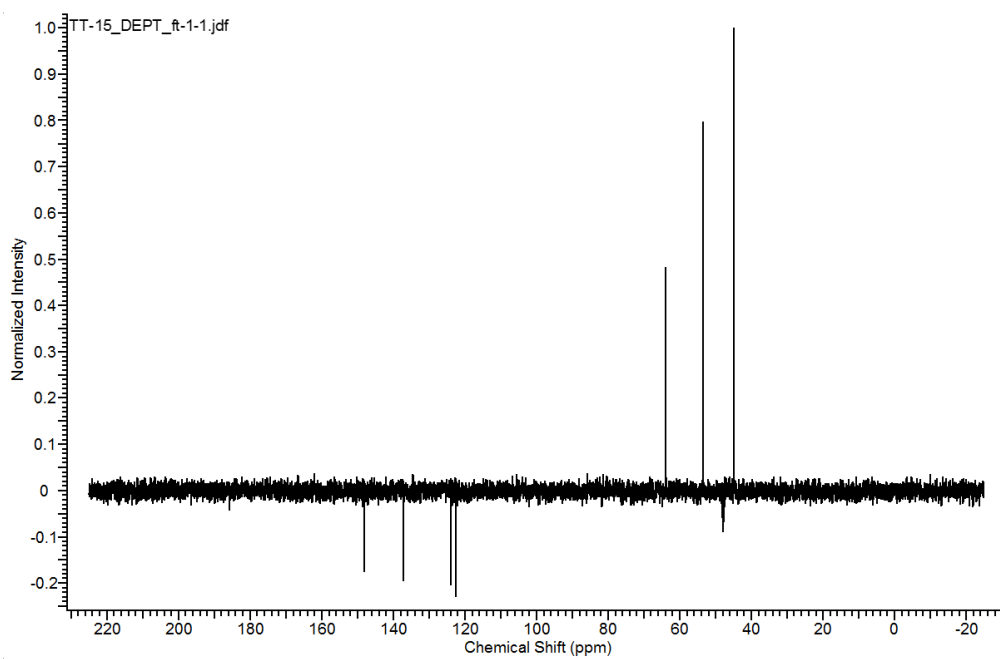


Figure 30: High-field DEPT NM for 2-PMP.

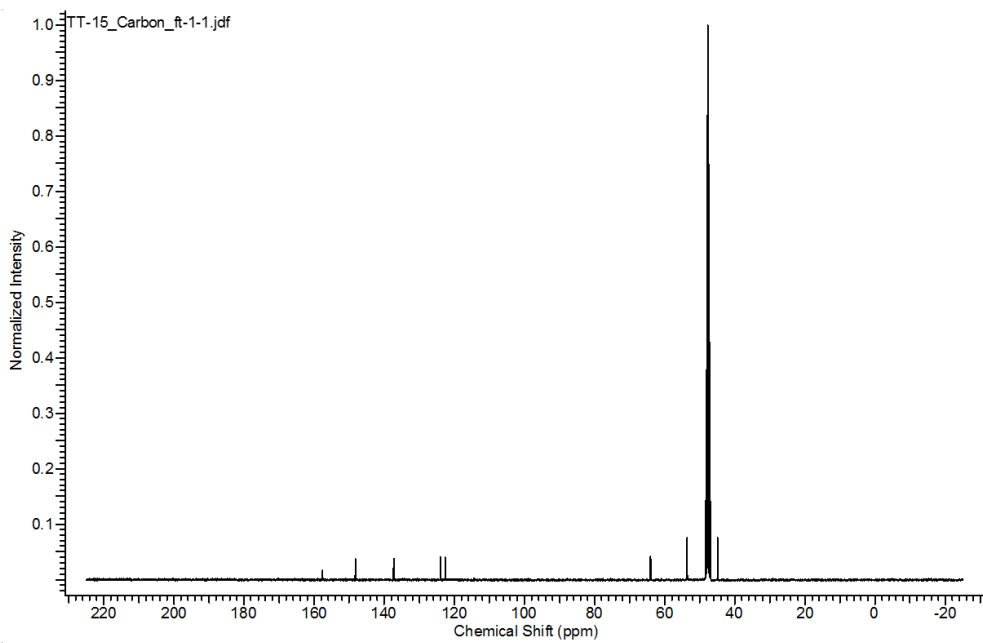


Figure 31: High-field  $^{13}\text{C}$  NMR for 2-PMP.

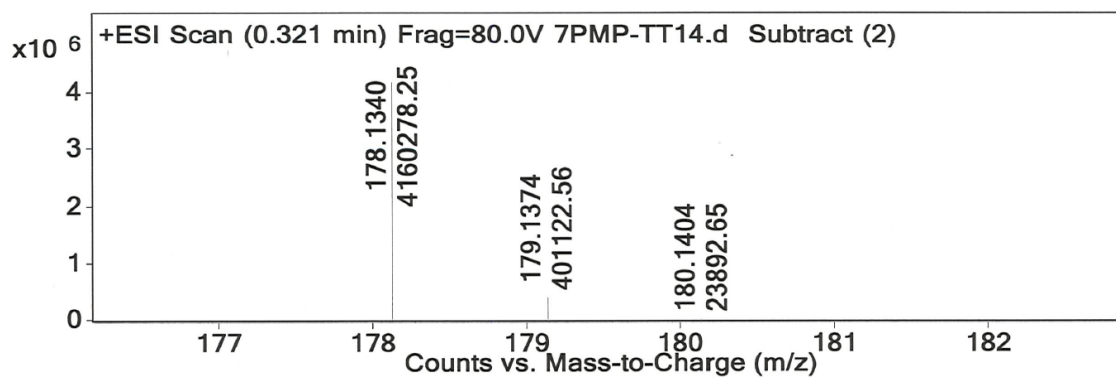


Figure 32 LC-MS spectrum for 2-PMP.



## 10.2. Characterisation Data for 3-PMP

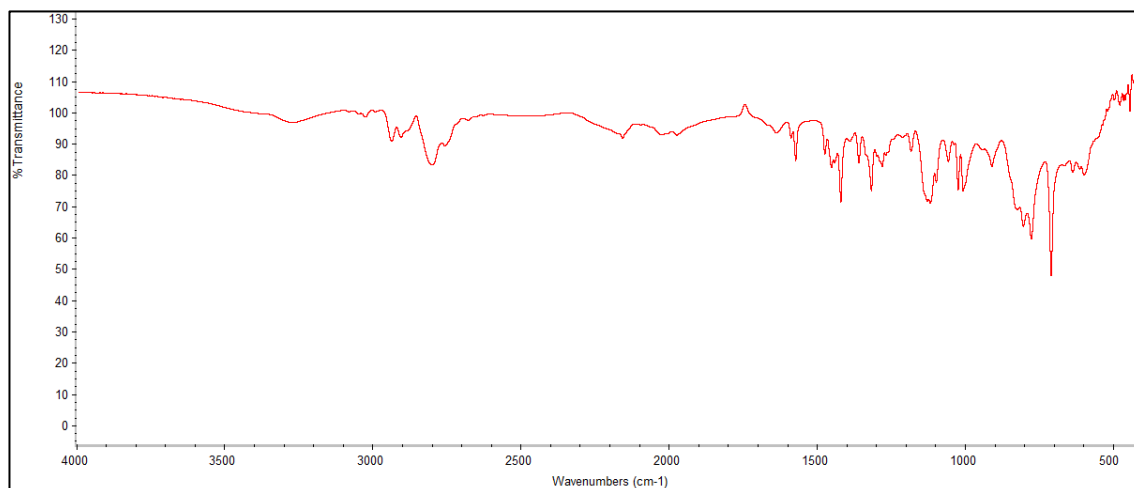


Figure 33: IR spectrum for 3-PMP.

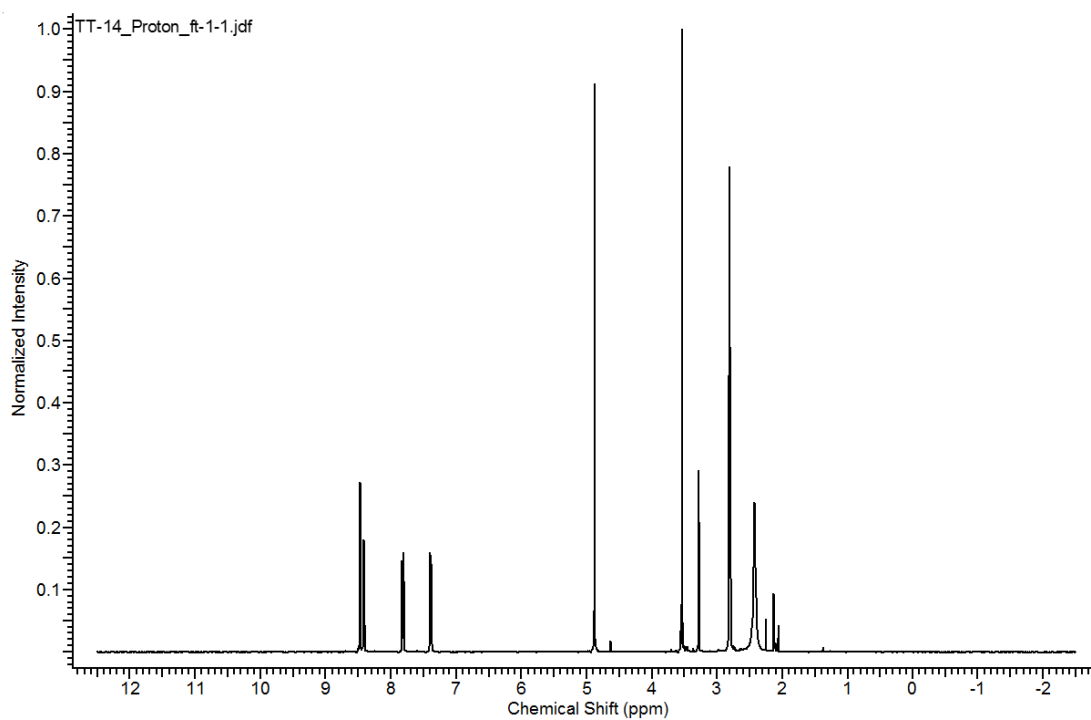


Figure 34: High-field <sup>1</sup>H NMR spectrum for 3-PMP.

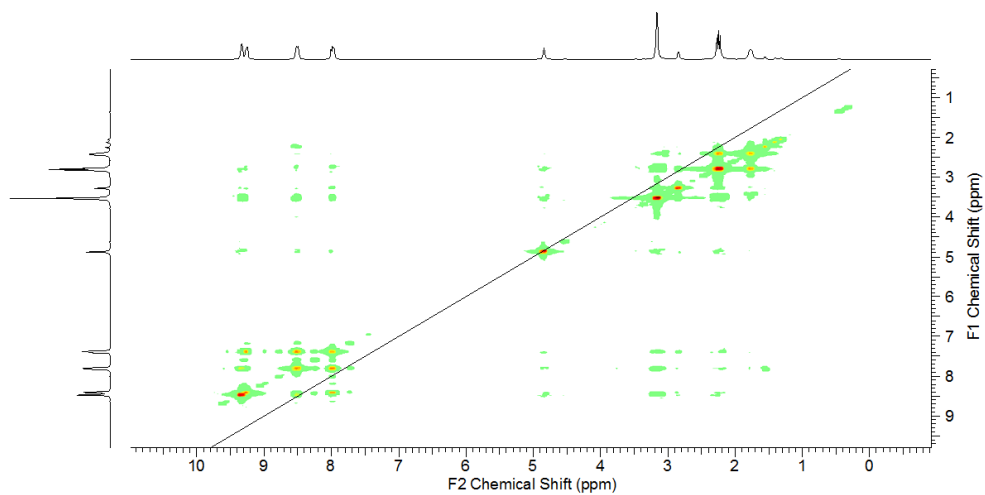


Figure 35: High-field  $^1\text{H}$ - $^1\text{H}$  COSY NMR for 3-PMP.

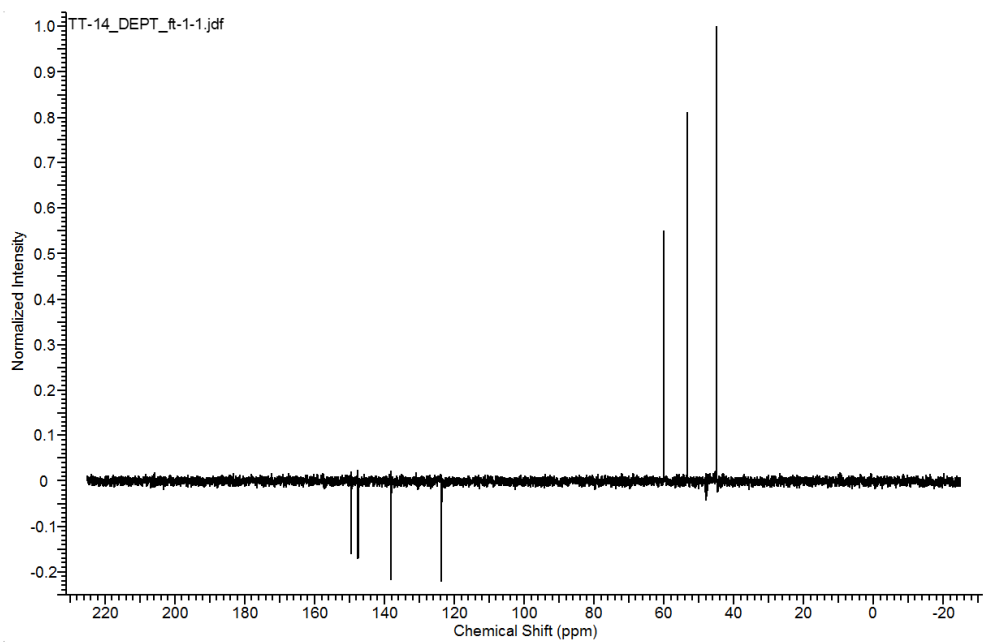


Figure 36: High-field DEPT NMR for 3-PMP.

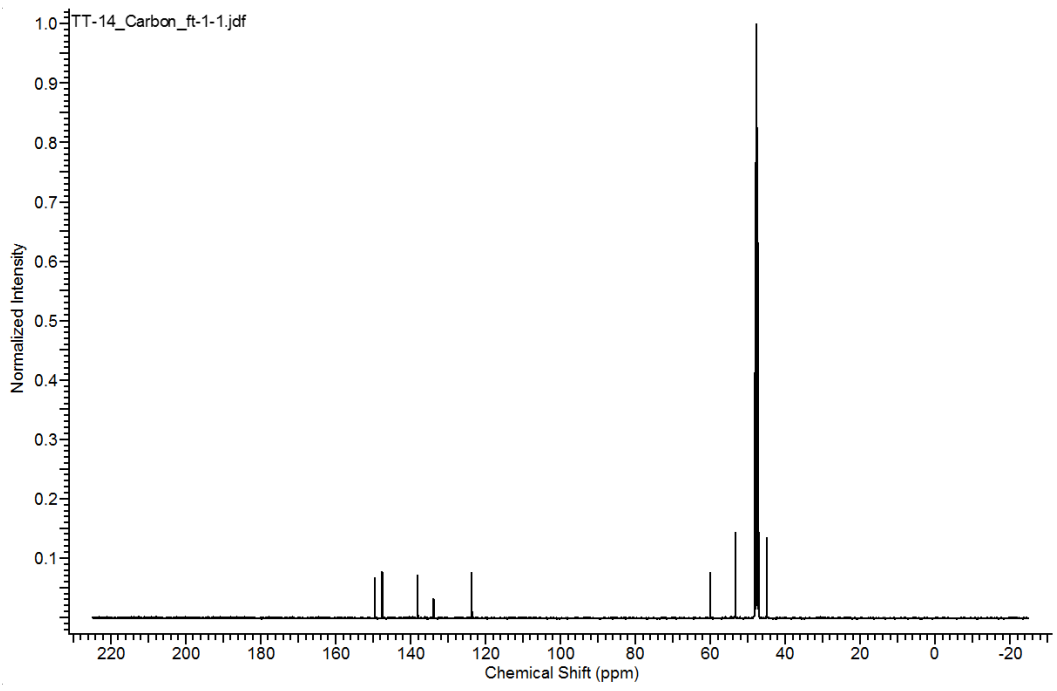


Figure 37: High-field  $^{13}\text{C}$  NMR.

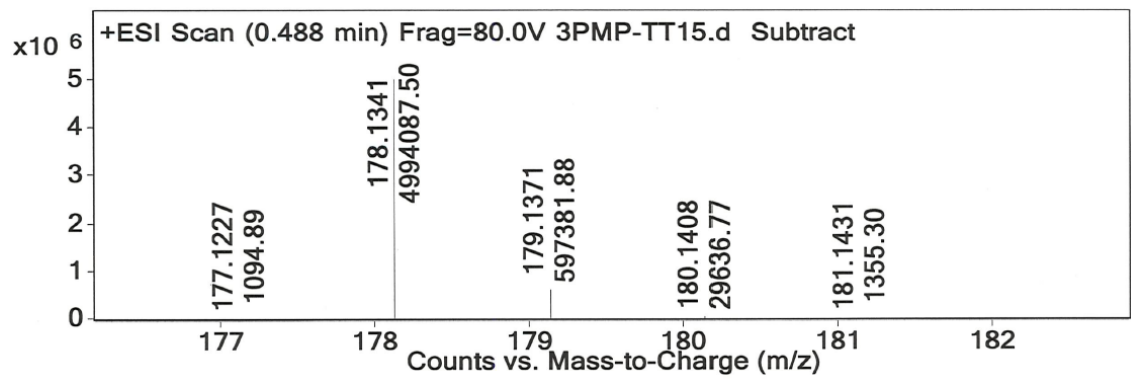


Figure 38: LC-MS spectrum for 3-PMP.

### 10.3. Characterisation Data for 4-PMP

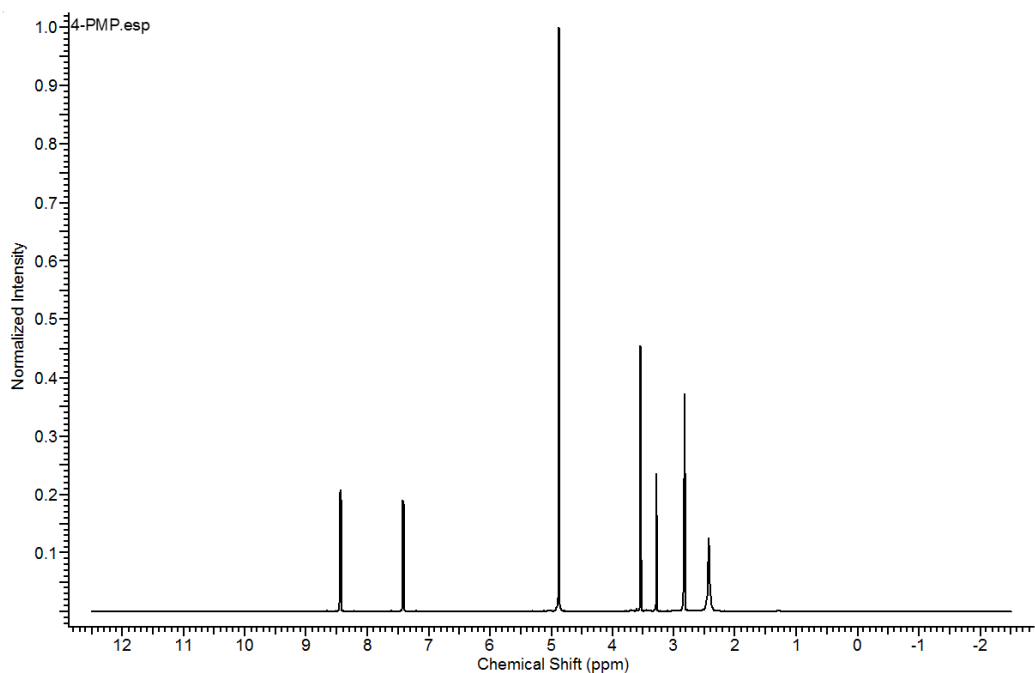


Figure 39: High-field  $^1\text{H}$  NMR spectrum for 4-PMP.

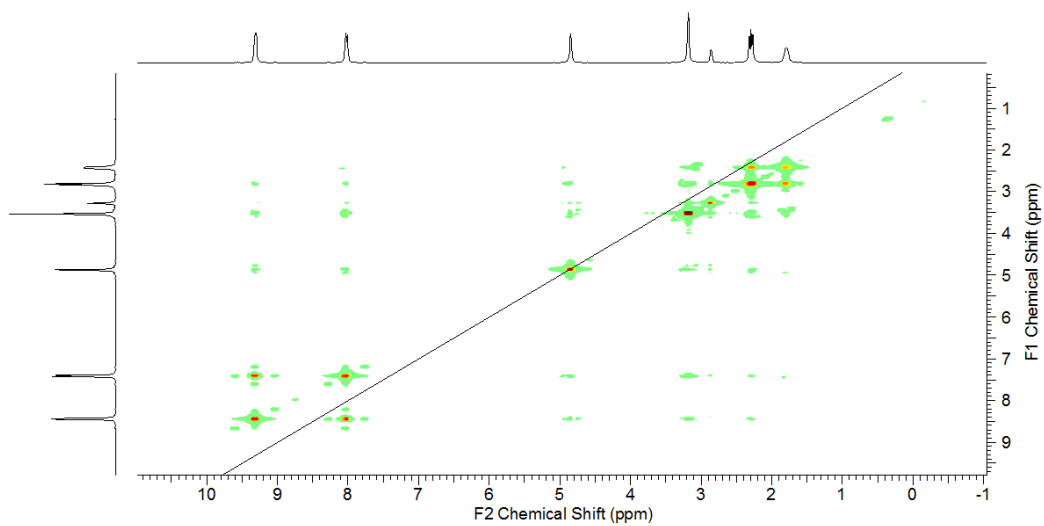


Figure 40: High-field  $^1\text{H}$ - $^1\text{H}$  COSY spectrum for 4-PMP.

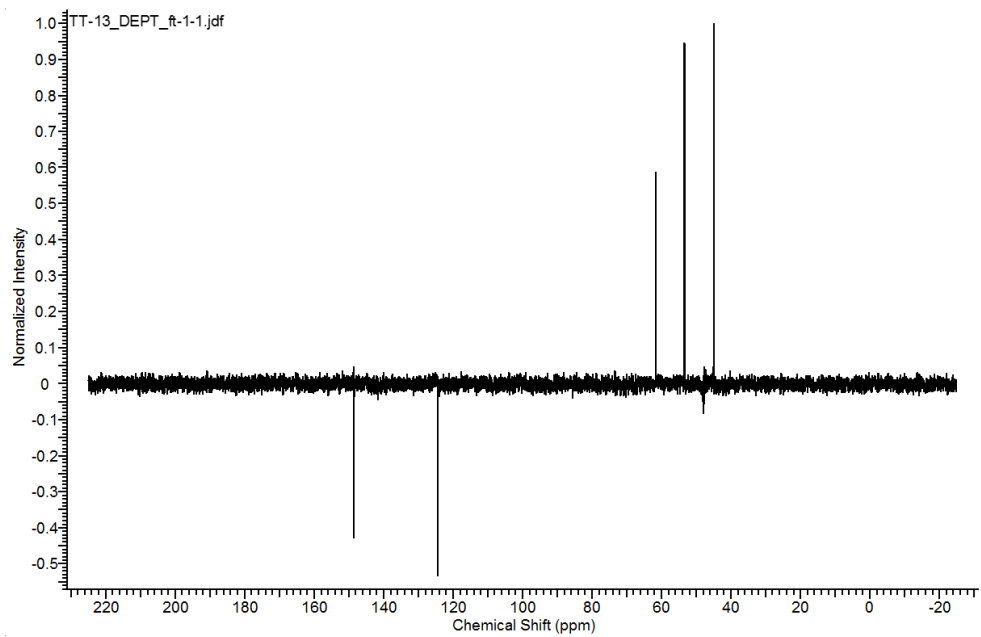


Figure 41: High-field DEPT NMR for 4-PMP.

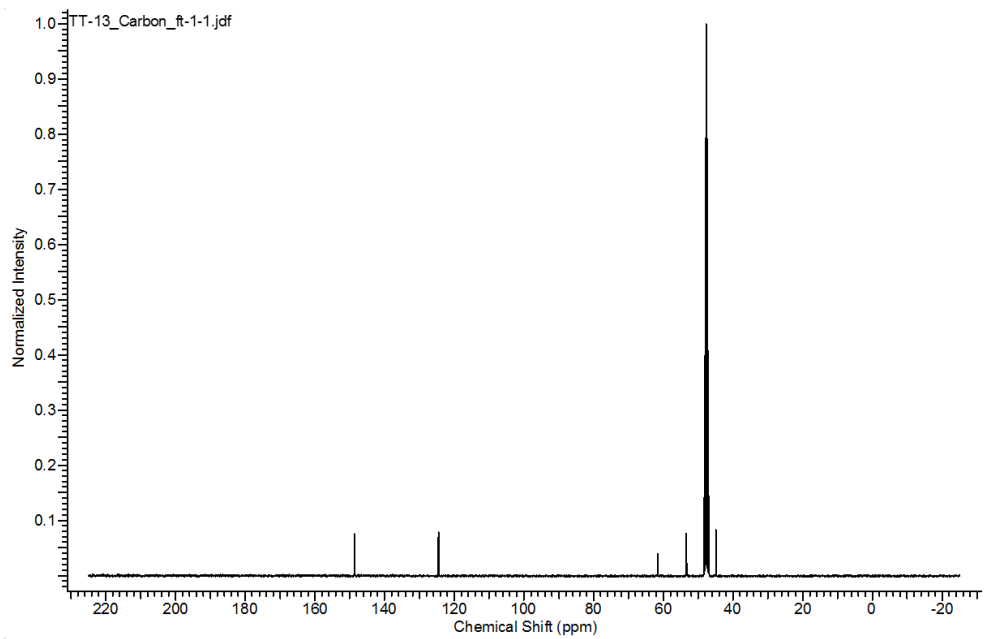


Figure 42: High-field  $^{13}\text{C}$  NMR for 4-PMP.

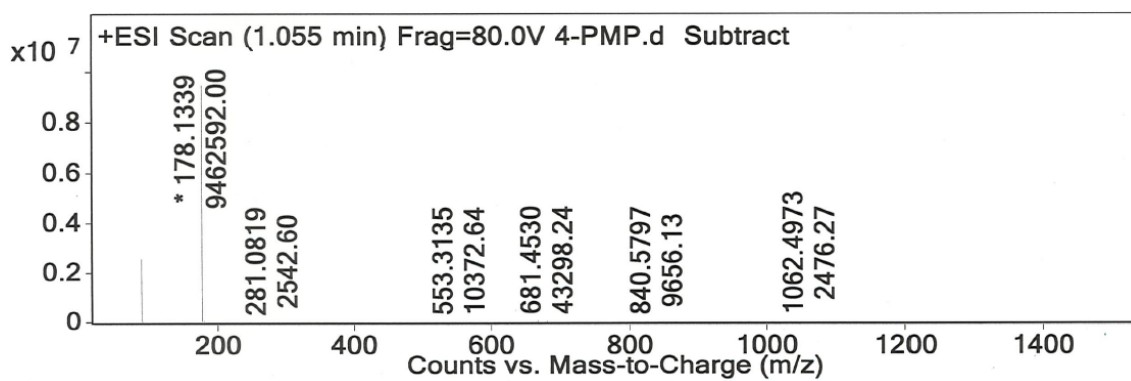


Figure 43: LC-MS spectrum for 4-PMP.

#### 10.4. Characterisation Data for 4-PMP.3HCl

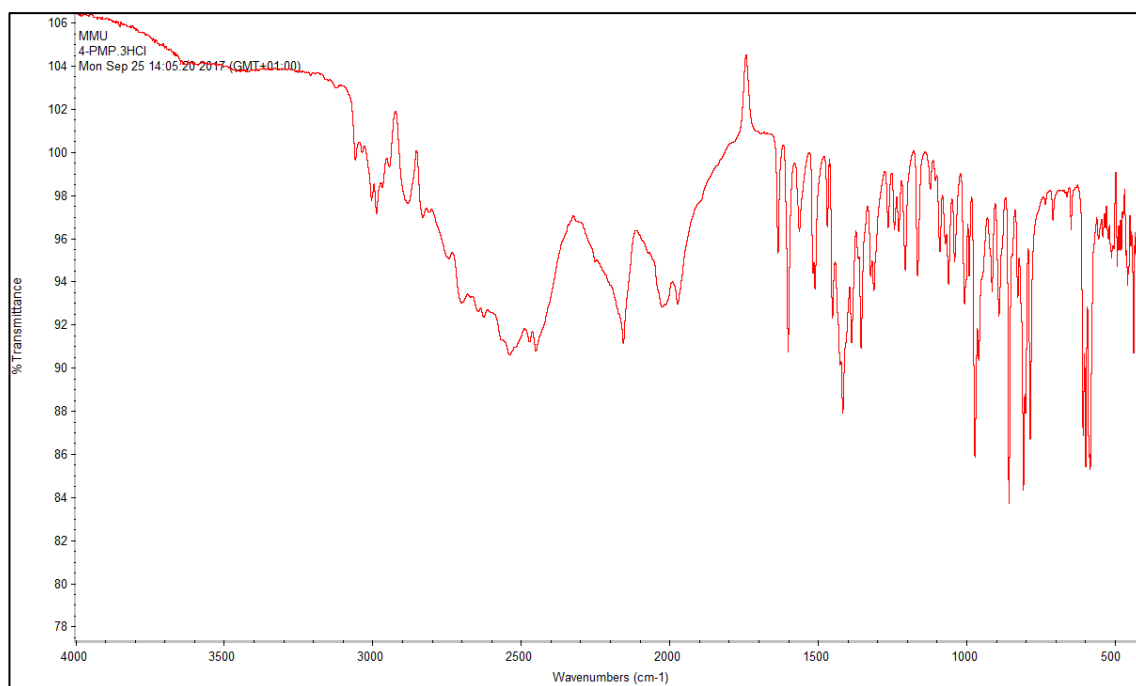


Figure 44: IR spectrum for 4-PMP.3HCl.

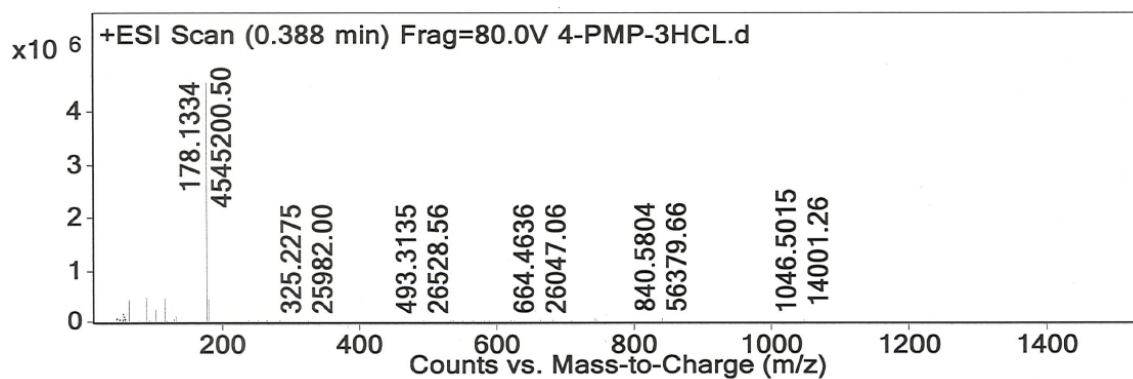


Figure 45: LC-MS spectrum for 4-PMP.3HCl.

10.5. Characterisation Data for 4-PMP.3HCl Tablet

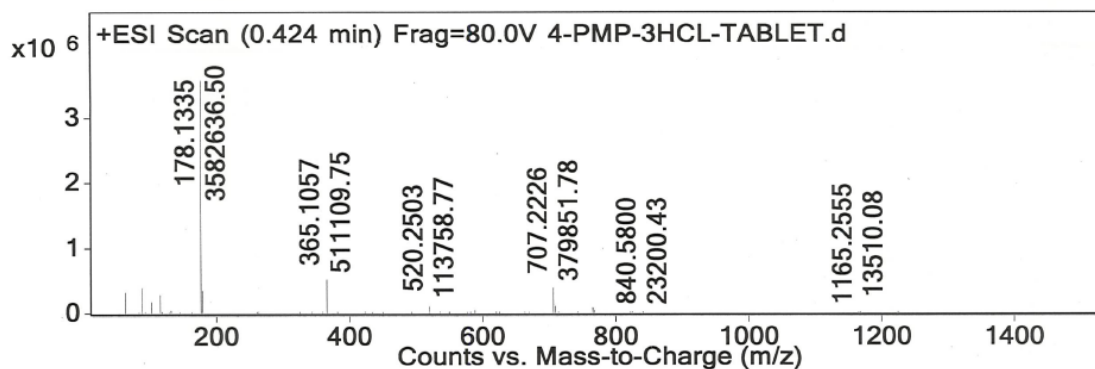


Figure 46: LC-MS spectrum for 4-PMP.3HCl tablet.

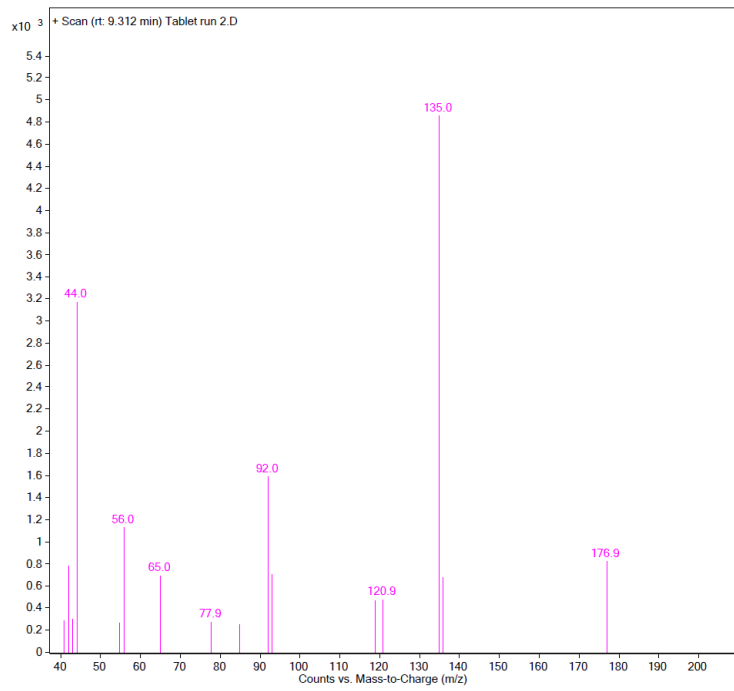


Figure 47: GC-MS for 4-PMP.3HCl tablet.



10.6. Characterisation Data for BB-22

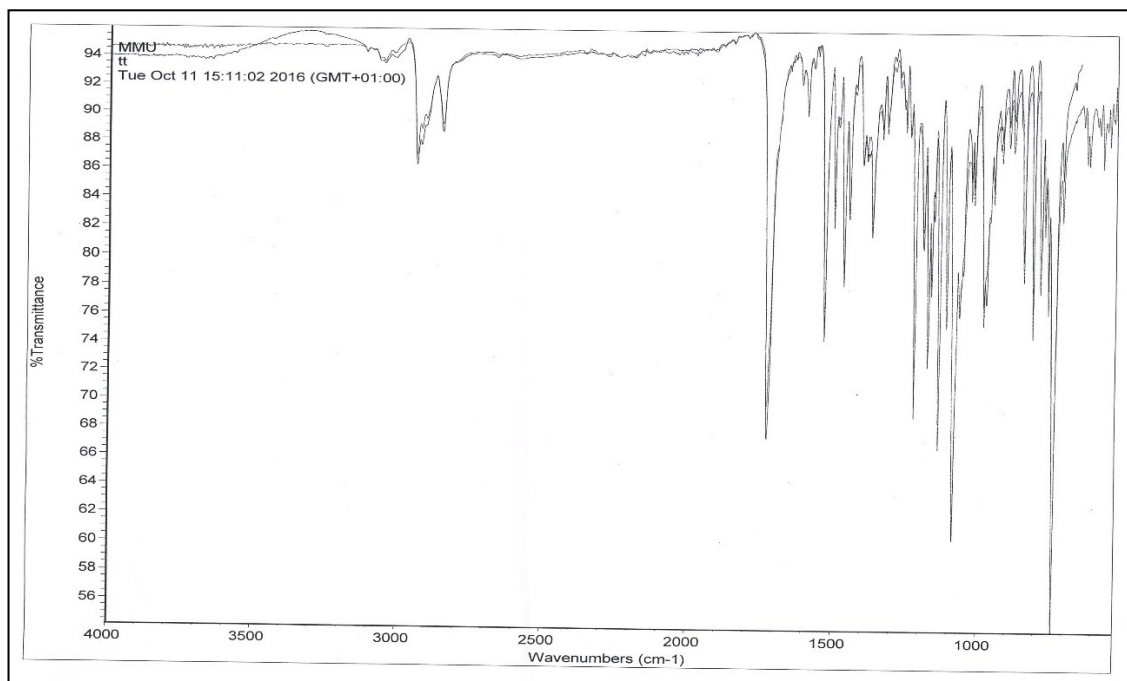


Figure 48: IR spectrum for BB-22.

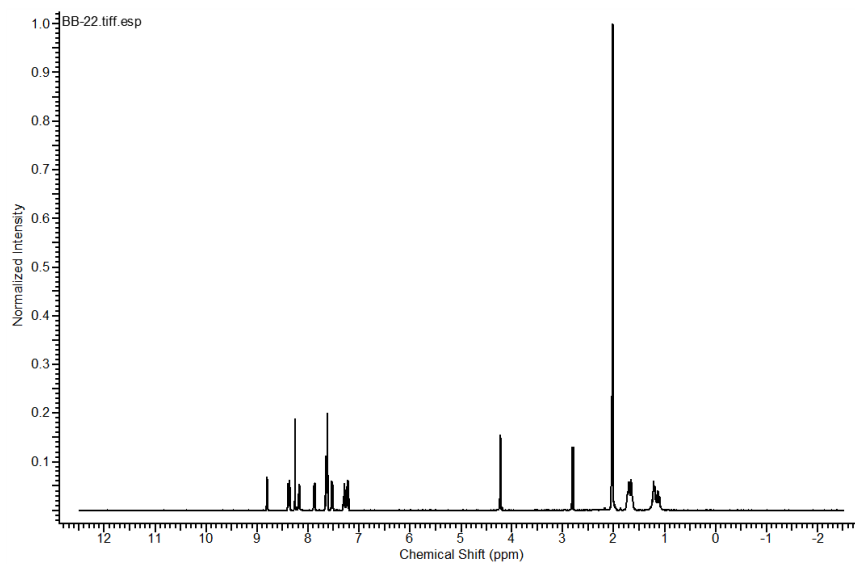


Figure 49: High-field  $^1\text{H}$  NMR spectrum for BB-22.

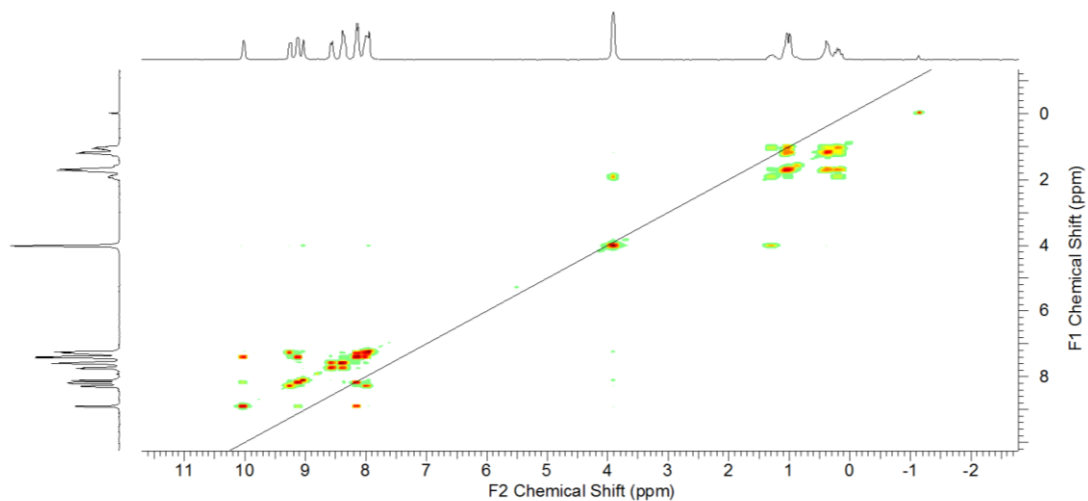


Figure 50: High-field <sup>1</sup>H-<sup>1</sup>H COSY NMR spectrum for BB-22.

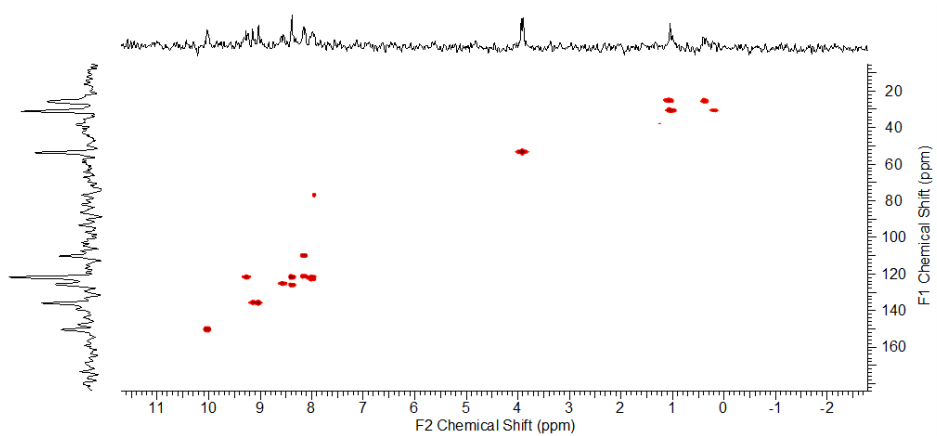


Figure 51: High-field HMQC NMR spectrum for BB-22.

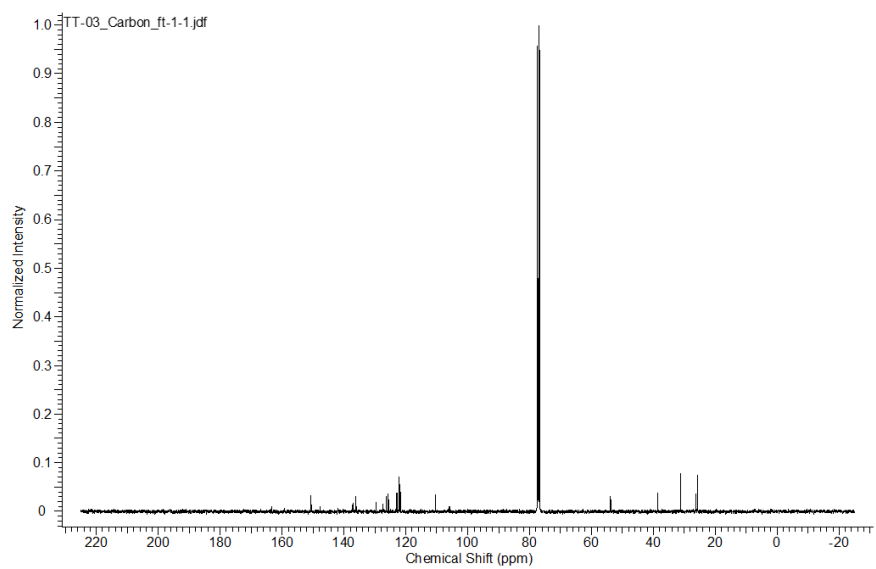


Figure 52: High-field  $^{13}\text{C}$  NMR spectrum for BB-22.

## 11. Bibliography

1. L. A. King and A. T. Kicman, *Drug testing and analysis*, 2011, **3**, 401-403.
2. P. Reuter and B. Pardo, *Int. J. Drug. Policy*, 2017, **40**, 117-122.
3. R. M. Baum, *Chem. Eng. News.*, 1985, **63**, 7-16.
4. G. P. Galloway, S. L. Frederick, F. E. Staggers, M. Gonzales, S. A. Stalcup and D. E. Smith, *Addiction*, 1997, **92**, 89-96.
5. F. Hutton, *Aust. NZ. J. Criminol.*, 2017, **50**, 282-306.
6. M. Coppola and R. Mondola, *Toxicol. Lett.*, 2012, **211**, 144-149.
7. S. Hudson and J. Ramsey, *Drug testing and analysis*, 2011, **3**, 466-478.
8. UNODC, *Market Analysis of Synthetic Drugs*, 2017.
9. DEA, *2016 National Drug Threat Assessment Summary*, U.S.A, 2016.
10. C. Bye, A. D. Munro-Faure, A. W. Peck and P. A. Young, 1973, **6**, 163-169.
11. S. Elliott, *Drug testing and analysis*, 2011, **3**, 430-438.
12. M. D. Arbo, M. L. Bastos and H. F. Carmo, *Drug. Alcohol. Depen*, 2011, **122**, 174-185.
13. The New Zealand Census of Population and Dwellings, <http://www.stats.govt.nz/Census/2013-census.aspx>, (accessed 12/09/2017, 2017).
14. Psychoactive Substances Act 2016, <http://www.legislation.gov.uk/ukpga/2016/2/contents>, (accessed 13/09/2017, 2017).
15. G. Murrow, M. Girling, P. Sweetsur, T. Huckle and J. Huakau, *Legal party pill use in New Zealand*, Wellington, 2006.
16. W. H. Organisation, *N-Benzylpiperazine (BZP) Critical Review Report*, 2014.
17. R. A. Butler and J. L. Sheridan, *Harm Reduct. J.*, 2007, **4**, 18-18.
18. B. M. Z. Cohen and R. Butler, *Int. J. Drug. Policy.*, 2011, **22**, 95-101.
19. E. M. Purcell, H. C. Torrey and R. V. Pound, *Phys. Rev.*, 1946, **69**, 37-38.
20. F. Bloch, W. W. Hansen and M. Packard, *Phys. Rev.*, 1946, **69**, 127-127.
21. H. Günther, *NMR spectroscopy: basic principles, concepts, and applications in chemistry*, Wiley, Chichester, 2 edn., 1995.
22. J. C. Edwards, *Journal*, 2015, 1-27.
23. **M. Nerz-Stormes**, The Basics Nuclear Magnetic Resonance Spectroscopy, [http://www.brynmawr.edu/chemistry/Chem/mnerzsto/The\\_Basics\\_Nuclear\\_Magnetic\\_Resonance%20Spectroscopy\\_2.htm](http://www.brynmawr.edu/chemistry/Chem/mnerzsto/The_Basics_Nuclear_Magnetic_Resonance%20Spectroscopy_2.htm), (accessed 02/09/2017, 2017).
24. V. Domenici, *Liquid Crystals Today*, 2017, **26**, 2-10.
25. E. Breitmaier, in *Structure Elucidation by NMR in Organic Chemistry*, John Wiley & Sons, Ltd, 2002, pp. 1-10.
26. M. Michigan State University, Nuclear Magnetic Resonance Spectroscopy, <https://www2.chemistry.msu.edu/faculty/reusch/virttxtjml/spectrpy/nmr/nmr1.htm>, (accessed 02/09/2017, 2017).
27. R. E. Mewis, R. A. Green, M. C. R. Cockett, M. J. Cowley, S. B. Duckett, G. G. R. Green, R. O. John, P. J. Rayner and D. C. Williamson, *J. Phys. Chem. B*, 2015, **119**, 1416-1424.
28. M. L. Hirsch, N. Kalechofsky, A. Belzer, M. Rosay and J. G. Kempf, *J. Am. Chem. Soc.*, 2015, **137**, 8428-8434.

29. A. Comment, J. Rentsch, F. Kurdzesau, S. Jannin, K. Uffmann, R. B. van Heeswijk, P. Hautle, J. A. Konter, B. van den Brandt and J. J. van der Klink, *J. Magn. Reson.*, 2008, **194**, 152-155.
30. M. E. Halse, *Trac-Trend. Anal. Chem.*, 2016, **83**, 76-83.
31. C. Griesinger, M. Bennati, H. M. Vieth, C. Luchinat, G. Parigi, P. Hofer, F. Engelke, S. J. Glaser, V. Denysenkov and T. F. Prisner, *Prog. Nucl. Mag. Res. Sp.*, 2012, **64**, 4-28.
32. E. Bouleau, P. Saint-Bonnet, F. Mentink-Vigier, H. Takahashi, J. F. Jacquot, M. Bardet, F. Aussenac, A. Porea, F. Engelke, S. Hediger, D. Lee and G. De Paepe, *Chem. Sci.*, 2015, **6**, 6806-6812.
33. N. J. Brownbill, D. Gajan, A. Lesage, L. Emsley and F. Blanc, *Chem. Commun.*, 2017, **53**, 2563-2566.
34. A. J. Rossini, A. Zagdoun, M. Lelli, A. Lesage, C. Copéret and L. Emsley, *Accounts Chem. Res.*, 2013, **46**, 1942-1951.
35. A. S. Edison and F. C. Schroeder, in *Comprehensive Natural Products II*, Elsevier, Oxford, 2010, DOI: <https://doi.org/10.1016/B978-008045382-8.00196-9>, pp. 169-196.
36. K. R. Keshari, A. P. Tikunov, H. Lee and J. M. Macdonald, in *Encyclopedia of Spectroscopy and Spectrometry (Third Edition)*, eds. G. E. Tranter and D. W. Koppenaal, Academic Press, Oxford, 2017, DOI: <https://doi.org/10.1016/B978-0-12-409547-2.12116-X>, pp. 143-148.
37. M. S. Rosen, T. E. Chupp, K. P. Coulter, R. C. Welsh and S. D. Swanson, *Rev. Sci. Instrum.*, 1999, **70**, 1546-1552.
38. T. G. Walker and W. Happer, *Rev. Mod. Phys.*, 1997, **69**, 629-642.
39. F. W. Hersman, I. C. Ruset, S. Ketel, I. Muradian, S. D. Covrig, J. Distelbrink, W. Porter, D. Watt, J. Ketel, J. Brackett, A. Hope and S. Patz, *Acad. Radiol.*, 2008, **15**, 683-692.
40. C. R. Bowers and D. P. Weitekamp, *J. Am. Chem. Soc.*, 1987, **109**, 5541-5542.
41. K. V. Kovtunov, M. L. Truong, D. A. Barskiy, I. V. Koptuyug, A. M. Coffey, K. W. Waddell and E. Y. Chekmenev, *Chem. Eur. J.*, 2014, **20**, 14629-14632.
42. R. E. Mewis, *Magn. Reson. Chem.*, 2015, **53**, 789-800.
43. S. B. Duckett and R. E. Mewis, *Accounts Chem. Res.*, 2012, **45**, 1247-1257.
44. L. T. Kuhn and J. Bargon, in *In Situ Nmr Methods in Catalysis*, eds. J. Bargon and L. T. Kuhn, Springer-Verlag Berlin, Berlin, 2007, vol. 276, pp. 25-68.
45. H. Sengstschmid, R. Freeman, J. Barkemeyer and J. Bargon, *J. Magn. Reson. Ser. A*, 1996, **120**, 249-257.
46. R. A. Green, R. W. Adams, S. B. Duckett, R. E. Mewis, D. C. Williamson and G. G. R. Green, *Prog. Nucl. Mag. Res. Sp.*, 2012, **67**, 1-48.
47. K. D. Atkinson, M. J. Cowley, S. B. Duckett, P. I. P. Elliott, G. G. R. Green, J. Lopez-Serrano, I. G. Khazal and A. C. Whitwood, *Inorg. Chem.*, 2009, **48**, 663-670.
48. M. J. Cowley, R. W. Adams, K. D. Atkinson, M. C. R. Cockett, S. B. Duckett, G. G. R. Green, J. A. B. Lohman, R. Kerssebaum, D. Kilgour and R. E. Mewis, *J. Am. Chem. Soc.*, 2011, **133**, 6134-6137.
49. L. S. Lloyd, A. Asghar, M. J. Burns, A. Charlton, S. Coombes, M. J. Cowley, G. J. Dear, S. B. Duckett, G. R. Genov, G. G. R. Green, L. A. R. Highton, A. J. J. Hooper, M. Khan, I. G. Khazal, R. J. Lewis, R. E. Mewis, A. D. Roberts and A. J. Ruddlesden, *Catal. Sci. Technol.*, 2014, **4**, 3544-3554.
50. S. Loukiala, J. Ratilainen, K. Airola, J. Valkonen and K. Rissanen, *Acta Chem. Scand.*, 1998, **52**, 593-602.

51. M. L. Hamad, *J. Chem. Educ.*, 2013, **90**, 1662-1664.
52. VALIDATION OF ANALYTICAL PROCEDURES: TEXT AND METHODOLOGY Q2(R1), [http://www.ich.org/fileadmin/Public\\_Web\\_Site/ICH\\_Products/Guidelines/Quality/Q2\\_R1/Step4/Q2\\_R1\\_Guideline.pdf](http://www.ich.org/fileadmin/Public_Web_Site/ICH_Products/Guidelines/Quality/Q2_R1/Step4/Q2_R1_Guideline.pdf), (accessed 10/10/16, 2016).
53. D. A. Barskiy, K. V. Kovtunov, I. V. Koptuyug, P. He, K. A. Groome, Q. A. Best, F. Shi, B. M. Goodson, R. V. Shchepin, M. L. Truong, A. M. Coffey, K. W. Waddell and E. Y. Chekmenev, *Chemphyschem*, 2014, **15**, 4100-4107.
54. V. Daniele, F. X. Legrand, P. Berthault, J. N. Dumez and G. Huber, *Chemphyschem*, 2015, **16**, 3413-3417.
55. S. Duckett, M. Fekete, P. J. Rayner and G. G. R. Green, *Magn. Reson. Chem*, 2017.
56. N. Eshuis, B. J. A. van Weerdenburg, M. C. Feiters, F. Rutjes, S. S. Wijmenga and M. Tessari, *Angew. Chem. Int. Edit.*, 2015, **54**, 1481-1484.
57. H. F. Zeng, J. D. Xu, J. Gillen, M. T. McMahon, D. Artemov, J. M. Tyburn, J. A. B. Lohman, R. E. Mewis, K. D. Atkinson, G. G. R. Green, S. B. Duckett and P. C. M. van Zijl, *J. Magn. Reson.*, 2013, **237**, 73-78.
58. P. J. Rayner, M. J. Burns, A. M. Olaru, P. Norcott, M. Fekete, G. G. R. Green, L. A. R. Highton, R. E. Mewis and S. B. Duckett, *Natl. Acad. Sci. U. S. A.*, 2017, **114**, E3188-E3194.
59. R. W. Adams, J. A. Aguilar, K. D. Atkinson, M. J. Cowley, P. I. P. Elliott, S. B. Duckett, G. G. R. Green, I. G. Khazal, J. Lopez-Serrano and D. C. Williamson, *Science*, 2009, **323**, 1708-1711.
60. S. Glogglar, M. Emondts, J. Colell, R. Muller, B. Blumich and S. Appelt, *Analyst*, 2011, **136**, 1566-1568.
61. M. L. Truong, F. Shi, P. He, B. Yuan, K. N. Plunkett, A. M. Coffey, R. V. Shchepin, D. A. Barskiy, K. V. Kovtunov, I. V. Koptuyug, K. W. Waddell, B. M. Goodson and E. Y. Chekmenev, *J. Phys. Chem. B*, 2014, **118**, 13882-13889.
62. R. V. Shchepin, M. L. Truong, T. Theis, A. M. Coffey, F. Shi, K. W. Waddell, W. S. Warren, B. M. Goodson and E. Y. Chekmenev, *J. Phys. Chem. Lett*, 2015, **6**, 1961-1967.
63. K. D. Atkinson, M. J. Cowley, P. I. P. Elliott, S. B. Duckett, G. G. R. Green, J. Lopez-Serrano and A. C. Whitwood, *J. Am. Chem. Soc.*, 2009, **131**, 13362-13368.
64. A. N. Pravdivtsev, K. L. Ivanov, A. V. Yurkovskaya, P. A. Petrov, H. H. Limbach, R. Kaptein and H. M. Vieth, *J. Magn. Reson.*, 2015, **261**, 73-82.
65. R. E. Mewis, K. D. Atkinson, M. J. Cowley, S. B. Duckett, G. G. R. Green, R. A. Green, L. A. R. Highton, D. Kilgour, L. S. Lloyd, J. A. B. Lohman and D. C. Williamson, *Magn. Reson. Chem.*, 2014, **52**, 358-369.
66. P. Spanning, I. Reile, M. Emondts, P. P. M. Schleker, N. K. J. Hermkens, N. G. J. van der Zwaluw, B. J. A. van Weerdenburg, P. Tinnemans, M. Tessari, B. Blumich, F. Rutjes and M. C. Feiters, *Chem. Eur. J.*, 2016, **22**, 9277-9282.
67. E. Danieli, J. Perlo, A. L. L. Duchateau, G. K. M. Verzijl, V. M. Litvinov, B. Blumich and F. Casanova, *Chemphyschem*, 2014, **15**, 3060-3066.
68. B. Pinter, T. Fievez, F. M. Bickelhaupt, P. Geerlings and F. De Proft, *Phys. Chem. Chem. Phys.*, 2012, **14**, 9846-9854.
69. C. L. Johnson, *J. Med. Chem.*, 1976, **19**, 600-605.
70. D. A. Barskiy, A. N. Pravdivtsev, K. L. Ivanov, K. V. Kovtunov and I. V. Koptuyug, *Phys. Chem. Chem. Phys.*, 2016, **18**, 89-93.
71. L. S. Lloyd, R. W. Adams, M. Bernstein, S. Coombes, S. B. Duckett, G. G. R. Green, R. J. Lewis, R. E. Mewis and C. J. Sleight, *J. Am. Chem. Soc.*, 2012, **134**, 12904-12907.

72. J. B. Bass, Jr., L. S. Farer, P. C. Hopewell, R. O'Brien, R. F. Jacobs, F. Ruben, D. E. Snider, Jr. and G. Thornton, *American journal of respiratory and critical care medicine*, 1994, **149**, 1359-1374.
73. K. M. Appleby, R. E. Mewis, A. M. Olaru, G. G. R. Green, I. J. S. Fairlamb and S. B. Duckett, *Chem. Sci.*, 2015, **6**, 3981-3993.
74. S. B. Duckett and R. E. Mewis, in *Hyperpolarization Methods in Nmr Spectroscopy*, ed. L. T. Kuhn, 2013, vol. 338, pp. 75-103.
75. M. Houllberghs, A. Hoffmann, D. Dom, C. E. A. Kirschhock, F. Taulelle, J. A. Martens and E. Breynaert, *Anal. Chem.*, 2017, **89**, 6940-6943.
76. S. M. S. A. D. Gift, P. K. Bokashanga, *J. Chem. Educ.*, 2012, **89**, 11.
77. M. Bader, *J. Chem. Educ.*, 1980, **57**, 703.
78. L. Cuadros-Rodriguez, M. G. Bagur-Gonzalez, M. Sanchez-Vinas, A. Gonzalez-Casado and A. M. Gomez-Saez, *J. Chromatogr. A*, 2007, **1158**, 33-46.
79. P. Giraudeau, I. Tea, G. S. Remaud and S. Akoka, *J. Pharmaceut. Biomed.*, 2014, **93**, 3-16.
80. J. Meija, E. Pagliano and Z. Mester, *Anal. Chem.*, 2014, **86**, 8563-8567.
81. E. C. d. Oliveira, E. I. Muller, F. Abad, J. Dallarosa and C. Adriano, *Quim. Nova*, 2010, **33**, 984-987.
82. D. Orazbayeva, B. Kenessov, J. A. Koziel, D. Nassyrova and N. V. Lyabukhova, *Chromatographia*, 2017, **80**, 1249-1256.
83. P. M. Geyer, M. C. Hulme, J. P. B. Irving, P. D. Thompson, R. N. Ashton, R. J. Lee, L. Johnson, J. Marron, C. E. Banks and O. B. Sutcliffe, *Anal. Bioanal. Chem.*, 2016, **408**, 8467-8481.
84. H. Lord and J. Pawliszyn, *J. Chromatogr. A*, 2000, **885**, 153-193.